UNIVERSITÀ DEGLI STUDI DI GENOVA

Doctorate in
Sciences and Technologies
of
Chemistry and Materials

Curriculum: Drug Discovery

ISTITUTO ITALIANO DI TECNOLOGIA
Drug Discovery and Development department

Study of sphingolipid-mediated signaling and metabolism during aging

PhD Candidate
Valentina Vozella

Advisor
Prof. Daniele Piomelli
Co-advisor
Prof. Olga Bruno

Academic years 2014-2017

“The secret of getting ahead is getting started”

Mark Twain

Contents

Summary and aim of the thesis

Sphingolipids are a class of bioactive signaling molecules that regulate key cellular processes including cell growth, senescence and apoptosis, and have been implicated in age-related neurodegeneration. Previous studies have reported elevated ceramide levels in the brain of old rodents, but a systematic investigation of the impact of age on brain sphingolipid metabolism was still lacking. In the present study we quantified 17 key sphingolipid species in the hippocampus of young (3 months), middle-aged (12 months) and old (21 months) male and female mice. Lipids were extracted and quantified by liquid chromatography/mass spectrometry; transcription of enzymes involved in sphingolipid biosynthesis was evaluated by qPCR. Age-dependent changes of multiple sphingolipid species - including ceramide (d18:1/18:0), sphingomyelin (d34:1), hexosylceramide (d18:1/16:0), ceramide (d18:1/24:0) - were found in mice of both sexes. Moreover, sex-dependent changes were seen with hexosylceramide (d18:1/18:0), ceramide (d18:1/22:0), sphingomyelin (d36:1) and sphingomyelin (d42:1). Importantly, an age-dependent accumulation of sphingolipids containing nervonic acid (24:1) was observed in 21 month-old male ($p = 0.04$) and female mice ($p < 0.001$). Consistent with this increase, transcription of the nervonic acid-synthesizing enzyme, stearoyl-CoA desaturase (*Scd1* and *Scd2*), was upregulated in 21 month-old female mice (*Scd1* $p = 0.006$; *Scd2* $p = 0.009$); a similar trend was observed in males (*Scd1* $p = 0.07$). In conclusion, the results suggest that aging is associated with profound sex-dependent and -independent changes in hippocampal sphingolipid profile. The results also highlight the need to examine the contribution of sphingolipids, and particularly of those containing nervonic acid, in normal and pathological brain aging.

Nevertheless, also the circulating ceramids are altered in persons affected by age-dependent pathologies such as metabolic syndrome, mild cognitive impairment and Alzheimer's disease, but the potential impact of age and gender on plasma ceramide trajectories in healthy subjects has not been systematically examined. In this study we quantified a panel of circulating ceramides and dihydroceramides in a cohort of 164 healthy subjects (84 female, 80 male; 19-80 years of age). The results show that plasma ceramide levels are significantly lower

($p < 0.05$) in pre-menopausal women (aged 20-54 years) compared to age-matched men (aged 19-54 years). This difference disappears after menopause, such that plasma ceramide levels in post-menopausal women (aged 47-78 years) are statistically identical to those measured in aged-matched men (aged 55-80 years). In women of all ages, but not in men, circulating levels of ceramide (d18:1/24:1) were negatively correlated with plasma estradiol levels. Finally, in vitro experiment showed that incubation with estradiol (10 nM, 24 h) lowers ceramide levels in the human MCF7 breast cancer cell line. Together the results suggest the existence of gender- and age-dependent alterations in circulating ceramide concentrations, which are dependent on estradiol. In addition to my previous study on rodent model, the present work introduces menopause and fluctuating estradiol levels as new variables to keep into account in the study of aging.

Aging is the main risk factor for the development of neurodegenerative diseases such as Alzheimer's disease but also chronic diseases such as metabolic syndrome. Indeed, it is becoming increasingly evident that cellular and biochemical alterations observed in metabolic syndrome like, among others, alterations in lipid mediators, may represent a pathological bridge between age-related neurological disorders and metabolic syndrome.

Sphingolipids have been implicated in the pathogenesis of metabolic dysfunction, but physiological signals regulating their formation and deactivations in hypothalamus are unknown. Hypothalamus is an especially important node in central and peripheral regulation of feeding behavior. We studied the effect of high-fat diet (HFD) or food deprivation (FD) on sphingolipid levels and on the expression of enzymes involved in sphingolipid metabolism in the hypothalamus. To study the effect of HFD, mice were divided into two groups: standard diet (2.66 kcal/g) and HFD (5.24 kcal/g) and killed at different time points (1-3-7-14-28 days). To study the effect of fasting, male mice were subjected to 4 feeding conditions: 1) free feeding (FF); 2) 12h food deprivation (FD); 3) 1h refeeding after FD; 4) 6h refeeding after FD. Hypothalamic sphingolipids were extracted and quantified by LC-MS/MS. Transcription of enzymes involved in sphingolipid biosynthesis was evaluated by qPCR. After 1 day and 14 days, mice exposed to a HFD showed lower levels of ceramide (d18:1/24:0), its precursor dihydroceramide (d18:0/24:0), and ceramide (d18:1/24:1) compared to mice fed standard diet. Significant decrease in sphingosine-1-phosphate (SO-1-P) was also observed after 7 and 14 days of HFD. Relative to FF,

fasting: 1) decreased SO-1-P levels; 2) increased sphingosine, the precursor of sphingosine-1-phosphate; 3) reduced the levels of dihydroceramide (d18:0/18:0), a product of *de novo* ceramide biosynthesis; 4) down-regulated transcription of sphingosine kinases (SphK) and ceramide synthase 1 (CerS1). Our results suggest that hypothalamic levels of SO-1-P, its precursor sphingosine and enzymes involved in their metabolism (SphK) are influenced by feeding status. Feeding also regulates the *de novo* synthesis of sphingolipid, suggesting additional roles for these lipids in the control of energy balance. Finally, a single intracerebroventricular injection of an acid ceramidase inhibitor, ARN14974, which has been shown to imbalance the ceramide/sphingosine-1-phosphate rheostat, was able to alter some parameters of feeding behavior such as meal size.

The aim of my studies was to explore the complexity of sphingolipid metabolism and understand the role of sphingolipids as lipid-derived mediators of cell signaling in physiological or altered conditions in rodent model and in human. Aging and feeding states are strongly correlated since aging has been associated with development of obesity and metabolic disorders, which depend, in turn, on altered feeding status; on the other hand, hyperphagia or fasting may have respectively detrimental or beneficial effect on aging and longevity. Furthermore, since a variety of studies have been published on the relevance of dimorphism in the development of age-related disorders, I pursued my research keeping into account sex-related differences. Brain areas and plasma have been chosen as target tissues for my studies. My research has been focused on specific cerebral areas involved respectively in aging and cognition (hippocampus) and feeding control and energy balance (hypothalamus). To investigate the role of ceramides in human, I had access to plasma from healthy subjects recruited by Santa Lucia Foundation. Plasma is widely used to assess biomarkers of pathological states in human studies. Liquid chromatography-tandem mass spectrometry (LC-MS/MS), a unique technology with the requisite of specificity, sensitivity and quantitative precision capabilities, allowed me to qualify and quantify target sphingolipids.

Keywords

Lipidomics, sphingolipids; ceramides; sphingosine and sphingosine-1-phosphate; fatty acids; estradiol; liquid chromatography/mass spectrometry; sex-dependent; healthy aging; neurodegeneration; menopause; high fat diet; obesity; fasting; feeding behavior; hippocampus; hypothalamus; rodent models; human.

Chapter 1

Sphingolipids

1.1 Why to study Sphingolipids?

Sphingolipids, the second largest class of membrane lipids, were initially considered just as structural components of cellular membranes, having little relevance in cellular signaling. Nowadays, however, they are regarded as multifunctional bioactive lipids. The term “sphingosin” was coined and first published in 1884 by J.L.W. Thudichum (1829–1901), the German-born physician who identified sphingolipids in brain (Hawthorne 1975). The name for this enigmatic family of lipids was taken from the *Sphynx* of Greek mythology which was well known for its love of riddles. Through extensive research the secrets of sphingolipids have now become known. Over the past thirty years, research in the sphingolipid field has revealed that these molecules are involved in multiple regulatory functions in health and disease (Hannun and Obeid 2008). They are involved in the pathogenesis of cancer (Ogretmen and Hannun 2004), inflammation (Maceyka and Spiegel 2014), pain (Patti, Yanes et al. 2012), metabolic disorders (Chaurasia and Summers 2015), aging and senescence (Venable, Lee et al. 1995).

However, *Sphynx*-lipids continue to keep us guessing.

1.2 Sphingolipids: chemical structures and biosynthesis

Sphingolipids are essential lipids consisting of a sphingoid backbone that is *N*-acylated via amide bond with various fatty acids. Ceramides, which are considered the metabolic hub, can differ from each other by the chain-length, hydroxylation, or saturation of both the sphingoid base and fatty acid moieties (Fig.1). Sphingoid bases are of three general chemical types: sphingosine, dihydrosphingosine (also known as sphinganine) and phytosphingosine. Based on the nature of the sphingoid base backbone, we can distinguish three main species: ceramide, which contains sphingosine, has a trans-double bond at the C4–5 position in the sphingoid base backbone; dihydroceramide, which contains sphinganine, presents a saturated sphingoid backbone devoid of the 4,5-trans-double bond; phytoceramide, the yeast counterpart of the mammalian ceramide, which contains phytosphingosine, has an hydroxyl group at the C4 position (Hannun and Obeid 2008; Pruett, Bushnev et al. 2008).

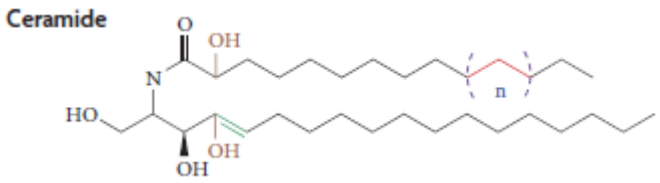

Fig.1. The generic 'ceramide' is a family of >50 distinct molecular species, as ceramide may exist without the double bond (dihydroceramide), with the double bond (ceramide), with a 4'-hydroxy sphingoid base (phytoceramide), with a 2'-hydroxy (α-hydroxyceramide), or both hydroxyl groups (α-hydroxy-phytoceramide). Each of these can have various *N*-linked acyl chains. Adapted from Hannun and Obeid, 2008.

The fatty acid components of ceramides vary widely in composition, but they typically range from 14 to 26 carbon atoms, although the most common fatty acids are palmitic (C16:0), stearic (C18:0), lignoceric (C24:0) and nervonic (C24:1), non-hydroxy fatty acids.

Sphingolipid family includes ceramide (Cer), dihydroceramide (dHCer), sphinganine (SA), sphinganine-1-phosphate (SA-1-P), sphingosine (SO), sphingosine-1-phosphate (SO-1-P) and more complex sphingolipids such as glucosylceramide (GluCer) and sphingomyelin (SM). Sphingolipid metabolic pathway shows a complex

network which results in the formation of different metabolites where ceramide occupies a central position in the biosynthesis and catabolism of sphingolipids.

Multiple metabolic pathways converge upon ceramide formation which can be synthesized by *de novo* pathway, hydrolysis of complex sphingolipids or salvage pathway (Fig.2).

In the *de novo* synthesis, the first step is the condensation of L-serine and palmitoyl-CoA catalyzed by the enzyme serine palmitoyltransferase (SPT) which leads to the formation of 3-ketosphinganine. Stereoselective reduction of the keton by 3-ketosphinganine reductase generates sphinganine. *N*-acylation by ceramide synthase (CerS) forms dihydroceramide which is then converted into ceramide by dihydroceramide desaturase (DES) that catalyzes the introduction of the *trans*-double bond at carbon 4-5. In mammals, six genes that encode ceramide synthases have been cloned and called longevity-assurance homologues (LASS1-6) or ceramide synthases (CerS1-6). From a biochemical point of view, each isoform has substrate preference for a specific chain-length fatty acyl-CoA, thus generating distinct ceramides with distinct N-linked fatty acid (for example, LASS1 shows significant preference for fatty acid C18:0). The *de novo* pathway is activated in response to tumor necrosis factor (TNF)-α and chemotherapeutic agents; in fact this pathway may be the mechanism by which several chemotherapeutics agents induce apoptosis. *De novo* pathway is also activated by free palmitoyl-CoA and this has been proposed to play a role in mediating complications of diabetes and obesity. The ceramide coming from the *de novo* synthesis is accumulated in the endoplasmatic reticulum and later transported to the Golgi apparatus to be used as substrate for the biosynthesis of complex sphingolipids; specific protein transfers, termed CERTs, are responsible for the transit of ceramide (Hanada, Kumagai et al. 2003). In the Golgi apparatus, the primary alcohol of ceramide can undergo glycosylation forming glucosylceramide or can incorporate a phosphocholine head group from phosphatidylcholine, producing sphingomyelin.

The hydrolysis of sphingomyelin leads to ceramide accumulation catalyzed by the sphingomyelinases (SMases). These enzymes are distinguished according to their optimum pH and subcellular localization, and although several mammalian SMases have been identified and characterized, the neutral sphingomyelinase 2 (nSMase 2,

SMPD3) and acid sphingomyelinase (aSMase, SMPD1) are the most extensively studied (Jenkins, Canals et al. 2010). Acid sphingomyelinase has an optimum pH of 4.5–5.5 and it is localized in the lysosome. The neutral sphingomyelinase acts at neutral pH, it is stimulated by cation Mg^{2+} or Mn^{2+} and it is essentially located in the plasma membrane, cytosol, endoplasmatic reticulum or nuclear membrane. The sphingomyelinases (neutral and acid) are a class of phosphodiesterases activated by stress-signaling molecules such as the TNF-α and interleukin-1β and by other stress stimuli as exposure to ultraviolet (UV) light or radioactive radiation.

Finally, the salvage pathway occurs within the lysosome and it is based on the generation of ceramide by catabolism of complex sphingolipids such as sphingomyelin and hexosylceramide. The common metabolic product, ceramide, can be further hydrolyzed by acid ceramidase to form sphingosine and free fatty acid, both of which are able to leave the lysosome. Sphingosine may then re-enter the pathway for synthesis of ceramide through reacylation or can be phosphorylated to sphingosine-1-phosphate (SO-1-P) by sphingosine kinases (SphK). The conversion of ceramide to SO-1-P has been termed as “sphingolipid rheostat” and it involves enzymes which may be potential targets to tilt the balance between these bioactive molecules, eventually contributing to determine cell fate (Cuvillier, Pirianov et al. 1996). In fact, ceramide generally exerts pro-senescent and pro-apoptotic effects in both normal and tumour cells, while SO-1-P enhances cell survival and proliferation by activating selective G protein-coupled receptors named S1PR1-5.

The enzymes responsible to regulate the ceramide/SO-1-P axis are the ceramidases, ubiquitous amido-hydrolases responsible for the cleavage of ceramide into sphingosine and fatty acid. Five mammalian ceramidases have been cloned and biochemically characterized due to the differences in substrate specificity, cellular localization, optimum pH, tissue distribution and expression level: acid ceramidase; neutral ceramidase; alkaline ceramidase 1; alkaline ceramidase 2; alkaline ceramidase 3.

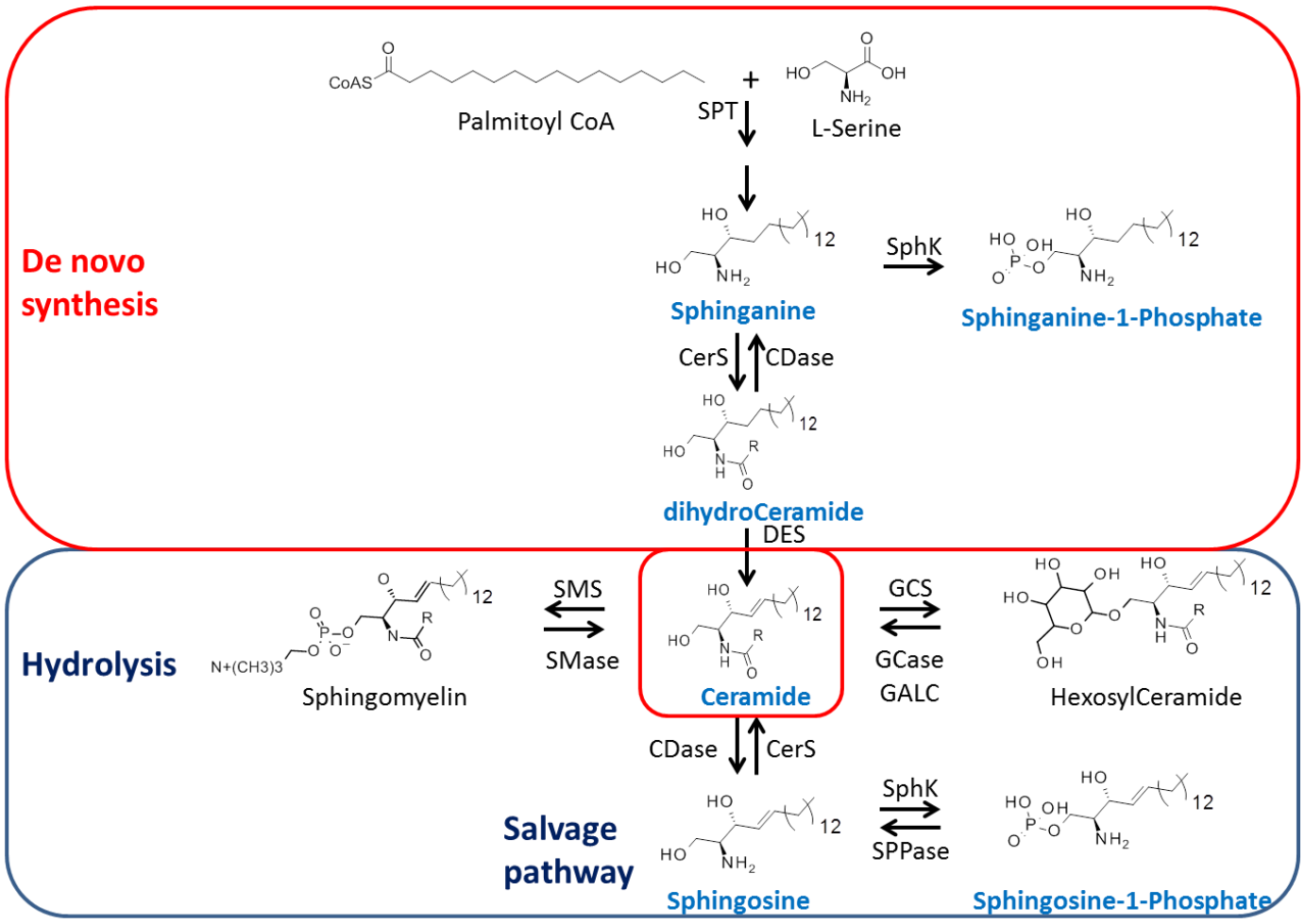

Fig. 2. Sphingolipid metabolism: bioactive sphingolipid metabolites and key enzymes. SPT (serine palmitoyltransferase); CerS (ceramide synthase); CDase (ceramidase); DES (desaturase); SphK (sphingosine kinase); SPPase (sphingosine-1-phosphate phosphatase); SMS (sphingomyelin synthase); SMase (sphingomyelinase); GCS (glucosylceramide synthase); GCase (glucosylceramidase); GALC (galactosylceramidase).

Chapter 2

Age-dependent changes in nervonic acid-containing sphingolipids in mouse hippocampus

2.1 Introduction

Sphingolipids are a class of bioactive signaling molecules that regulate key cellular processes including cell growth, senescence and apoptosis (Venable, Lee et al. 1995; Hetz, Hunn et al. 2002; Bartke and Hannun 2009; Jana, Hogan et al. 2009). Ceramides occupy a central place in sphingolipid metabolism (Fig. 1): they are synthesized *de novo* from the condensation of serine and palmitoyl-coenzyme A by the action of serine palmitoyltransferase (SPT), from the reacylation of sphingoid long-chain bases, or from the breakdown of more complex sphingolipids such as sphingomyelins and hexosylceramides (Gault, Obeid et al. 2010). Moreover, ceramides give rise to sphingosine, which is phosphorylated by sphingosine kinases to produce the transcellular messenger sphingosine-1-phosphate (Hannun and Obeid 2008).

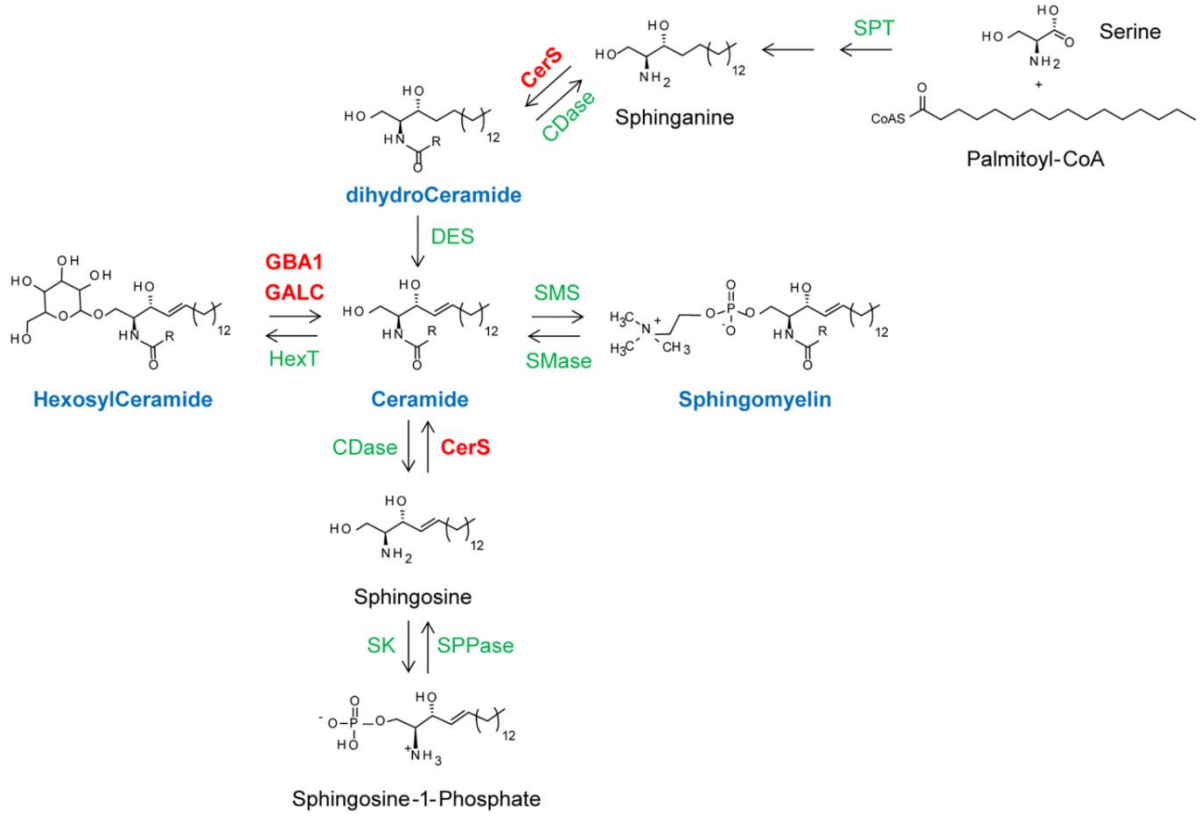

Fig. 1. Schematic view of sphingolipid metabolism, highlighting metabolites and enzymes targeted by the present study. Abbreviations: SPT (serine palmitoyltransferase); CerS (ceramide synthase); CDase (ceramidase); DES (desaturase); GBA1 (glucosylceramidase); GALC (galactosylceramidase); HexT (hexosyltransferase); SMS (sphingomyelin synthase); SMase (sphingomyelinase); SK (sphingosine kinase); SPPase (sphingosine-1-phosphate phosphatase).

Evidence from animal and human studies suggests that Alzheimer's disease (AD) and Parkinson's disease (PD) are associated with abnormalities in sphingolipid metabolism (Han, D et al. 2002; Cutler, Kelly et al. 2004; Mielke, Haughey et al. 2010; Mielke, Maetzler et al. 2013). Aging is the primary risk factor for AD and PD (Collier, Kanaan et al. 2011; Niccoli and Partridge 2012). Multiple lines of evidence indicate that tissue ceramide profiles change during aging and in response to a variety of age-related stress factors (e.g. oxidative stress) (Lightle, Oakley et al. 2000; Cutler, Kelly et al. 2004; Costantini, Kolasani et al. 2005; Perez, Jurisicova et al. 2005; Astarita, Avanesian et al. 2015). Despite this growing body of evidence, a systematic study of the impact of age on brain sphingolipid metabolism remains to be performed. Such a study should take into consideration as an independent variable sex along with age, because of the dimorphic trajectory of both healthy aging and neurodegenerative disorders (Fratiglioni, Launer et al. 2000; Moser and Pike 2016).

In the present study, we used a targeted lipidomic approach to identify age- and sex-dependent alterations in sphingolipid metabolism in mouse hippocampus. We selected this brain region because it is one of the first to become damaged in AD, leading to memory loss and cognitive impairment (Lauterborn, Palmer et al. 2016). The results suggest that aging is accompanied by multiple, sexually dimorphic changes in hippocampal sphingolipid profile. Notably, we found that sphingolipid species containing the long-chain monounsaturated fatty acid, nervonic acid (24:1), are markedly affected by aging, pointing to these lipids as potential contributors to age-dependent cognitive impairment.

2.2 Materials and methods

2.2.1 Animals

Male and female C57Bl/6J mice (3, 12 and 21 months) were purchased from Charles River Laboratories (Calco, Lecco, Italy). Upon arrival, they were acclimatized to the vivarium and kept in a temperature (22 °C) and humidity controlled environment under a 12h light/12h dark cycle (lights on at 7:00 A.M.). Animals were housed under enriched conditions (Mattson, Duan et al. 2001; Segovia, del Arco et al. 2009) with bedding changes every 15 days in mice aged 3-12 months, and every 21 days in mice aged 21 months. Standard chow and water were available *ad libitum*. All procedures were performed in accordance with the Ethical Guidelines of the European Community Council (Directive 2010/63/EU of 22 September 2010) and accepted by the Italian Ministry of Health.

2.2.2 Chemicals

Standards such as ceramide (d18:1/16:0), ceramide (d18:1/17:0), ceramide (d18:1/18:0), ceramide (d18:1/20:0), ceramide (d18:1/22:0), ceramide (d18:1/24:0), ceramide (d18:1/24:1(15Z)), dihydroceramide (d18:0/16:0), dihydroceramide (d18:0/18:0), dihydroceramide (d18:0/24:0), dihydroceramide (d18:0/24:1), sphingomyelin (d34:1), sphingomyelin (d35:1), sphingomyelin (d36:1), sphingomyelin (d42:1), sphingomyelin (d42:2), glucosylceramide (d18:1/12:0), glucosylceramide (d18:1/16:0), glucosylceramide (d18:1/18:0), glucosylceramide (d18:1/24:1) were purchased from Avanti Polar Lipids (Alabaster, Alabama, USA). Fatty acid standards such as heptadecanoic acid (17:0), nervonic acid (24:1), palmitic acid (16:0), stearic acid (18:0), oleic acid (18:1), eicosaenoic acid (20:1) and erucic acid (22:1) were purchased from Sigma-Aldrich (Milan, Italy).
LC-MS grade solvents such as acetonitrile, isopropanol, water, methanol and chloroform and other chemicals such as trifluoroacetic acid and formic acid were from Sigma-Aldrich (Milan, Italy).

2.2.3 Tissue collection

Mice were anesthetized with isoflurane and sacrificed by cervical dislocation. Brains were removed; hippocampi were dissected on an ice-cold glass plate and were immediately flash frozen in liquid N_2. Samples were stored at -80 °C before analyses.

2.2.4 Lipid extraction

Lipid extractions were performed according to a modified Bligh and Dyer protocol, as previously reported (Basit, Piomelli et al. 2015). Briefly, frozen hippocampi (10-20 mg) were homogenized in 2 mL of a methanol/chloroform mixture (2:1 vol/vol) containing trifluoroacetic acid (TFA, 0.1% final concentration), and spiked with a mixture of internal standards consisting of the following unnatural odd-chain lipids: 200 nM ceramide (d18:1/17:0), 400 nM sphingomyelin (d18:1/17:0) and 500 nM heptadecanoic acid (17:0). Glucosylceramide (d18:1/12:0) 200 nM was added as internal standard for hexosylceramides after having verified the absence from hippocampal extracts. After mixing for 30 s, lipids were extracted with chloroform (0.6 mL) and extracts were washed with purified water (0.6 mL). Samples were centrifuged for 15 min at 2800×*g* at 15 °C. After centrifugation, the organic phases were collected and transferred to a new set of glass vials. To increase the extraction efficiency, the aqueous fractions were subjected to a second extraction. The organic phases were pooled, dried under N_2 and residues were dissolved in 0.2 mL of methanol/chloroform (9:1 vol/vol). 0.1 mL of the total extract was saved for the measurement of more polar analytes such as sphingomyelins and hexosylceramides. The remaining solvent was evaporated under N_2. Lipid pellets were reconstituted in chloroform (2 mL), loaded and fractionated using small glass columns packed with Silica Gel G (60-Å 230–400 Mesh ASTM; Whatman, Clifton, NJ). The flow through was discarded and ceramides and fatty acids were eluted with 2 mL of chloroform/methanol (9:1 vol/vol). The solvent was evaporated under N_2; dried material was resuspended in 0.1 mL of methanol/chloroform (9:1 vol/vol) and transferred to glass vials for liquid chromatography/mass spectrometry (LC/MS) analyses.

2.2.5 Sphingolipid analyses

An Acquity® UPLC system coupled with a Xevo triple quadrupole mass spectrometer (TQ-MS) were used as previously described (Basit, Piomelli et al. 2015). Lipids were separated using a BEH (Ethylene Bridged Hybrid) C18 column (2.1×50 mm, 1.7 µm particle size) and eluted at a flow rate of 0.4 mL/min. The mobile phase consisted of 0.1% formic acid in acetonitrile/water (20:80 vol/vol) as solvent A and 0.1% formic acid in acetonitrile/isopropanol (20:80 vol/vol) as solvent B. A step gradient program was used: 0.0–1.0 min 30% B, 1.0–2.5 min 30 to 70% B, 2.5–4.0 min 70 to 80% B, 4.0–5.0 min 80% B, 5.0–6.5 min 80 to 90% B, and 6.6–7.5 min 100% B. The column was then reconditioned to 30% B for 1.4 min. The total run time for analysis was 9 min and the injection volume was 3 µL. Mass spectrometric detection was done in the positive electrospray ionization (ESI) mode and analytes were quantified in the multiple reaction monitoring (MRM) mode. Capillary voltage was set at 3 kV and the cone voltage at 25 V for all transitions. The source temperature was 120 °C. Desolvation gas flow was set at 800 l/h and cone gas (N_2) flow at 20 l/h. Desolvation temperature was 600 °C. Analytes were identified by comparison of their retention times and MS^n fragmentation patterns with those of authentic standards. The following MRM transitions were used for identification and quantification: ceramide (d18:1/16:0) (*m/z* = 520.0 > 264.2); ceramide (d18:1/18:0) (*m/z* = 548.0 > 264.2); ceramide (d18:1/20:0) (*m/z* = 576.0 > 264.2); ceramide (d18:1/22:0) (*m/z* = 604.3 > 264.2); ceramide (d18:1/24:0) (*m/z* = 632.0 > 264.2); ceramide (d18:1/24:1 (15Z)) (*m/z* = 630.0 > 264.2). Dihydroceramide (d18:0/16:0) (*m/z* = 540.5 > 522.5); dihydroceramide (d18:0/18:0) (*m/z* = 568.5 > 550.5); dihydroceramide (d18:0/24:0) (*m/z* = 652.5 > 634.5); dihydroceramide (d18:0/24:1) (*m/z* = 650.5 > 632.5). Sphingomyelin (d34:1) (*m/z* = 703.25 > 184.1); sphingomyelin (d36:1) (*m/z* = 731.47 > 184.1); sphingomyelin (d42:1) (*m/z* = 815.14 > 184.1); sphingomyelin (d42:2) (*m/z* = 813.2 > 184.1). Hexosylceramide (d18:1/16:0) (*m/z* = 682.2 > 264.2); hexosylceramide (d18:1/18:0) (*m/z* = 710.1 > 264.2); hexosylceramide (d18:1/24:1) (*m/z* = 792.1 > 264.2). Data were acquired by the MassLynx software and quantified using the TargetLynx software.

2.2.6 Fatty acid analyses

An Acquity® UPLC system coupled with a Xevo triple quadrupole mass spectrometer were used. Lipids were separated using a HSS C18 column (2.1 × 100 mm, 1.8 µm particle size) and eluted at a flow rate of 0.4 mL/min. The mobile phase consisted of 20 mM ammonium acetate in water as solvent A and acetonitrile/isopropanol (50:50 vol/vol) as solvent B. A step gradient program was used: 0.0–0.5 min 50% B, 0.5–3.5 min 50 to 90% B, 3.5–4.5 min 90% B, 4.5–5.5 min 90 to 100% B, 5.5–7 min 100% B, 7–7.5 min 100 to 50% B and 7.5–9 min 50% B. The total run time for analysis was 9 min and the injection volume was 5 µL. Mass spectrometric detection was done in the negative ESI mode and analytes were quantified in the MRM mode. Capillary voltage was set at 3 kV and cone voltage was set at 30 V for all transitions. The source temperature was 120 °C. Desolvation gas flow was set at 800 l/h and cone gas (N_2) flow at 20 l/h. Desolvation temperature was 450 °C. Analytes were identified by comparison of their retention times and matching MRM transitions with authentic standards. MRM transitions were: nervonic acid (24:1) (*m/z* = 365.30 > 365.30), palmitic acid (16:0) (*m/z* = 255.04 > 255.04), stearic acid (18:0) (*m/z* = 283.25 > 283.25), oleic acid (18:1) (*m/z* = 281.22 > 281.22), eicosaenoic acid (20:1) (*m/z* = 309.22 > 309.22), erucic acid (22:1) (*m/z* = 337.23 > 337.23) CE set at 5 eV. Data were acquired by the MassLynx software and quantified using the TargetLynx software.

2.2.7 mRNA isolation, cDNA synthesis and quantitative real-time PCR

Total RNA was extracted from tissues using TRIzol (Life Technologies, Carlsbad, California) and the Ambion Purelink RNA mini-kit, as directed by the supplier (Life Technologies). Samples were rendered genomic DNA-free by treatment with DNase (PureLink DNase, Life Technologies). Reverse transcription of purified mRNA (1 µg) was carried out using SuperScript VILO complementary DNA (cDNA) synthesis kit according to the protocol (Invitrogen, Carlsbad, California). First-strand cDNA was amplified using the iTaq Universal SYBR Green Supermix (Biorad, Segrate, Milan, Italy) following manufacturer's instructions. The primer sequences were: ceramide synthase 1 (*Lass1*) forward: TCTGCTGTTGCTCCTGATGGTC, reverse: CTTGGCTGTCTGAGCTTCCAGA; ceramide synthase 2 (*Lass2*) forward: CCTTCTACTGGTCCCTGCTCTT, reverse: TGGCAAACCAGGAGAAGCAGAG;

stearoyl-CoA desaturase 1 (*Scd1*) forward: GCAAGCTCTACACCTGCCTCTT, reverse: CGTGCCTTGTAAGTTCTGTGGC; stearoyl-CoA desaturase 2 (*Scd2*) forward: GTCTGACCTGAAAGCCGAGAAG, reverse: GCAAGAAGGTGCTAACGCACAG; glucosylceramidase (*Gba1*) forward: GCCAGTTGTGACTTCTCCATCC, reverse: CGTGAGGACATCTTCAGGGCTT; lysosome membrane protein 2 (*Scarb2*) forward: TAGCCAACACCTCCGAAAACGC, reverse: CGAACTTCTCGTCGGCTTGGTA; prosaposin (*Psap*) forward: GTCTGATGTCCAGACTGCTGTG, reverse: CTGGACACAGACCTCGGAATAC; galactosylceramidase (*Galc*) forward: ATCTCTGGGAGCCGATTTCCTC, reverse: CCACACTGTGTAGGTTCCAGGA; elongase 1 (*Elovl1*) forward: CTGGCTCTTCATGCTTTCCAAGG, reverse: AAGCACCGAGTGGTGGAAGACA; elongase 6 (*Elovl6*) forward: CGGCATCTGATGAACAAGCGAG, reverse: GTACAGCATGTAAGCACCAGTTC.

Quantitative PCR was performed in 96-well PCR plates. Real-time PCR reactions were performed using ViiA™7 Real-Time PCR detection system (Applied Biosystems by Life Technologies). Thermal cycling conditions were: 95 °C for 10 min, followed by 40 cycles, each cycle consisting of 15 s at 95 °C and 1 min at 60 °C. The freely available Bestkeeper software (Pfaffl, Tichopad et al. 2004) was used to determine the expression stability and the geometric mean of two different housekeeping genes (glyceraldehyde 3-phosphate dehydrogenase, *Gapdh*, and hypoxanthine phosphoribosyltransferase, *Hprt*). The relative expression of genes of interest was measured by the $2^{-\Delta\Delta Ct}$ method (Livak and Schmittgen 2001), where ΔCt was calculated by subtracting the cycle threshold (Ct) value of the geometric mean of the housekeeping genes from the Ct value of the gene of interest. Data for 12 and 21 month-old mice are reported as fold change relative to 3 month-old mice.

2.2.8 Statistical analyses

Results are presented as mean ± SEM (standard error of the mean). Comparisons of parameters between two groups were made by unpaired Student's *t*-test. Comparisons of parameters among more than two groups were made by one-way ANOVA. GraphPad Prism software V5.03 (GraphPad Software, Inc., USA) was used. Differences between groups were considered statistically significant if $p<0.05$.

2.3 Results

2.3.1 Age and sex-dependent changes in ceramides

To investigate the impact of aging on brain sphingolipid metabolism we measured levels of several key sphingolipid species in healthy male and female mice at three different ages: young (3 months), middle aged (12 months) and old (21 months). Lipid extracts of hippocampal tissue were fractionated by normal phase open-bed chromatography, and ceramides and other sphingolipids were identified and quantified by liquid chromatography/mass spectrometry (LC/MS). Significant bidirectional age- and sex-dependent changes were seen with multiple ceramide species. Marked increases were observed in the levels of ceramide (d18:1/24:1) in both male and female mice at 12 and 21 months of age (Fig. 2A, C). A small but significant increase in ceramide (d18:1/24:0) was also noted in 21 month-old female mice (Fig. 2C). By contrast, decreases were observed with ceramide (d18:1/18:0) in both male and female mice at 21 months, but not 12 months of age (Fig. 2B, D). A decrease was also seen with ceramide (d18:1/24:0) in middle-aged and old male mice (Fig. 2A). The results suggest that age can differentially influence the accumulation of specific ceramides in mouse hippocampus. Most striking and consistent among these effects was an increase in the levels of nervonic acid-containing ceramide (d18:1/24:1).

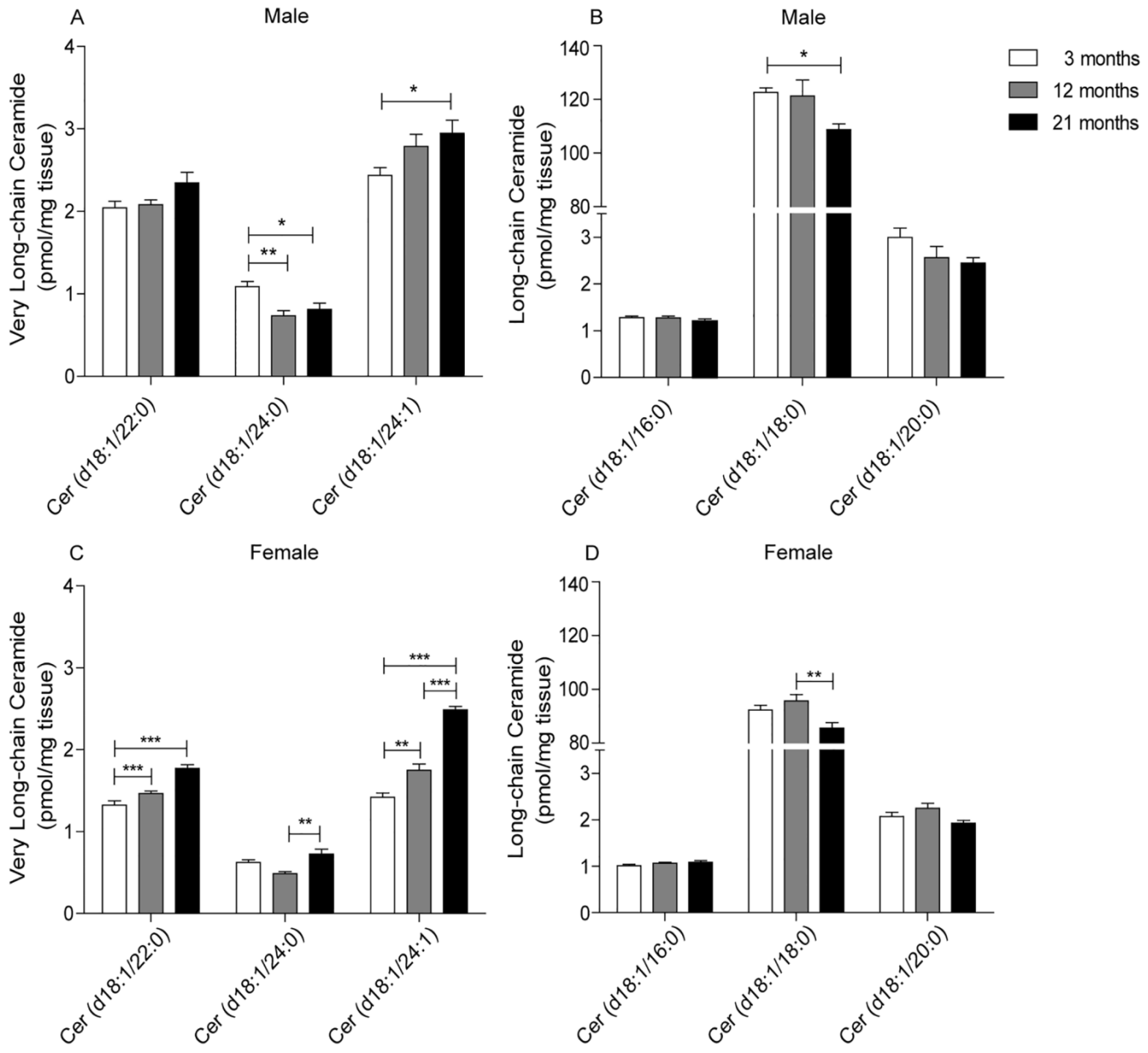

Fig. 2. Age and sex-dependent changes in ceramide (Cer) levels in mouse hippocampus. (A) and (B) male hippocampus; (C) and (D) female hippocampus. Results are expressed as mean ± SEM (n = 8/group). * $p < 0.05$, ** $p < 0.01$, *** $p < 0.001$; one-way ANOVA followed by Tukey's multiple comparison test.

2.3.2 Age and sex-dependent changes in de novo ceramide biosynthesis

Next, we asked whether the changes reported above might be attributable to alterations in *de novo* ceramide biosynthesis (Fig. 1). We found that levels of dihydroceramide (d18:0/18:0), the precursor for ceramide (d18:1/18:0), were lower in middle-aged (12 months) and old (21 months) male mice compared to their younger counterparts (Fig. 3A). No such effect was seen, however, in female mice, in which dihydroceramide (d18:0/18:0) content was not affected by age (Fig. 3C). The precursors for very long-chain ceramides, dihydroceramide (d18:0/24:0) and (d18:0/24:1), were slightly albeit significantly increased in 21 month-old female mice (Fig. 3C).

Age and sex were also associated with changes in transcription of the ceramide-synthesizing enzymes, ceramide synthase (CerS) 1 and 2 (encoded by the *Lass1* and *Lass2* genes) (Levy and Futerman 2010). Transcription of CerS1, which is responsible for the biosynthesis of long-chain ceramides such as ceramide (d18:1/18:0) (Grosch, Schiffmann et al. 2012), was significantly reduced in 21 month-old male mice, but not in females of the same age (Fig. 3B). Conversely, in middle-aged and old females we observed an increased transcription of CerS2, which is involved in the formation of very long-chain ceramides such as ceramide (d18:1/24:0) and (d18:1/24:1) (Fig. 3D). Transcription of CerS1 and 2 in middle-age (12 months) mice could not be assessed in these studies since we did not have enough tissue left to perform further analyses. Thus, aging appears to be associated with changes in the transcription of genes encoding for enzymes of *de novo* ceramide biosynthesis.

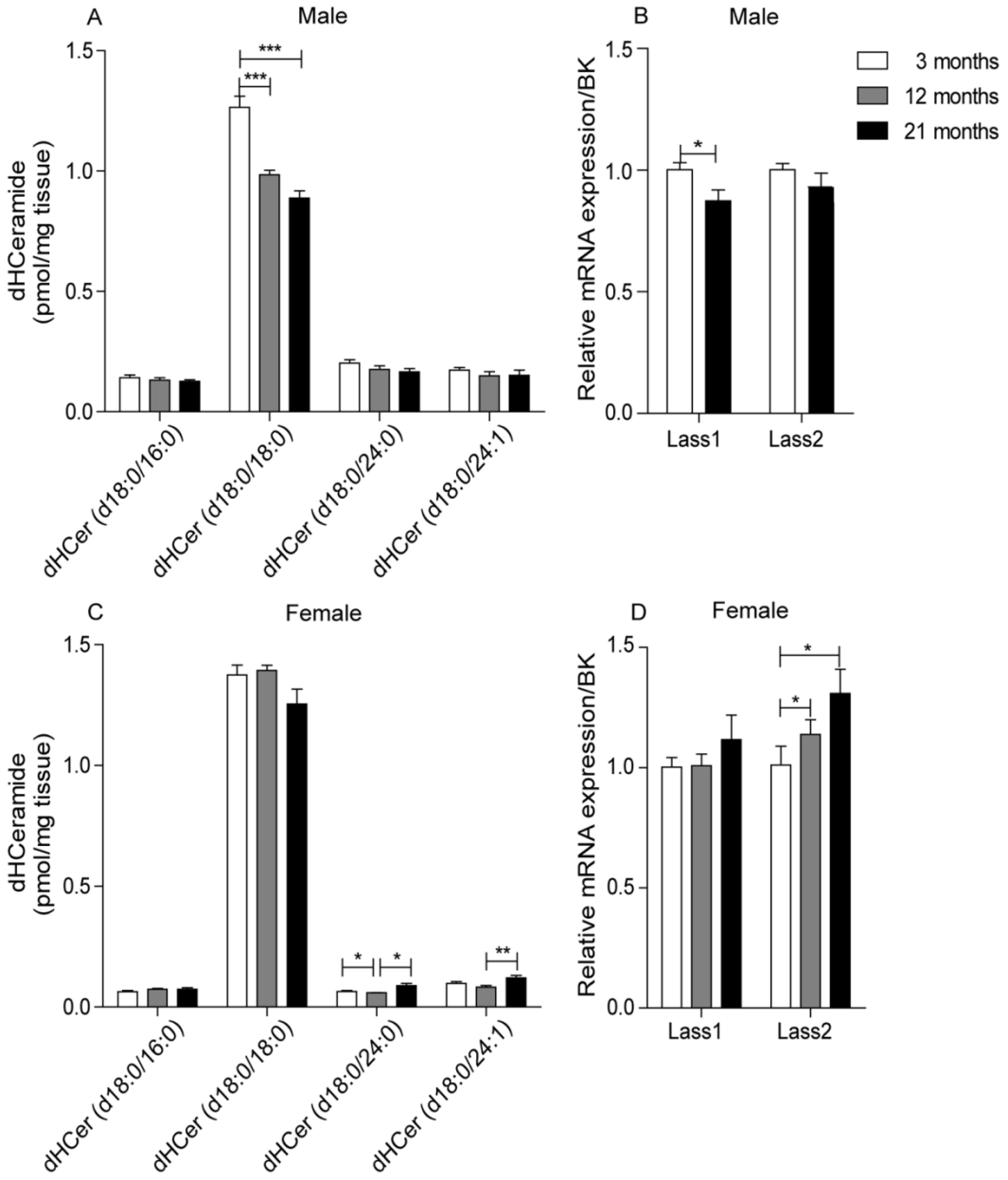

Fig. 3. Age and sex-dependent changes in dihydroceramide (dHCer) levels and *Lass1* (ceramide synthase 1) and *Lass2* (ceramide synthase 2) transcription in mouse hippocampus. (A) and (B) male hippocampus; (C) and (D) female hippocampus. Results are expressed as mean ± SEM (n = 5-8/group). * $p < 0.05$, ** $p < 0.01$, *** $p < 0.001$; Student's unpaired *t*-test or one-way ANOVA followed by Tukey's multiple comparison test.

2.3.3 Age and sex-dependent changes in sphingomyelin

In alternative to *de novo* biosynthesis, ceramides can also be produced through sphingomyelin hydrolysis (Fig. 1). We found that levels of sphingomyelin (d42:2) increased in an age-dependent manner in both male and female mice (Fig. 4A, B), as previously seen with ceramide (d18:1/24:1) (Fig. 2A, C). Sphingomyelin (d42:2) is likely to comprise the (d18:1/24:1) species, although others (e.g. d20:1/22:1) (Sugiura, Shimma et al. 2008) cannot be excluded. On the other hand, sex-dependent differences were observed for sphingomyelin (d36:1), which did not change with age in male mice (Fig. 4A), but showed small age-related fluctuations in females (Fig. 4B). Thus, since sphingomyelin (d42:1) and (d42:2) showed the same age-dependent trend as their catabolites ceramide (d18:1/24:0) and (d18:1/24:1), and since age-dependent increase in sphingomyelinase expression has been reported (Sacket, Chung et al. 2009), elevated sphingomyelin hydrolysis may contribute to the observed change in the levels of ceramides (d18:1/24:0) and (d18:1/24:1).

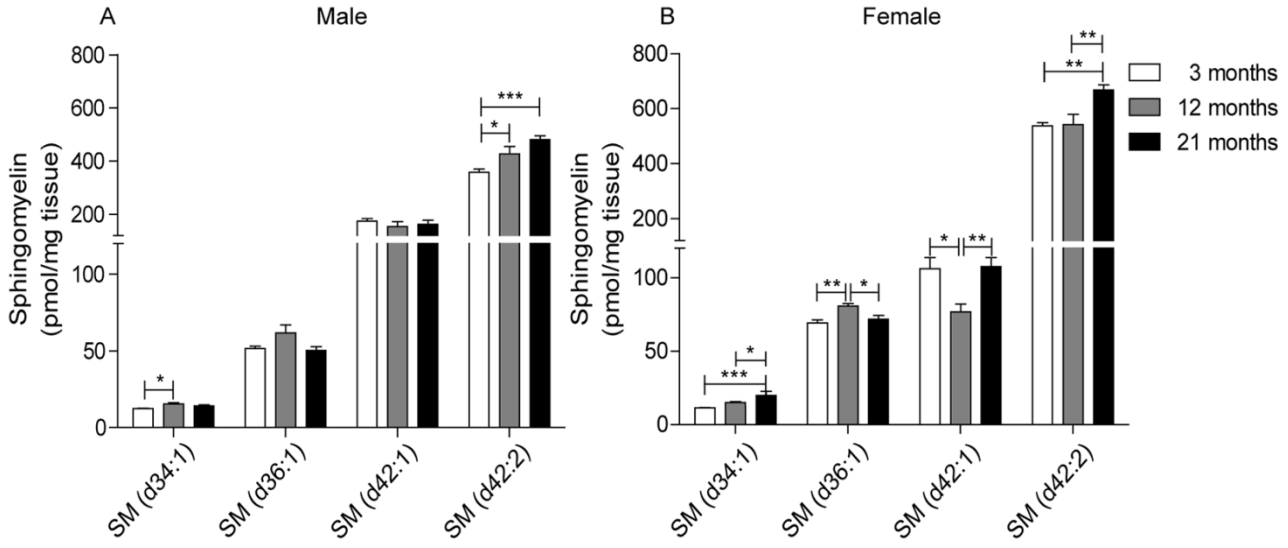

Fig. 4. Age and sex-dependent changes in sphingomyelin (SM) levels in mouse hippocampus. (A) and (B) male hippocampus; (C) and (D) female hippocampus. Results are expressed as mean ± SEM (n = 8/group). * $p < 0.05$, ** $p < 0.01$, *** $p < 0.001$; one-way ANOVA followed by Tukey's multiple comparison test.

2.3.4 Age and sex-dependent changes in hexosylceramide

The hexosylceramides, which contain either a glucosyl or a galactosyl sugar moiety, have been implicated in the pathogenesis of neurodegenerative disorders such as PD and Gaucher's disease (Mielke, Maetzler et al. 2013; Farfel-Becker, Vitner et al. 2014). As aging is the main risk factor for these disorders, we measured hexosylceramide content in the hippocampus of male and female mice at 3, 12 and 21 months of age. Fig. 5 illustrates our findings. Nervonic acid-containing hexosylceramide (d18:1/24:1) was elevated in 12 and 21 month-old male and female mice compared to 3 month-old animals. Moreover, age-dependent accumulation was observed with hexosylceramide (d18:1/16:0) in both sexes. By contrast, aging had no effect on hexosylceramide (d18:1/18:0) in female mice and caused a slight accumulation of this lipid molecule in 21 month-old males (Fig. 5).

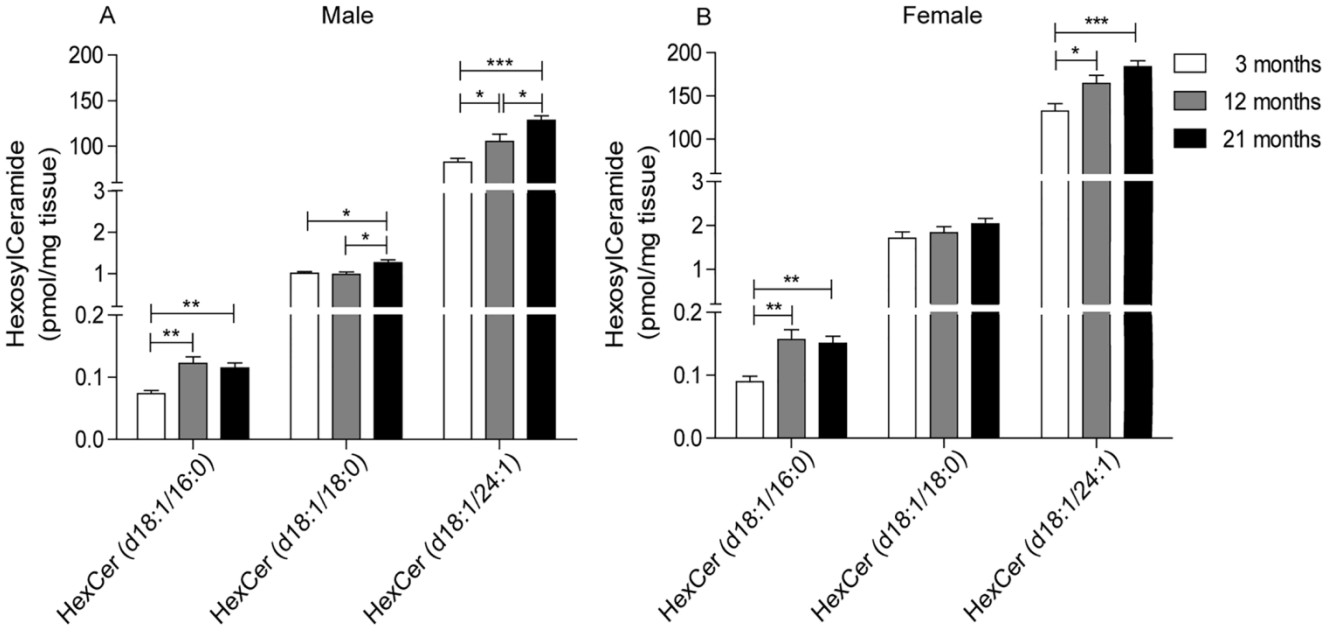

Fig. 5. Age and sex-dependent changes in hexosylceramides (HexCer) levels in mouse hippocampus. (A) male hippocampus; (B) female hippocampus. Results are expressed as mean ± SEM (n = 8/group). * $p < 0.05$, ** $p < 0.01$, *** $p < 0.001$; one-way ANOVA followed by Tukey's multiple comparison test.

Glucosylceramide accumulation in Gaucher's disease is due to impaired hydrolysis by β-glucosylceramidase 1, which is encoded by the *GBA1* gene (Brady, Kanfer et al. 1965; Brady, Kanfer et al. 1966; Tayebi, Stubblefield et al. 2003). To determine whether defective degradation might contribute to the high levels of hexosylceramide observed in the hippocampus of 12 and 21 month-old mice, we measured transcription of *Gba1* (Brady, Kanfer et al. 1965), lysosome membrane protein 2 (LIMP2, encoded by *Scarb2*), which acts as lysosomal receptor for glucosylceramidase (Gonzalez, Valeiras et al. 2014), and prosaposin (*Psap*), whose protein product is cleaved to generate the glucosylceramidase activators saposins A and C (Kishimoto, Hiraiwa et al. 1992). We also measured transcription of galactosylceramidase (*Galc*), which hydrolyzes the galactose ester bond of galactosylceramide (Nagano, Yamada et al. 1998). As shown in Fig. 6, no changes were detected in *Scarb2*, *Psap* and *Galc* expression. A small but significant downregulation of *Gba1* was observed in 21 month-old male, but not female mice (Fig. 6A, B), suggesting that changes in *Gba1* transcription only partially explain the observed alterations in hexosylceramide levels occurring in mice of both sexes at 12 and 21 months of age.

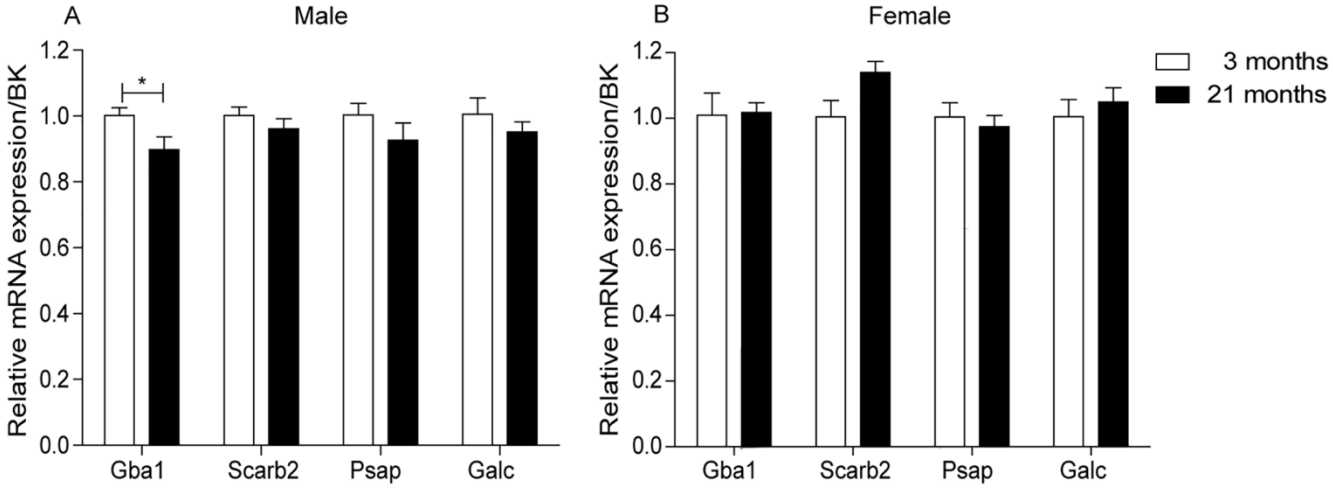

Fig. 6. Age and sex-dependent changes in *Gba1 (*β-glucosylceramidase 1), *Scarb2* (lysosome membrane protein 2), *Psap (*prosaposin), *Galc* (galactosylceramidase) transcription in mouse hippocampus. (A) male hippocampus; (B) female hippocampus. Results are expressed as mean ± SEM (n = 5/group). * $p < 0.05$, ** $p < 0.01$, *** $p < 0.001$; Student's unpaired *t*-test

2.3.5 Age and sex-dependent changes in nervonic acid and its biosynthesis

A common finding throughout our experiments was an elevation in sphingolipid species containing nervonic acid (24:1), which suggests that the production and the degradation of this long-chain monounsaturated fatty acid might be regulated by age. Consistent with this idea, we found that the content of non-esterified nervonic acid was higher in the hippocampus of 21 month-old male and female mice, compared to 3 month-old mice (Fig. 7A, D). We analyzed a broad panel of fatty acids, and then we focused on those species that are precursor of nervonic acid-containing sphingolipids. A similar increasing trend was seen with another monounsaturated fatty acid, oleic acid (18:1), in male but not female mice, whereas no change was observed in eicosaenoic acid (20:1) and erucic acid (22:1) (Fig. 7B, E), palmitic acid (16:0) and stearic acid (18:0) (Fig. 7C, F). Other species were analyzed but are not reported here since they were not significantly altered or because not directly involved in nervonic acid biosynthesis.

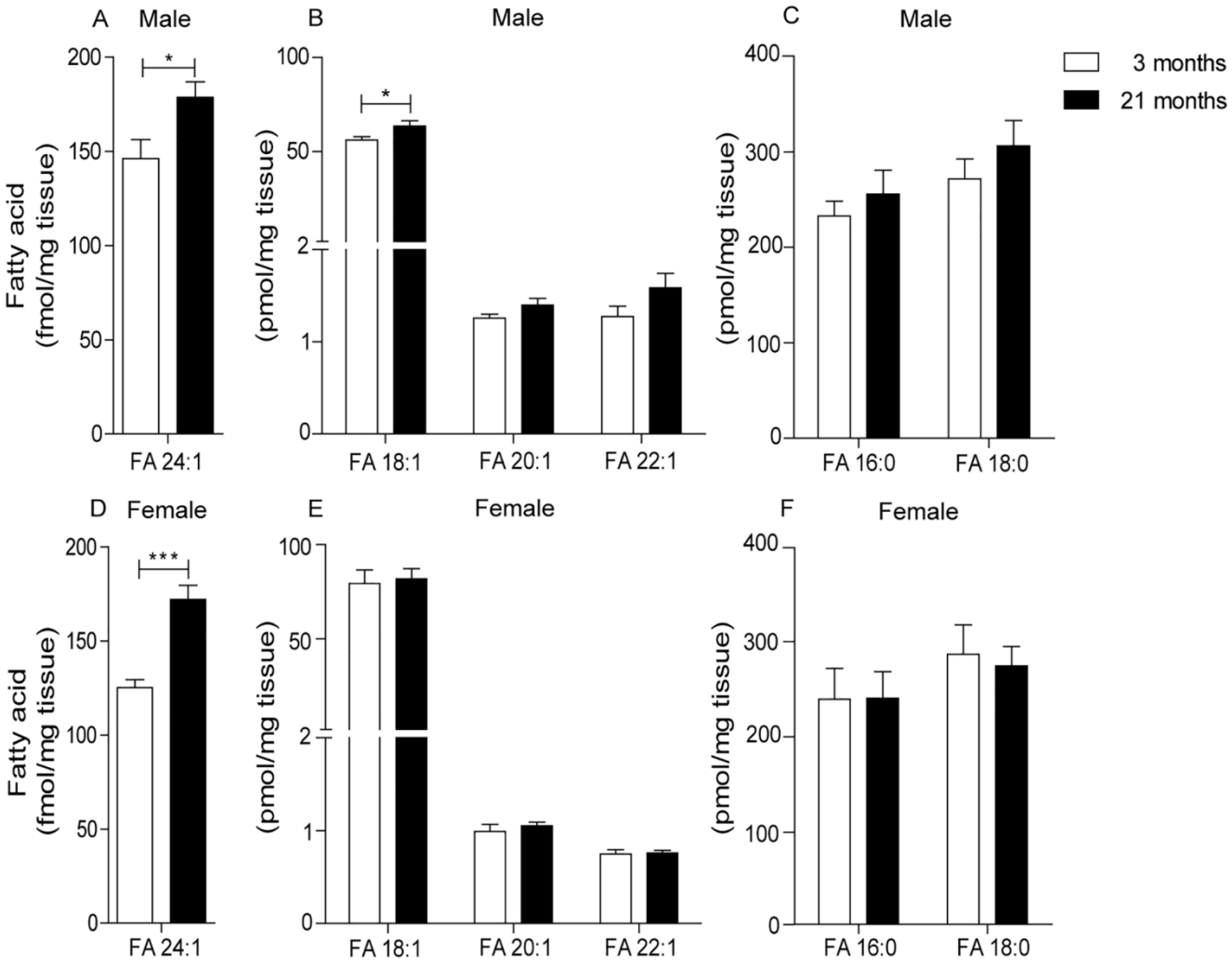

Fig. 7. Age and sex-dependent changes in fatty acids (FA): nervonic (24:1), oleic (18:1), eicosaenoic (20:1), erucic (22:1), palmitic (16:0) and stearic (18:0) acid levels in mouse hippocampus. (A), (B) and (C) male hippocampus; (D), (E) and (F) female hippocampus. Results are expressed as mean ± SEM (n = 5-8/group). * $p < 0.05$, ** $p < 0.01$, *** $p < 0.001$; Student's unpaired *t*-test.

The first committed step in the biosynthesis of nervonic acid is catalyzed by stearoyl-CoA desaturase (SCD) (Ntambi, Buhrow et al. 1988; Kaestner, Ntambi et al. 1989; Zheng, Prouty et al. 2001; Miyazaki, Jacobson et al. 2003), which converts stearic acid (18:0) into oleic acid (18:1). Elongase enzymes (ELOVL1 and ELOVL6 in brain) progressively insert two-carbon units to yield nervonic acid (24:1). We used quantitative RT-PCR to examine whether transcription of *Scd1* and *Scd2*, the most abundant *Scd* isoforms expressed in the rodent brain, might be elevated in old animals. Indeed, significant increases in *Scd1* and *Scd2* mRNA levels were observed in the hippocampus of 21 month-old female mice (Fig. 8C). A similar trend was seen in males, but did not reach

statistical significance (Fig. 8A). By contrast, transcription of *Elovl1* and *Elovl6* was reduced in male mice (Fig.8B), whereas transcription of *Elovl6* was slightly increased in female mice (Fig. 8D). Together, these findings are suggestive of an age-dependent dysregulation in nervonic acid homeostasis in the mouse hippocampus.

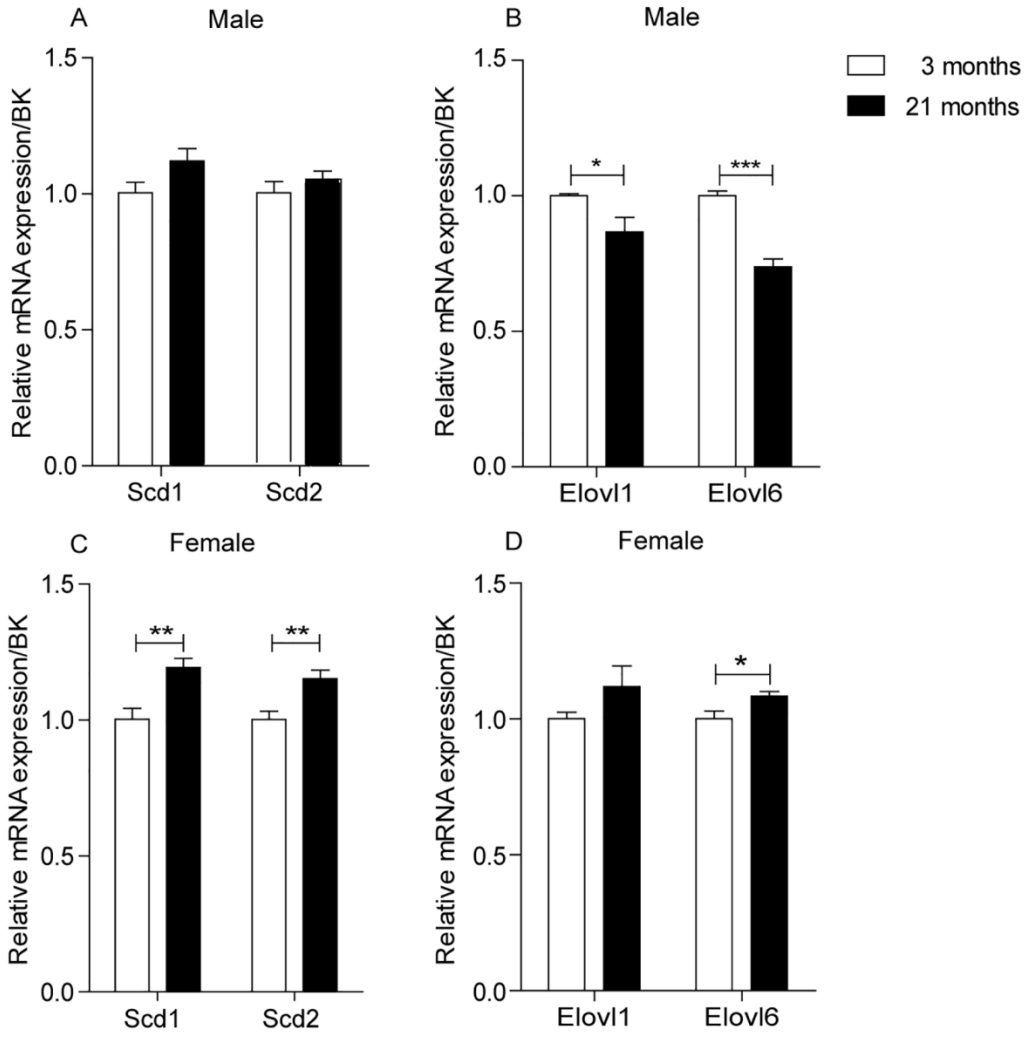

Fig. 8. Age and sex-dependent changes in *Scd* (stearoyl-CoA desaturase) and *Elovl* (elongase) transcription in mouse hippocampus. (A) and (B) male hippocampus; (C) and (D) female hippocampus. Results are expressed as mean ± SEM (n = 5/group). * $p < 0.05$, ** $p < 0.01$, *** $p < 0.001$; Student's unpaired *t*-test.

2.4 Discussion

The role of sphingolipids in normal aging and age-related disorders has been the object of multiple studies (for review see (Huang, Withers et al. 2014)). In the present work, we describe a series of previously unreported alterations in hippocampal sphingolipid metabolism, which are both age- and sex-dependent. As schematically summarized in Figure 9A, bidirectional changes in the levels of ceramide (d18:1/18:0), ceramide (d18:1/24:0), sphingomyelin (d34:1) and hexosylceramide (d18:1/16:0) were seen in mice of both sexes. Sex-restricted modifications were also observed with increased hexosylceramide (d18:1/18:0) only in males, increased ceramide (d18:1/22:0) and fluctuating sphingomyelin (d36:1) and (d42:1) only in females. These effects could be partially, but not completely, accounted for by alterations in *de novo* ceramide biosynthesis and sphingomyelin hydrolysis. However, the most striking and consistent finding in our study was the discovery of an age-dependent increase in sphingolipid species containing the monounsaturated fatty acid nervonic acid (24:1), whose levels were also heightened by aging (Fig. 9B). This increase was linked to, at least in female mice, transcriptional elevation of *Scd1* and *Scd2*, the rate-limiting enzymes of nervonic acid biosynthesis.

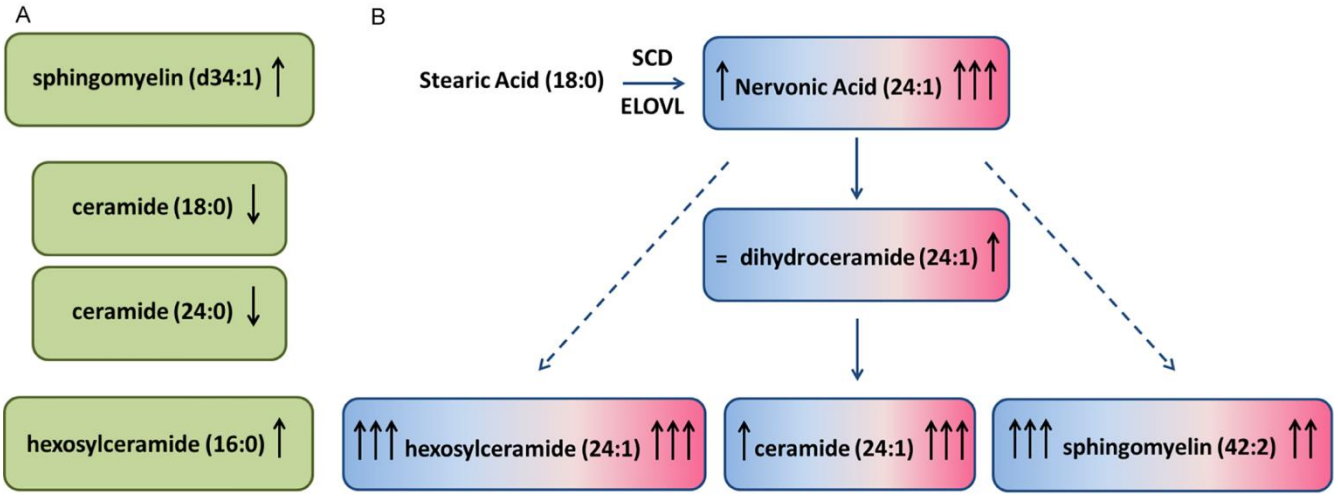

Fig. 9. Schematic overview of the main results obtained in the present study. (A) Age-dependent lipid changes observed in mice of both sexes. (B) Age-dependent changes in nervonic acid (24:1) and nervonic acid-containing sphingolipids found in both male (blue) and female (pink) mice. Symbols: =, no change; ↑, ↑↑, ↑↑↑, increases of varying magnitude.

Previous studies have documented alterations in ceramide profile in mouse cortex (Cutler, Kelly et al. 2004) and rat hippocampus (Costantini, Weindruch et al. 2005; Babenko and Semenova 2010; Babenko and Shakhova 2014) at ages varying from 6 to 32 months. Furthermore, abnormally high levels of ceramides (d18:1/18:0), (d18:1/22:0), (d18:1/24:0) and (d18:1/24:1) have been reported in the mid-frontal cortex (Cutler, Kelly et al. 2004), white matter (Han, D et al. 2002) and plasma of persons with AD (Mielke, Haughey et al. 2010).

Previous work from our laboratory has shown that the levels of non-esterified nervonic acid are substantially elevated in mid-frontal cortex, temporal cortex and hippocampus of AD patients, compared to age- and sex-matched control subjects (Astarita, Jung et al. 2011). Importantly, these increases were shown to be strongly correlated with cognitive impairment and to be accompanied by parallel changes in the transcription of *SCD1*, *SCD5a* and *SCD5b*, three *SCD* isoforms that are predominantly expressed in the human brain (Astarita, Jung et al. 2011). Furthermore, increases in SCD activity and SCD1 expression in human frontal cortex during normal aging were reported by McNamara et al. (McNamara, Liu et al. 2008).

Human studies have demonstrated a critical role for SCD in the development of obesity and metabolic syndrome, including insulin resistance, hyperlipidemia and abdominal adiposity (Corpeleijn, Feskens et al. 2006; Mar-Heyming, Miyazaki et al. 2008; Paillard, Catheline et al. 2008). Experiments with genetically modified mice have provided mechanistic support to these observations: *Scd1*-deficient mice are lean and protected from diet-induced obesity (Miyazaki, Kim et al. 2001; Ntambi, Miyazaki et al. 2002; Jiang, Li et al. 2005) and have increased insulin sensitivity in skeletal muscle, brown adipose tissue, liver and heart (Rahman, Dobrzyn et al. 2003; Rahman, Dobrzyn et al. 2005; Gutierrez-Juarez, Pocai et al. 2006; Flowers, Rabaglia et al. 2007; Dobrzyn, Sampath et al. 2008). Because of these findings, SCD has emerged as a potential target for the treatment of metabolic syndrome (Cohen, Ntambi et al. 2003; Dobrzyn and Ntambi 2005). Furthermore, nervonic acid content in human serum was found to be associated with metabolic syndrome and peroxisomal dysfunction, whose frequency is increased by aging (Yamazaki, Kondo et al. 2014). The present results support a role for nervonic acid in normal brain aging and point to a possible connection between this lipid and age-dependent neurodegeneration.

A number of studies have documented the occurrence of sphingolipid alterations in neurodegenerative disorders. Mielke and co-workers (Mielke, Bandaru et al. 2015) have found that the plasma concentrations of dihydroceramides (d18:0/20:0) and (d18:0/24:0) are elevated in men and women aged 55 years and older, compared to younger men and women. Moreover, transcriptional upregulation of enzymes that control *de novo* ceramide biosynthesis (*LASS1* and *LASS2*) was reported in brain areas of subjects at the earliest stage of AD or with varying severity of AD and dementia (Katsel, Li et al. 2007). Together with our results, these data suggest a potential involvement of *de novo* ceramide biosynthesis in aging and age-related disorders. Ceramides can be produced from the breakdown of sphingomyelins and hexosylceramides (Fig. 1). Very-long chain sphingomyelin (d42:1) increases in the brain of 6 month-old male mice compared to 3 and 25 month-old animals (Cutler, Kelly et al. 2004). Hexosylceramides, which include glucosyl- and galactosylceramides, have been implicated in neurodegenerative diseases. For example, plasma hexosylceramides (d18:1/18:1) and (d18:1/24:1) were found to be elevated in people affected by dementia with Lewy Bodies (DLB) and AD (Savica, Murray et al. 2016). Hexosylceramides were also shown to be abnormally high in PD patients and to be highest among those patients who displayed cognitive impairment (Mielke, Maetzler et al. 2013).

The observed age-associated changes in sphingolipid levels may occur in one or more of the multiple cell types present in the hippocampus. One limitation of the present study is that the specific cell populations in which such changes take place were not identified. This would be technically very challenging since the analysis of lipids in individual neuronal types is still in its infancy (Merrill, Basit et al. 2017). Thus, we cannot exclude the possibility that the changes reported here may reflect subtle modifications in the cytology of the aging hippocampus, which have been reported by some studies (Ball 1977; Landfield, Rose et al. 1977; Landfield, Braun et al. 1981; Nichols, Day et al. 1993; Ogura, Ogawa et al. 1994; West, Coleman et al. 1994; Di Stefano, Casoli et al. 2001; Cerbai, Lana et al. 2012; Yamada and Jinno 2014) but not others (Geinisman, Bondareff et al. 1977; Morrison and Hof 1997; Peters, Morrison et al. 1998; Hof and Morrison 2004; Hattiangady and Shetty 2008). For example, despite reductions in cortical thickness, unbiased stereological assessment revealed that overall neuronal numbers in the human brain decline <10% over the age range of 20–90 years (Pakkenberg,

Pelvig et al. 2003). While the hilar region of hippocampus appears to undergo mild age-related neuron loss, other hippocampal subregions show increased dendritic and synaptic complexity with increasing age (Flood, Buell et al. 1987; Flood, Guarnaccia et al. 1987). Our data illustrate the rich and significant sphingolipid alterations that occur in the hippocampus across the lifespan. However, the cell types to which these changes are localized are unknown at present and future studies are needed to address whether cytological alterations correlate with sphingolipids changes.

2.5 Conclusions

A substantial body of prior work has documented a role for sphingolipids in aging and age-related disorders. A new and significant result of the present report is that nervonic acid-containing sphingolipids accumulate in the aging hippocampus of both male and female mice. Because of the previously described association between nervonic acid levels and cognitive impairment in AD (Astarita, Jung et al. 2011), it will be important to examine the possible functional roles of nervonic acid-containing sphingolipids in the development of age-related neurodegeneration.

Chapter 3

Elevated plasma ceramide levels in post-menopausal women

-

3.1 Introduction

Ceramides are lipid-derived molecules that play both structural and functional roles in mammalian cells. In addition to contributing to the biophysical properties of membranes (van Blitterswijk, van der Luit et al. 2003; Castro, Prieto et al. 2014), these lipids also regulate the localization and oligomerization of membrane-associated proteins, including hormone and neurotransmitter receptors (Salem, Litman et al. 2001; Hering, Lin et al. 2003; Grassme, Riethmuller et al. 2007; Schneider, Levant et al. 2017). Moreover, ceramides are thought to participate in many intracellular and transcellular signaling processes, including regulation of cell survival (Garcia-Barros, Coant et al. 2016), growth and proliferation (Saddoughi and Ogretmen 2013), differentiation (Bieberich 2012), senescence (Venable and Yin 2009) and apoptosis (Satoi, Tomimoto et al. 2005; Maeng, Song et al. 2017). It has been suggested that dysfunctions in ceramide-mediated signaling may contribute to the initiation and progression of a variety of disease states, including atherosclerosis (Edsfeldt, Duner et al. 2016), depression (Gracia-Garcia, Rao et al. 2011; Dinoff, Herrmann et al. 2017) and Alzheimer's disease (AD) (Jazvinscak Jembrek, Hof et al. 2015). Human studies have demonstrated the existence of an association between plasma levels of ceramides and proinflammatory cytokines in persons with cardiovascular disease (de Mello, Lankinen et al. 2009), obesity (Majumdar and Mastrandrea 2012) and type-2 diabetes (Haus, Kashyap et al. 2009). Similarly, elevated serum levels of long-chain ceramides – including ceramides (d18:1/18:0), (d18:1/22:0), (d18:1/24:0) and (d18:1/24:1) – have been associated with increased risk of memory impairment (Mielke, Bandaru et al. 2010) and may be predictive of cognitive decline and hippocampal volume loss in persons with mild cognitive impairment (MCI) (Mielke, Haughey et al. 2010). Importantly, abnormal plasma ceramide levels may not only be associated with cognitive disturbances and MCI progression (Ewers, Mielke et al. 2010; Mielke, Haughey et al. 2010), but also with other age-related pathologies such as obesity (Hojjati, Li et al. 2005; Samad, Hester et al. 2006; Chaurasia and Summers 2015), type-2 diabetes (Summers 2006; Chavez and Summers 2012; Jiang, Hsu et al. 2013) and atherosclerosis (Ichi, Nakahara et al. 2006).

While many previous studies have documented changes in plasma ceramide levels in human pathological states, there is still limited information about how age influences such levels in healthy people. In the present study, we have begun to address this question by profiling six ceramide and dihydroceramide species in plasma of 164 healthy men and women between 19 and 80 years of age. Our results suggest that plasma ceramide levels are lower in pre-menopausal women than they are in men of the same age group. Importantly, this difference between women and men disappears after menopause, when plasma ceramide levels become approximately equal in the two sexes. We also found that in women, but not in men, circulating levels of the long-chain ceramide (d18:1/24:1) - which was previously implicated in increased risk of memory impairment, AD development (Mielke, Bandaru et al. 2010) and type-2 diabetes (Haus, Kashyap et al. 2009) - are negatively correlated with circulating estradiol levels, which is suggestive of a modulatory control by estradiol on ceramide mobilization.

3.2 Materials and Methods

3.2.1 Study subjects

We recruited 164 healthy Italian subjects (84 female, 80 male) from 19 to 80 years of age (Table 1). There were no significant differences between male and female subjects with respect to age, education and cognitive status, as assessed by the Mini-Mental State Examination (MMSE). Exclusion criteria were: (i) suspicion of cognitive impairment or dementia based on MMSE (Folstein, Folstein et al. 1975) (score ≤ 26, consistent with normative data collected in the Italian population) and confirmed by a detailed neuropsychological evaluation using the Mental Deterioration Battery (MDB) (Carlesimo, Caltagirone et al. 1996) and clinical criteria for Alzheimer's dementia (McKhann, Knopman et al. 2011) or MCI (Petersen and Morris 2005); (ii) subjective complaints of memory difficulties or other cognitive deficits, regardless of whether or not these interfered with daily life; (iii) vision and hearing loss that could potentially influence testing results; (iv) major medical illnesses (i.e., unstable diabetes; obesity; obstructive pulmonary disease or asthma; hematological and oncological disorders; pernicious anemia; significant gastrointestinal, renal, hepatic, endocrine, or cardiovascular system diseases; recently treated hypothyroidism); (v) current or reported psychiatric disease, as assessed by the Structured Clinical Interview for Diagnostic and Statistical Manual of Mental Disorders, 4th Edition, Text Revision (DSM-IV-TR SCID) (First and Pincus 2002) or neurological disease, as assessed by clinical evaluation; (vi) known or suspected history of alcoholism or drug addiction; (vii) brain abnormalities or vascular lesions revealed by conventional FLAIR-scans; in particular, presence, severity, and location of vascular lesions were determined using a recently published semi-automated method (Iorio, Spalletta et al. 2013).

Menopausal status was prospectively assessed during clinical interviews. Women were defined as post-menopausal after 12 consecutive months of amenorrhea, for which there was no other obvious pathological or physiological cause (1996). Blood collection was approved and undertaken in accordance with the guidelines of the Santa Lucia Foundation Ethics Committee. A written consent form was signed by all participants after they received a full explanation of the study procedures.

Characteristic	Whole sample (n=164)	Men (n=80)	Women (n=84)	t	p-value
Age	49.3 ±16.6 (range 19-80)	49.6±16.8 (range 19-80)	49±16.6 (range 20-78)	0.73	0.46
Education (years)	14.4±3.8 (range 5-25)	14.6±4 (range 5-25)	14.2±3.7 (range 5-24)	0.19	0.85
MMSE	29.4±1 (range 26-30)	29.4±1 (range 26-30)	29.4±1 (range 26-30)	-0.18	0.82

Table 1. Sociodemographic and clinical characteristics of healthy men and women subjects. Data are expressed as mean ± SD. Differences between groups are considered statistically significant at $p < 0.05$; unpaired Student's *t*-test. MMSE: Mini Mental State Examination. MMSE was corrected for age and education levels of the subjects.

3.2.2 Chemicals

Ceramide standards such as ceramide (d18:1/16:0), ceramide (d18:1/17:0), ceramide (d18:1/18:0), ceramide (d18:1/24:0), ceramide (d18:1/24:1(15Z)), dihydroceramide (d18:0/24:0) and dihydroceramide (d18:0/24:1) were from Avanti Polar Lipids (Alabaster, AL, USA). LC-MS grade solvents as acetonitrile, isopropanol, water, methanol and chloroform were purchased from Sigma Aldrich (Milan, Italy). The formic acid and estradiol were also purchased from Sigma Aldrich (Milan, Italy).

3.2.3 Blood collection

Blood was drawn by venipuncture in the morning after an overnight fast, and collected into 10-ml tubes containing spray-coated EDTA (EDTA Vacutainer, BD Biosciences, San Diego, CA, USA). Plasma was obtained by blood centrifugation at 400 × *g* at 4 °C for 15 min. The plasma divided into aliquots was stored at −80 °C until analyses.

3.2.4 Lipid extraction

Lipids were extracted using a modified Bligh and Dyer method (Basit, Piomelli et al. 2015). Briefly, plasma samples (50 µL) or cell pellets were transferred to glass vials and liquid-liquid extraction was carried out using 2 mL of a methanol/chloroform mixture (2:1 vol/vol) containing the odd-chain saturated ceramide (d18:1/17:0) as an internal standard. After mixing for 30 s, lipids were extracted with chloroform (0.5 mL) and extracts were washed with liquid chromatography (LC)-grade water (0.5 mL), mixing after each addition. The samples were centrifuged for 15 min at 3500 x *g* at room temperature. After centrifugation, the organic phases were collected and transferred to a new set of glass vials. To increase overall recovery, the aqueous fractions were extracted again with chloroform (1 mL). The two organic phases were pooled, dried under a stream of N_2 and residues were dissolved in methanol/chloroform (9:1 vol/vol, 0.07 mL). After mixing (30 s) and centrifugation (10 min, 5000 x *g*, room temperature) the samples were transferred to glass vials for analyses.

3.2.5 Ceramide quantification

Ceramides were analyzed by liquid chromatography/mass spectrometry (LC/MS) using an Acquity® UPLC system coupled to a Xevo triple quadrupole mass spectrometer (TQ-MS) interfaced with electrospray ionization (ESI) (Waters, Milford, MA), as previously described (Basit, Piomelli et al. 2015). Lipids were separated on a Waters Acquity® BEH C18 column (2.1 × 50 mm, 1.7 µm particle size) at 60 °C and eluted at a flow rate of 0.4 mL/min. The mobile phase consisted of 0.1% formic acid in acetonitrile/water (20:80 vol/vol) as solvent A and 0.1% formic acid in acetonitrile/isopropanol (20:80 vol/vol) as solvent B. A gradient program was used: 0.0–1.0 min 30% B, 1.0–2.5 min 30 to 70% B, 2.5–4.0 min 70 to 80% B, 4.0–5.0 min 80% B, 5.0–6.5 min 80 to 90% B, and 6.6–7.5 min 100% B. The column was reconditioned to 30% B for 1.4 min. The injection volume was 3 µL. Detection was done in the positive ESI mode. Capillary voltage was 3.5 kV and cone voltage was 25 V. The source and desolvation temperatures were set at 120 °C and 600 °C respectively. Desolvation gas and cone gas (N_2) flow were 800 L/h and 20 L/h, respectively. Plasma and cell-derived ceramides were identified by comparison of their LC retention times and MS/MS fragmentation patterns with those of authentic standards.

Extracted ion chromatograms were used to identify and quantify the following ceramides and dihydroceramides (d18:1/16:0) (*m/z* 520.3 > 264.3), (d18:1/18:0) (*m/z* = 548.3 > 264.3), (d18:1/24:0) (*m/z* = 632.3 > 264.3), (d18:1/24:1) (*m/z* = 630.3 > 264.3), (d18:0/24:0) (*m/z* = 652.5 > 634.5) and (d18:0/24:1) (*m/z* = 650.5 > 632.5). Data were acquired by the MassLynx software and quantified using the TargetLynx software (Waters).

3.2.6 Estradiol quantification

Plasma 17-β-estradiol (E2) levels were quantified using a competitive binding immunoassay kit (Human E2 ELISA kit, Invitrogen, Italy) following manufacturer's instructions. Briefly, plasma samples, controls and standard curve samples (50 µL) were incubated with E2-horseradish peroxidase conjugate (50 µL) and anti-estradiol antibody (50 µL) in a 96-well plate for 2h, at room temperature, on a shaker set at 700 ± 100 rpm. Washing was carried out by completely aspirating the liquid, filling the wells with diluted wash buffer (0.4 mL) provided in the kit and then aspirating again. After repeating this procedure 4 times, chromogen solution (200 µL) was added to each well; reactions were run for 15 min and stopped adding 50 µL of the stop solution provided in the kit. Absorbance was measured at 450 nm and estradiol concentrations were calculated by interpolation from the reference curve.

3.2.7 Cell cultures and treatment

The MCF7 human breast cancer cell line was a kind gift of Dr. Gennaro Colella (Mario Negri Institute, Milan, Italy). Cells were cultured in Dulbecco's Modified Eagle's Medium (DMEM) supplemented with L-glutamine (2 mM), fetal bovine serum (10%) and penicillin/streptomycin (100 µg/mL), in a humidified atmosphere (5% CO_2, 37 °C). Cells were seeded in 6-well plates (3 x 10^5 cells/well) and cultured for 24 h. Estradiol was dissolved in DMSO and diluted in DMEM to a final concentration of 10 nM (0.1% final DMSO concentration). After 24 h incubation, the media were removed, cells were washed with phosphate-buffered saline, scraped and centrifuged (800 x *g*, 4 °C, 10 min). Protein concentrations were measured using the bicinchoninic acid assay (Pierce, Rockford, IL, USA) and cell pellets were stored at -80 °C until analyses.

3.2.8 Statistical analyses

Results are expressed as mean ± SEM (standard error of the mean). Data were analyzed by unpaired Student's *t*-test or 2-way ANOVA followed by Bonferroni post-hoc test. Pearson's correlation coefficient was calculated to evaluate pairwise correlation between estradiol and ceramide levels. Significant outliers were excluded using the Grubbs' test. Differences between groups were considered statistically significant at values of $p < 0.05$. The GraphPad Prism software (GraphPad Software, Inc., USA) was used for statistical analyses.

3.3 Results

3.3.1 Association between menopause and plasma ceramide levels in healthy women

We recruited 164 healthy subjects (84 female, 80 male) aged 19 to 80 years. Their demographic and clinical information are provided in Table 1. Exclusion parameters are described under Materials and Methods. There were no significant differences between men and women with regard to age, education and cognitive status. A single blood draw was made in fasting subjects, and ceramides were identified and quantified by LC-MS/MS in lipid extracts of plasma samples, using a previously described method (Basit, Piomelli et al. 2015). The following panel of ceramide and dihydroceramide species was monitored: ceramides (d18:1/16:0), (d18:1/18:0), (d18:1/24:0) and (d18:1/24:1); dihydroceramides (d18:0/24:0) and (d18:0/24:1). Pearson's analysis of the data revealed a statistically significant positive correlation between total ceramide levels and age ($r = 0.378$; $p = 0.0004$). Because the largest accrual in plasma ceramides occurred between the age of 40 and 50 years, which is coincident with menopause, in a secondary analysis we grouped the data according to the subjects' menopausal status. This analysis revealed a statistically detectable difference between pre-menopausal (20-54 years) and post-menopausal (47-78 years) women (Fig. 1B). In particular, the levels of long-chain ceramide (d18:1/18:0), very long-chain ceramides (d18:1/24:0) and (d18:1/24:1), and dihydroceramide (d18:0/24:1) were higher in post-menopausal relative to pre-menopausal women (Fig. 1B). The levels of ceramide (d18:1/16:0) and dihydroceramide (d18:0/24:0) were unchanged.

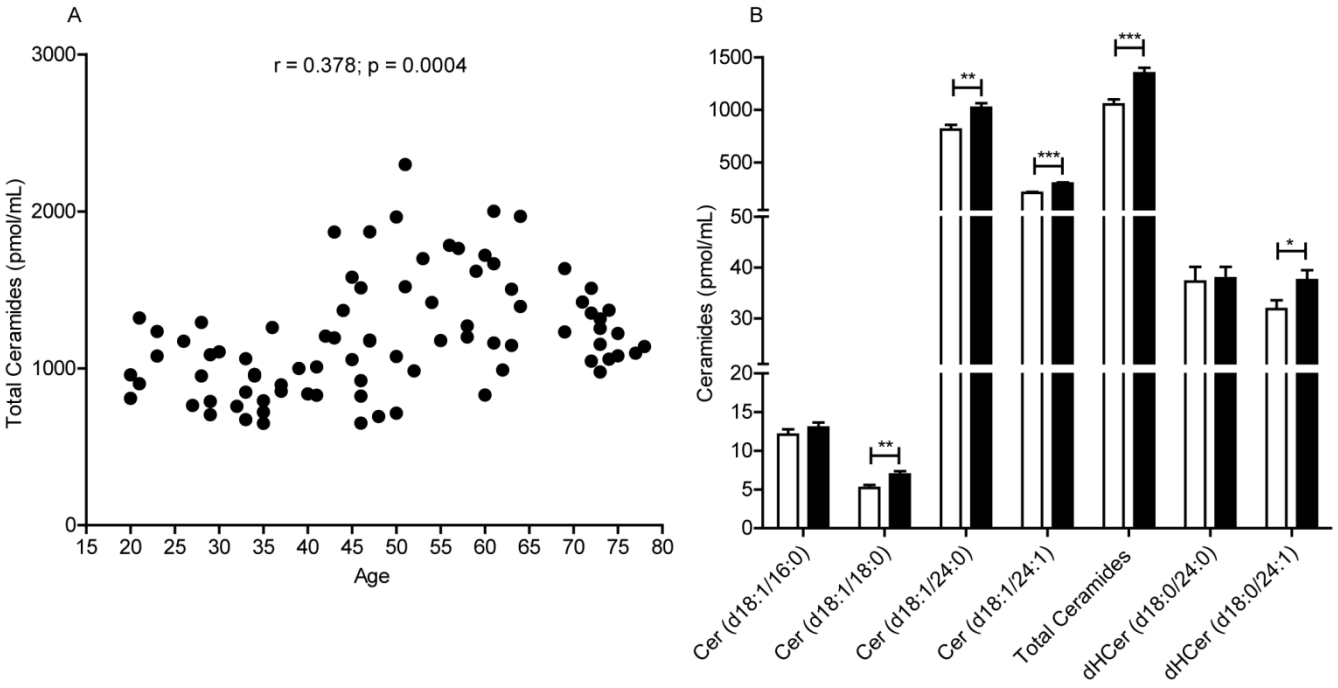

Fig. 1. Scatter plot of plasma ceramide concentrations in women aged 20 to 78 years. (A) Total ceramide levels in 84 female subjects included in the study. Pearson's correlation is considered statistically significant at $p < 0.05$. (B) Average levels of individual ceramide (Cer) and dihydroceramide (dHCer) species in pre-menopausal women (20-54 years, n = 44, open bars) and post-menopausal women (47-78 years, n = 40, closed bars). Results are expressed as mean ± SEM. *$p < 0.05$, **$p < 0.01$, ***$p < 0.001$; unpaired Student's *t*-test.

In contrast with these findings in women, no time-dependent changes in plasma ceramide levels were noticeable in men (Fig. 2A). Male subjects in the age groups 19-54 and 55-80 displayed similar levels of plasma ceramides (d18:1/18:0), (d18:1/24:0) and (d18:1/24:1) and dihydroceramides (d18:0/24:1). Noteworthy, however, levels of dihydroceramide (d18:0/24:0) were significantly lower in men >55 years, compared to younger men (Fig. 2B).

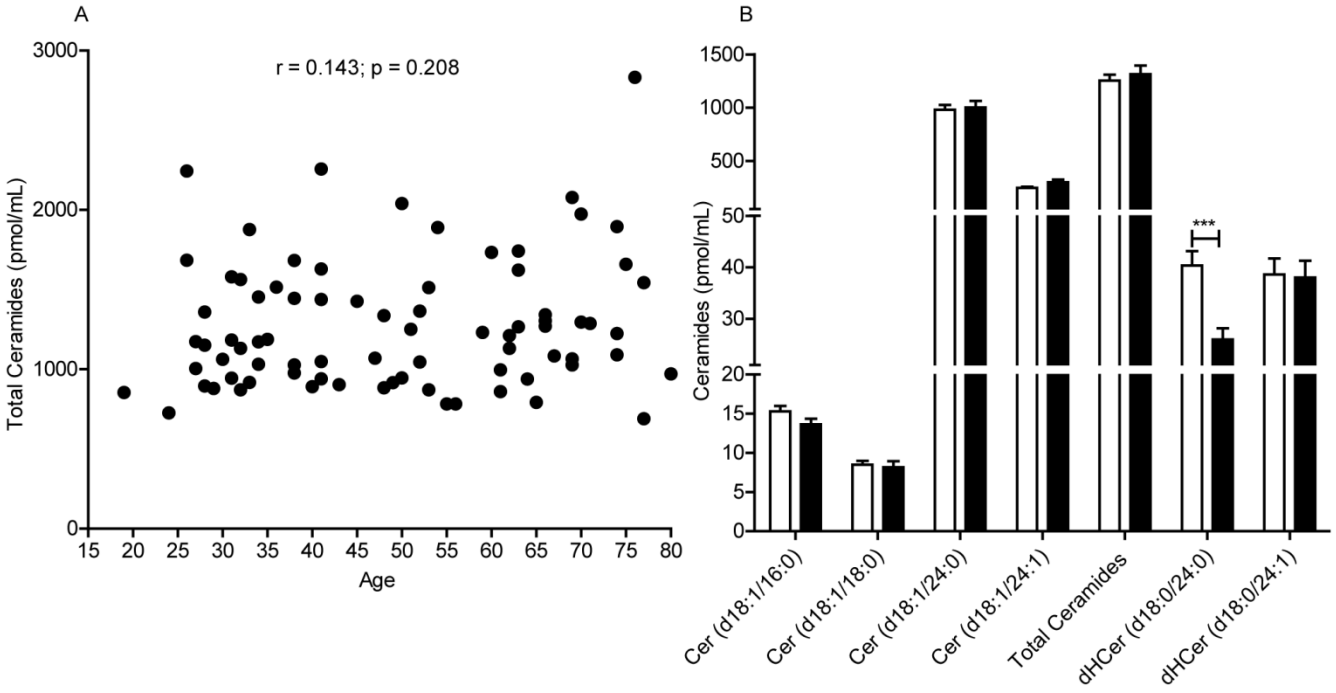

Fig. 2. . Scatter plot of plasma ceramide concentrations in men aged 19 to 80 years. (A) Total ceramide levels in 80 male subjects included in the study. Pearson's correlation is considered statistically significant at $p < 0.05$. (B) Average levels of individual ceramide (Cer) and dihydroceramide (dHCer) species in men aged 19-54 years (n = 48, open bars) and 55-80 years (n = 32, closed bars). Results are expressed as mean ± SEM. *p < 0.05, **p < 0.01, ***p < 0.001; unpaired Student's *t*-test.

In an additional analysis, we compared total ceramide levels in plasma of pre- and post-menopausal women with those observed in age-matched men (Fig. 3). The data show that pre-menopausal women have significantly lower levels of circulating ceramides, relative to men of the same age (Fig. 3A). This difference disappeared, however, following menopause (Fig. 3A).

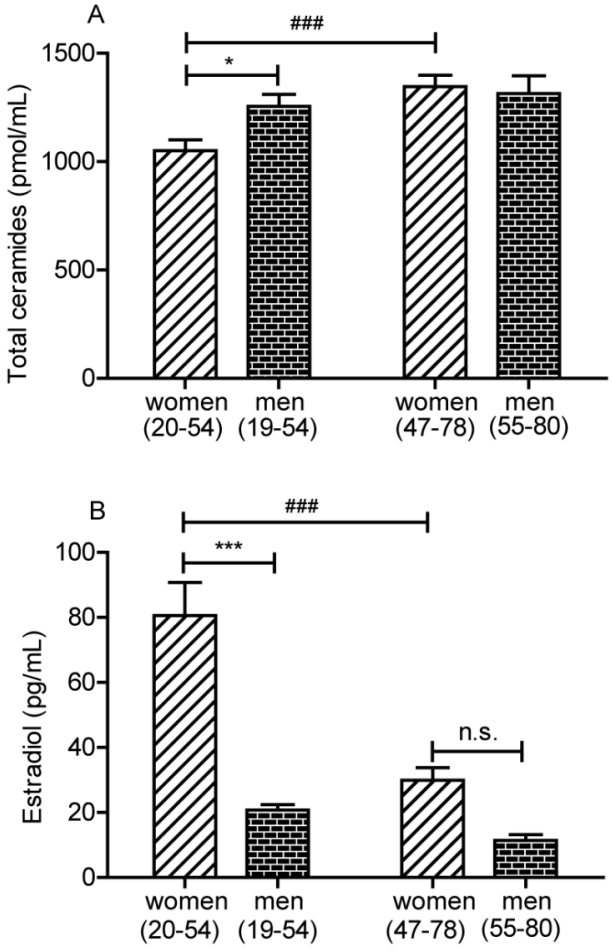

Fig. 3. Plasma ceramide and estradiol concentrations in men and women. (A) Plasma ceramide levels in, left, pre-menopausal women (20-54 years, n = 44) and age-matched men (19-54 years, n = 48) and, right, post-menopausal women (47-78 years, n = 40) and age-matched men (55-80 years, n = 32). (B) Plasma estradiol levels in, left, pre-menopausal women (20-54 years, n = 44) and age-matched men (19-54 years, n = 48) and, right, post-menopausal women (47-78 years, n = 40) and age-matched men (55-80 years, n = 32). Results are expressed as mean ± SEM. *p < 0.05, **p < 0.01, ***p < 0.001; 2-way ANOVA followed by Bonferroni post-hoc test (women 20-54 years versus men 19-54 years). # p < 0.05, ## p < 0.01, ### p < 0.001; 2-way ANOVA followed by Bonferroni post-hoc test (women 20-54 years versus women 47-78 years)

3.3.2 Plasma ceramide levels are negatively correlated with estradiol in women, but not in men

To determine whether changes in circulating estradiol might account for the observed age-dependent alterations in plasma ceramides, we quantified estradiol in pre- and post-menopausal women and age-matched men using a competitive binding immunoassay. As expected, levels of estradiol were higher in pre-menopausal women (<55 years) than in men of the same age group (Fig. 3B). After menopause, estradiol levels sharply

decreased in both sexes (Fig 3B). Next, we explored the occurrence of a possible functional interaction between estradiol and ceramide. In women of all ages, Pearson's statistical analyses revealed a significant negative correlation between the levels of estradiol and those of ceramide (d18:1/24:1) ($p = 0.007$ and $r = -0.294$), a non-significant negative trend between estradiol and ceramide (d18:1/24:0) ($p = 0.066$ and $r = -0.202$) and no correlation between estradiol and other ceramide species (Fig. 4).

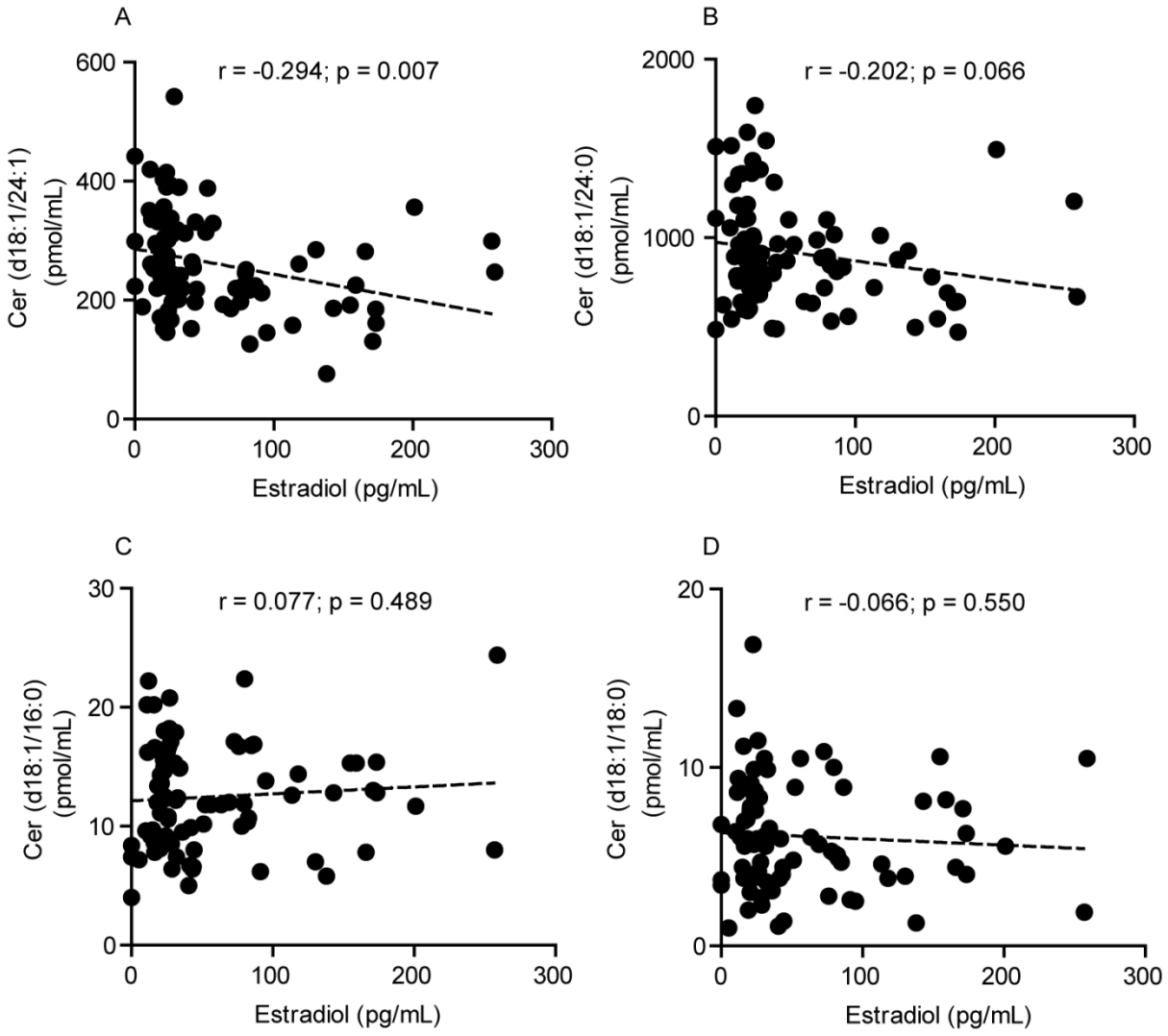

Fig. 4. Pearson's correlation analysis between estradiol and levels of various ceramide (Cer) species in plasma from 84 healthy women aged 20 to 78 years. (A) Ceramide (d18:1/24:1); (B) Ceramide (d18:1/24:0); (C) Ceramide (d18:1/16:0); (D) Ceramide (d18:1/18:0). Correlation is considered statistically significant at $p < 0.05$.

Notably, no correlation was found between estradiol and any ceramide species in male subjects (Fig. 5). These findings point to the existence of a gender-specific association between plasma levels of estradiol and ceramides in healthy female, but not male subjects.

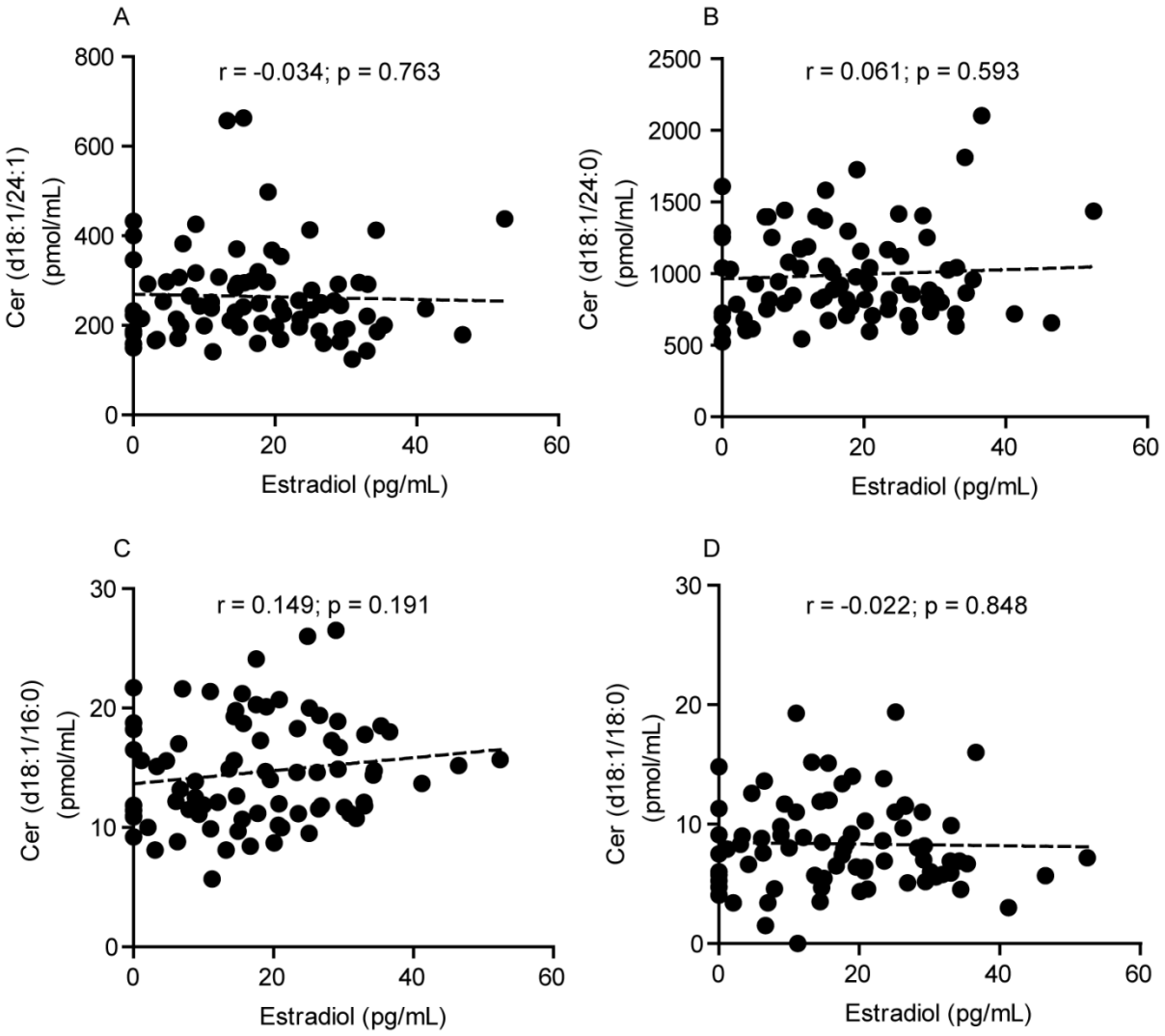

Fig. 5. Pearson's correlation analysis between estradiol and level of various ceramide (Cer) species in plasma from 80 healthy men aged 19 to 80 years. (A) Ceramide (d18:1/24:1); (B) Ceramide (d18:1/24:0); (C) Ceramide (d18:1/16:0); (D) Ceramide (d18:1/18:0). Correlation is considered statistically significant at $p < 0.05$.

3.3.3 Estradiol suppresses ceramide accumulation in vitro

Sphingolipid-derived mediators regulate steroidogenesis (Lucki and Sewer 2010), but it is still unknown whether estradiol receptor activation influences sphingolipid metabolism. To gain insights into the functional link between plasma levels of estradiol and ceramides in healthy women, we evaluated whether exposure to estradiol might alter ceramide accumulation in human MCF7 breast cancer cells, which express high levels of estrogen receptor α (ERα) and β (ERβ) (Brooks, Locke et al. 1973; Simstein, Burow et al. 2003). The cells were treated with estradiol (10 nM) for 24 h and cellular ceramide levels were measured by LC-MS/MS. The results indicate that exposure to estradiol causes a substantial reduction in ceramides (d18:1/16:0), (d18:1/24:0) and (d18:1/24:1) (Table 2), which is suggestive of a modulatory role for estradiol on ceramide formation and/or degradation.

	Vehicle	**17-β-estradiol**	**p-value**
Ceramide (d18:1/16:0)	57.4 ± 6.2	41.8 ± 0.8	0.02
Ceramide (d18:1/18:0)	16.9 ± 1,3	13.3 ± 1,6	0.12
Ceramide (d18:1/24:0)	209.4 ± 14.1	134.6 ± 7.4	0.0002
Ceramide (d18:1/24:1)	265.6 ± 13.4	184.6 ± 12.6	0.0006
Total Ceramides	148.3 ± 18.6	98.2 ± 12.6	0.03

Table 2. Effects of estradiol on ceramide levels in MCF7 human breast cancer cells. Cells were treated for 24 h with vehicle (0.1% DMSO in DMEM) or estradiol (10 nM in DMEM) and ceramide levels (pmol/mg protein) were measured by LC-MS/MS. Results are expressed as mean ± SEM of three independent experiments. Differences between groups are considered statistically significant at $p < 0.05$; unpaired Student's *t*-test.

3.4 Discussion

In the present study, we investigated potential age- and gender-dependent alterations in plasma ceramide levels of healthy subjects aged between 19 and 80 years. LC-MS/MS based analyses revealed that the levels of several ceramides [(d18:1/18:0), (d18:1/24:0) and (d18:1/24:1)] as well as dihydroceramide (d18:0/24:1) were elevated in post-menopausal relative to pre-menopausal women. In striking contrast, no such difference was found in age-matched men. A comparison between the circulating levels of individual ceramide species and those of estradiol revealed a significant negative correlation between ceramide (d18:1/24:1) and estradiol levels in women of all ages, but not in men. To explore the possible causal basis of such a correlation, we incubated human MCF breast cancer cells with estradiol (10 nM, 24 h) and measured ceramides by LC-MS/MS. The results show that exposure to estradiol causes a significant decrease in the content of ceramides (d18:1/18:0), (d18:1/24:0) and (d18:1/24:1). We interpret these findings to suggest that estradiol may regulate circulating ceramide levels in women.

Several human studies have reported gender-dependent differences in circulating ceramide levels. In one study on 10 Caucasian volunteers (5 males aged 27-33 years and 5 females aged 26-33 years), higher ceramide (42:1) levels were found in serum from female subjects, compared to males (Ishikawa, Tajima et al. 2013). In another study conducted on a large cohort of young Mexican Americans (1,076 individuals, 39.1% males), a strong positive correlation was demonstrated between age and plasma total ceramides. Moreover, an association between ceramides and gender was revealed after adjusting for age and body mass index (BMI): ceramide levels in young women were lower than in young men (25-49 years) (Weir, Wong et al. 2013). These disparities were mostly driven by long-chain ceramides (d18:1/22:0), (d18:1/24:0) and (d18:1/24:1). Furthermore, a multiethnic population sample of 366 women and 626 men aged 55-94 years enrolled in the Baltimore Longitudinal Study of Aging (BLSA), displayed age- and gender-dependent increases in ceramide and dihydroceramide blood levels, with stronger trajectory in women. In this study the female population (aged 55-94 years) showed higher plasma ceramide concentrations than man (Mielke, Bandaru et al. 2015).

Here we found lower total ceramide concentrations in plasma from pre-menopausal women, compared to age-matched men. However, no difference was observed between women aged 47 to 78 years and men of the same age group (55-80 years). Comparisons between different studies must take into account which demographic and clinical factors are included in the analysis, thus our partially contrasting results may be explained by the different clinical characteristics of study participants. In the selection of our subjects, we excluded variables that have been shown to affect plasma ceramide levels such as obesity (Samad, Hester et al. 2006), diabetic or pre-diabetic status (Galadari, Rahman et al. 2013), oncological disorders (Kizhakkayil, Thayyullathil et al. 2012), renal diseases (Mitsnefes, Scherer et al. 2014), and cardiovascular system diseases (Alewijnse and Peters 2008), but we maintained the menopause status as an important variable.

In their 2015 study, Mielke and collaborators did not consider menopause as a variable, but did suggest that menopause and estradiol may influence ceramide levels. Our present result confirms this prediction. Menopause is mainly linked to decreasing levels of estradiol, which acts not only as gonadal hormone, but also as neurosteroid and neuromodulator in particular in hippocampus and frontal cortex, two regions highly affected by neurodegeneration and enriched in estrogen receptors, ERα and ERβ (Almey, Milner et al. 2015). Estradiol exerts anti-inflammatory effect in the brain acting through ERα (De Marinis, Acaz-Fonseca et al. 2013; Zhang, Wang et al. 2014) and promoting the secretion of anti-inflammatory cytokines, such as interleukin (IL)-10 while preventing the production of pro-inflammatory cytokines, such as IL-1β, IL-6 and tumor necrosis factor-α (TNFα). Estradiol has neurotrophic effects in hippocampal neurons of women treated with estrogen replacement therapy and enhances neural growth of glial cells (Brinton, Chen et al. 2000; Gerstner, Sifringer et al. 2007; Saravia, Beauquis et al. 2007). In post-menopausal women, administered estradiol also improves certain cognitive functions such as verbal memory and short-term memory, possibly via modulation of the spine sprouting of hippocampal CA1 pyramidal neurons (Wolf, Kudielka et al. 1999; Shaywitz, Naftolin et al. 2003; Baker, Asthana et al. 2012; Velazquez-Zamora, Gonzalez-Tapia et al. 2012). Therefore, variations in estrogen levels may significantly affect brain functioning and might be, at least in part, behind the manifestation of the cognitive impairments often reported by post-menopausal women (Sullivan et al. 2001;

Maki et al. 2001; Kampen et al. 1994; Sherwin, 1997). Whether estrogens are able to influence sphingolipid signaling remains still unclarified, however the likelihood of developing pathologies as MCI and AD appears to be particularly strong in elderly women who show higher ceramide levels (Mielke, Haughey et al. 2010). Furthermore, post-menopausal women have also greater morbidity and mortality from cardiovascular disease (CVD), compared with pre-menopausal women: sex hormone dynamics (Karim, Hodis et al. 2008) as well as upregulation of circulating ceramides (Ichi, Nakahara et al. 2006) are related to subclinical atherosclerosis progression.

3.5 Conclusions

A weakness of the present study is that we did not investigate subtle longitudinal changes in cognitive performances or metabolic function which may have occurred in our healthy sample in relation to variation in ceramide and estrogen levels. Further studies will be needed to address this important question. Despite this limitation, here we found for the first time that post-menopausal women, who are sensible to estrogen imbalance, are much more exposed to ceramide accumulation so they may be more affected by ceramide-driven impairments.

Chapter 4

Feeding regulates sphingolipid-mediated signaling in mouse hypothalamus

4.1 Introduction

Aging is the main risk factor for the development of neurodegenerative diseases such as Alzheimer's disease (Fjell, McEvoy et al. 2014) but also chronic diseases such as metabolic syndrome, which is a cluster of pathologies as obesity, dyslipidemia, atherosclerosis, hypertension, insulin resistance and diabetes (Dominguez and Barbagallo 2016). Obesity results from an imbalance of food intake, basal metabolism and energy expenditure (Jequier 1989). Furthermore, it is widely regarded that chronic inflammation is a common link among all these age-related diseases (Guarner and Rubio-Ruiz 2015). Several studies have revealed a close relationship between nutrient excess and derangements in inflammatory mediators and this has given birth to the concept of meta-inflammation, which describes the chronic low-grade inflammatory response to obesity (Hotamisligil 2006). Importantly, obesity is not only age-related but also sex-dependent. It has been reported that males and females respond differently to obesity and related disorders, due to the influence of sex steroids (Palmer and Clegg 2015). Estrogen decline in post-menopausal women is associated with increased propensity to accumulate fat and development of obesity (Gambacciani, Ciaponi et al. 1997). Moreover, female mice gain less weight than male in response to high fat diet (HFD), a response that is lost in ovariectomized mice (Hamilton, Minze et al. 2016). At cerebral level this difference may be explained by the fact that glial cells have sexually dimorphic characteristics and responses due to the influence of sex hormones (Melcangi, Magnaghi et al. 2001; Acaz-Fonseca, Avila-Rodriguez et al. 2016). Indeed, sex steroids not only modulate glial response to HFD (Morselli, Fuente-Martin et al. 2014; Morselli, Frank et al. 2016) but they also exert neuroprotective effects in brain regions so that they could protect against the deleterious effects of HFD-induced obesity on hypothalamic control of metabolism.

The hypothalamus plays an essential role in feeding regulation (Schwartz, Woods et al. 2000) as it integrates neural, humoral and nutritional signals to control feeding, as well as it governs peripheral metabolic processes to regulate food intake and energy homeostasis. In particular, it has been demonstrated that activation of hypothalamic glial cells in response to HFD is involved in central inflammation, pointing to the important role for glia in metabolic control (Thaler, Yi et al. 2012; Buckman, Thompson et al. 2013).

Modulation of inflammatory responses in the central nervous system leads to alterations in the hypothalamic body weight-appetite-satiety set point, resulting in the initiation and development of metabolic syndrome and obesity. Furthermore, metabolic syndrome has been found to be a risk factor for neurological disorders such as stroke, depression and Alzheimer's disease (Farooqui, Farooqui et al. 2012). The molecular mechanism underlying the relationship between metabolic syndrome and neurological disorders is not fully understood. However, it is becoming increasingly evident that cellular and biochemical alterations observed in metabolic syndrome like, among others, alterations in lipid mediators, may represent a pathological bridge between age-related neurological disorders and metabolic syndrome.

A growing body of evidence indicates that sphingolipids, a major lipid class in mammalian cells, are involved in the control of feeding, energy balance, obesity and related metabolic disorders (Yang, Badeanlou et al. 2009; Bikman and Summers 2011; Choi and Snider 2015). Sphingolipids are emerging as bioactive lipids that play key roles in cellular signaling and regulatory function (Hannun and Obeid 2008) and they are involved in multiple physiological and pathological events (Bartke and Hannun 2009), in addition to their structural role in eukaryotic cells. In vivo experiments revealed that ICV infusion of C6-ceramide in rats resulted in increased ceramide (d18:1/16:0) and hypothalamic inflammation, leading to lipotoxicity and feeding-independent weight gain (Contreras, Gonzalez-Garcia et al. 2014). By contrast, inhibition of *de novo* synthesis of ceramides by myriocin, resulted in reduced food intake and body weight, suggesting that disruption of *de novo* pathway may have a beneficial effect (Yang, Badeanlou et al. 2009). Furthermore, carnitine palmitoyltransferase 1c (CPT1c, a brain-specific isoform located in the endoplasmic reticulum) is implicated in the central control of food intake and energy homeostasis, and regulates hypothalamic ceramide levels (Deng, Wang et al. 2011; Ramirez, Martins et al. 2013). Overexpression of CPT1c in the arcuate nucleus blocks the effect of leptin through the increase of ceramide levels. All these data suggest a role of ceramide metabolism in the hypothalamic control of feeding.

Since the balance between ceramide and its metabolites in hypothalamic cells may have an impact on the control of feeding, we evaluated whether the consumption of high amounts of dietary fat or an opposite condition of fasting can produce a sphingolipid imbalance in this brain region.

In the present study, we measured endogenous sphingolipids and we found that short and mid-term exposures (1-3-7-14-28 days) to a HFD affect long-chain dihydroceramide, ceramide and its metabolite sphingosine-1-phosphate (SO-1-P). 12 h fasting downregulates the *de novo* biosynthesis, which results in sphinganine and dihydroceramide reduction, due to genetic down-regulation of *Sptlc2* (gene encoding the serine palmitoyltransferase enzyme) and *Lass1* (gene encoding the Ceramide Synthase 1 enzyme). However, food deprivation does not affect ceramide levels. Similarly, also sphingosine/sphongosine-1-phosphate (SO/SO-1-P) balance is altered, as we observed an increase in SO after food deprivation and a concomitant decrease in SO-1-P. Finally, we used a potent acid ceramidase inhibitor designed and synthesized by our lab, ARN14974 (Pizzirani, Bach et al. 2015), as a pharmacological tool to investigate the possible effects of ceramide/SO/SO-1-P imbalance on food intake and feeding behavior.

4.2 Materials and methods

4.2.1 Animals

Male C57BL/6J mice (8 weeks) were purchased from Charles River Laboratories (Calco, Lecco, Italy). Upon arrival animals were acclimatized to the vivarium and kept in a temperature (22 °C) and humidity controlled environment under a 12h light/12h dark cycle (lights on at 7 a.m.). All procedures were performed in accordance with the Ethical Guidelines of the European Community Council (Directive 2010/63/EU of 22 September 2010) and accepted by the Italian Ministry of Health. All the experiments performed at the University of California Irvine met the National Institute of Health guidelines for the care and use of laboratory animals and were approved by the Institutional Animal Care and Use Committee at University of California, Irvine.

4.2.2 Diets

Mice were fed a standard diet (SD)(2.66 kcal/g, 4RF21 GLP, Mucedola s.r.l., Settimo Milanese, MI, Italy) or high fat diet (HFD) (60 kcal% as fat and 7 kcal% as sucrose, 5.24 kcal/g, D12492, Research Diets Inc., New Brunswick, NJ, USA).

4.2.3 Drugs and treatments

ARN14974 was synthesized by our lab as described by Pizzirani et al. ARN 14974 (50 pmoles) was dissolved in DMSO for intracerebroventricular injections and administered 2h before the dark phase onset.

4.2.4 Experimental design

4.2.4.1 Effects of HFD.

Mice were single housed and randomly divided into two groups: fed *ad libitum* for 1, 3, 7, 14 or 28 days with rodent standard chow (control group) or HFD. Mice body weight and energy intake were daily monitored and recorded at 9 a.m. Food intake and food spillage were determined by measuring the difference between the weight of food given and the weight of food at the end of a 24 h period and the energy intake was calculated (Ellacott, Morton et al. 2010). The day of established time points, food was removed from cages two hours before mice were killed (Figure A).

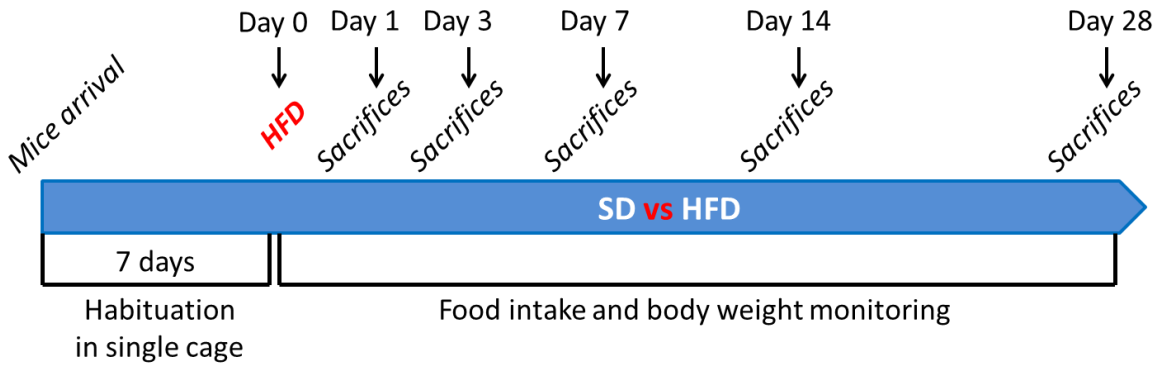

Figure A. Graphical representation of experiment workflow. Upon arrival, mice were divided into single cage and acclimatized to the vivarium for 7 days. At day 0 one cohort was assigned to the high fat diet (HFD), the other one to standard diet (SD) and body weight and food were measured. Mice were daily monitored. They were sacrificed and tissues were collected at established time points: 1 day, 3 days, 7 days, 14 days or 28 days.

4.2.4.2 Effects of food deprivation and refeeding.

Mice were single housed in bottom-wired cages to prevent coprophagia during food deprivation and randomly assigned to the following groups: free feeding (FF), 12-h food deprivation (FD), 1-h refeeding after food deprivation (RF 1h) and 6-h refeeding after food deprivation (RF 6h). Water and standard chow pellets were provided *ad libitum*, except when mice were food deprived. After 4 days of habituation to the experimental

settings, food deprivation was conducted for 12 h during the dark phase (from 7 p.m. to 7 a.m.). The refeeding group was food deprived for 12 h and then provided access to the food for 1 h or 6 h before animals were sacrificed. During refeeding the food consumed was weighted at 1 hour-intervals and energy intake was calculated (Figure B).

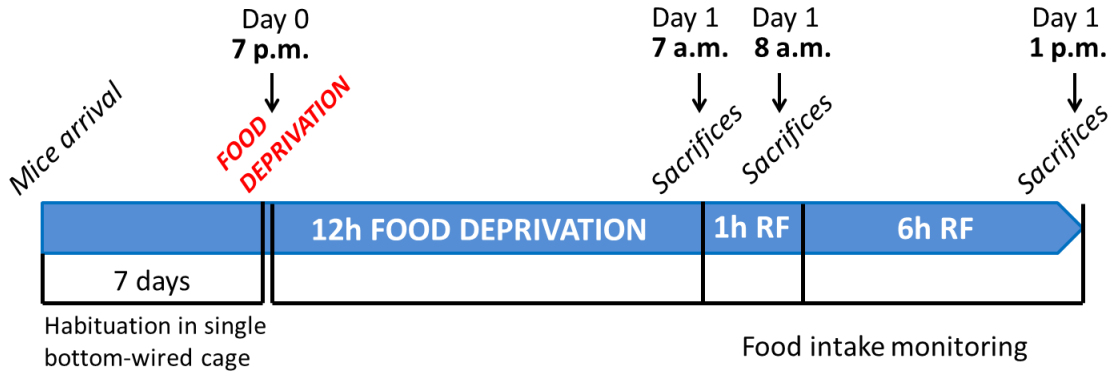

Figure B. Graphical representation of experiment workflow. Upon arrival, mice were divided into single cage and acclimatized to the vivarium for 7 days. After habituation to bottom-wired cages, one group of mice was allowed to have food *ad libitum* from 7 p.m. to 7 a.m. (free feeding, FF) and three groups were food deprived for 12 hours (7 p.m. to 7 a.m.). Of these three groups, one was sacrificed at 7 a.m. after 12 hours of fasting, the second group was re-exposed to standard diet for 1 hour before being sacrificed (re-feeding 1h, RF 1h), the third group was re-exposed to standard diet for 6 hours before being sacrificed (re-feeding 6h, RF 6h).

4.2.5 Tissues collection

Mice were anesthetized with isoflurane and sacrificed by cervical dislocation. Brain was removed, hypothalamus was dissected on an ice-cold glass plate and immediately flash frozen in liquid N_2. Samples were stored at -80 °C until analyses.

4.2.6 Lipid extraction

Lipid extractions of the samples were carried out as described by Basit et al., 2015.

4.2.7 Sphingolipid analyses

Lipid analyses were performed applying the same LC-MS/MS conditions previously described in this manuscript (Chapter 2).

Ceramides, sphingosine, sphinganine and their phosphate metabolites sphingosine-1-phosphate and sphinganine-1-phosphate were identified by comparison of their retention times and MS^n fragmentation patterns with those of authentic standards. The following MRM transitions were used for identification and quantification: sphingosine (*m/z* 300.2 > 282.2), sphingosine-1-phosphate (*m/z* 380.3 > 264.2), sphinganine (*m/z* 302.2 > 284.2), sphinganine-1-phosphate (*m/z* 382.2 > 284.2), ceramide (d18:1/18:0) (*m/z* 548.0 > 264.2), ceramide (d18:1/24:0) (*m/z* = 632.0 > 264.2); ceramide (d18:1/24:1 (15Z)) (*m/z* = 630.0 > 264.2). Dihydroceramide (d18:0/18:0) (*m/z* = 568.5 > 550.5); dihydroceramide (d18:0/24:0) (*m/z* = 652.5 > 634.5); dihydroceramide (d18:0/24:1) (*m/z* = 650.5 > 632.5).

4.2.8 mRNA isolation, cDNA synthesis and quantitative real-time PCR

qRT-PCR was performed following the protocol previously described.

The primer sequences were: sphingosine kinase 1 (*Sphk1)* forward: GCTTCTGTGAACCACTATGCTGG, reverse: ACTGAGCACAGAATAGAGCCGC; sphingosine kinase 2 (*Sphk2)* forward: GGTGCCAATGATCTCTGAAGCTG, reverse: CTCCAGACACAGTGACAATGCC; sphingosine-1-phosphate receptor 1 (*S1PR1*) forward: CGCAGTTCTGAGAAGTCTCTGG, reverse: GGATGTCACAGGTCTTCGCCTT; Serine Palmitoyltransferase Long Chain Base Subunit 2 (*Sptlc2*) forward: CCAGACTGTCAGGAGCAACCAT, reverse: CTTCTTGTCCGAGGCTGACCAT; ceramide synthase 1 (*Lass1*) forward: TCTGCTGTTGCTCCTGATGGTC, reverse: CTTGGCTGTCTGAGCTTCCAGA.

4.2.9 Microsomal protein extracts preparation

Frozen tissues were homogenized in 500 µL of resuspension buffer (HEPES 50 mM, pH 8, and EDTA 1 mM), and sonicated for 10 seconds at 50% power and 50% pulsation. Homogenates were centrifuged at 2,500 x *g* for 2 min. Supernatants were ultra-centrifuged at 46,000 rpm (MLA 130 rotor) for 30 min at 4 °C. Pellets were finally

resuspended in 500 µl of buffer (HEPES 50 mM, pH 8, and EDTA 1 mM) and protein concentrations were measured using the bicinchoninic acid protein assay (Pierce, Rockford, IL, USA).

4.2.10 Ceramide synthase 1 activity assay

Microsomal extracts (50 µg) were mixed in assay buffer (Bovine Serum Albumin (BSA)-fatty acid free 20 µM, HEPES 200 mM, pH 7.4, $MgCl_2$ 2 mM, DTT 0.5 mM, KCl 25 mM) in the presence of the substrates StearoylCoA (50 µM) and sphinganine (15 µM) to a final volume of 500 µL and incubated for 1h at 37 °C. Blank samples were added as controls (a sample without protein and a sample without substrate). Reactions were stopped by addition of a mixture of chloroform/methanol (2:1, vol/vol) containing the odd-chain ceramide (d18:1/17:0) (200 pmol/sample) as internal standard. Samples were centrifuged at 3000 rpm for 15 min at 4 °C. The organic phases were collected, dried under nitrogen and dissolved in 100 µL MeOH. LC-MS/MS analysis of samples was carried out using the method for sphingolipid measurements previously described and monitoring the reaction product dihydroceramide (d18:0/18:0).

4.2.11 SPT activity assay

Microsomal extracts (200 µg) were incubated in protein assay buffer (HEPES 50 mM at pH 8, EDTA1 mM, DTT 0.5 mM) in the presence of assay hot buffer (L-serine 0.5 mM, L-[^{3}H] serine 500 nM, palmitoyl-CoA 100 µM, pyridoxal 5'-phosphate 40 µM) for 3 hours at 37 °C. Blank samples without protein extracts or without substrates were used as negative controls. Reactions were stopped by addition of a mixture of MeOH-KOH:$CHCl_3$ = 4:1 (0.5 mL). Lipids were extracted by $CHCl_3$ (0.5 ml) and washed with alkaline water (0.5 ml). Samples were centrifuged at 12,000 x *g* for 1 minute at room temperature. The upper phase was removed and the lower phase was washed twice with 1 mL of alkaline water. 400 µl of organic phase were transferred to a polyethylene scintillation vial, dried under nitrogen and then 3 mL of scintillation liquid cocktail were added. The radioactivity incorporated in the reaction product was counted by a scintillation counter.

4.2.12 Intracerebroventricular (icv) drug infusions

Mice were anesthetized with a mixture of ketamine/xylazine (100 mg/kg and 10 mg/kg body weight, respectively) and placed in a stereotaxic frame with a mouse-adaptor. A 22-gauge guide cannula (3.1 mm in length, Plastics One) was stereotaxically implanted and positioned 1 mm above the right lateral ventricle at the following brain atlas coordinates, relative to bregma and dural surface: AP −0.2, ML −1.0, and DV −1.3 mm (Paxinos and Franklin, The Mouse Brain in Stereotaxic Coordinates). Animals were allowed to recover 10 days after surgery, during which they were single-housed and habituated to the feeding system cages. Infusions were made in wake animals through a 33-gauge infusion cannula (Plastics One) that extended 1 mm beyond the end of the guide cannula. The injector was connected to a 10-µL Hamilton syringe by PE-20 polyethylene tube. The syringe was driven by an automated pump (Harvard Apparatus) at a rate of 0.5 µL/min to provide a total infusion volume of 2 µL. Cannula placements were verified histologically.

4.2.13 Feeding behavior

Cannulated mice were transferred to individual test chambers to recover from surgery and to habituate to the new bottom-wired cages, 10 days before the test. Food intake was monitored for 24 hours as previously described (Fu, Gaetani et al. 2003; Gaetani, Oveisi et al. 2003; Schwartz, Fu et al. 2008), using an automated system (Scipro Inc., New York, NY), consisting of 24 cages equipped with baskets connected to weight sensors. The baskets contained standard chow pellets and were accessible to the animals through a hole in the wire lid of the cage. Each time food was removed from the basket the computer recorded the duration of the event, the amount of food retrieved, and the time at which the event occurred. Recorded data have been analyzed as food ingested/100g body weight/hour, and as cumulative food intake (g/100g body weight) across the test period. A detailed meal analysis has been performed adopting a minimum inter-response interval separating two meals of 10 minutes and the threshold for an eating episode was set at 0.12 g and >1 min.

Two categories of feeding parameters can be distinguished: “first meal parameters” and “average meal parameters”. The “average meal parameters” included:

- Meal size (g/100g body weight): the amount of food consumed during each meal
- Post-meal interval (min): the time interval between the end of one meal and the beginning of the next meal.
- Satiety ratio [min / (g/100g body weight)]: the ratio between post-meal interval and meal size.
- Meal frequency (meals/h): the ratio between total number of meals consumed within the trial period and trial duration.
- Eating rate [(g/100g body weight)/min]: the ratio of the average meal size and average meal duration.

4.2.14 Statistical analysis

Results are presented as mean $\pm$ SEM (standard error of the mean). Unpaired Student's *t*-test was used to compare one parameter between two groups. To compare one parameter among more than two groups one-way ANOVA followed by Tukey's multiple comparison post-hoc test was used. Two-way ANOVA followed by Bonferroni post-hoc test was used to analyze more than one factor among groups, with feeding status (standard diet or high fat diet; and re-feeding or free feeding) and time, or treatment (DMSO or ARN14974) and time as independent factors. GraphPad Prism software V5.03 (GraphPad Software, Inc., USA) was used. Differences between groups were considered statistically significant if $p < 0.05$.

4.3 Results

4.3.1 Effects of HFD on energy intake and body weight.

We were interested in the study of the effects of a fat-enriched diet on hypothalamic cerebral area at very early time points, prior to a significant weight gain, and at the time point when animals become obese (Wang and Liao 2012). As shown in Fig. 1A, mice fed an HFD exhibited a robust peak in energy intake during the first four days but without a significant increase of body weight until day 14 of HFD exposure (Fig. 1B). After 14 days, body weight differences between the two groups increased and a clear separation occurred, until became significant at day 28.

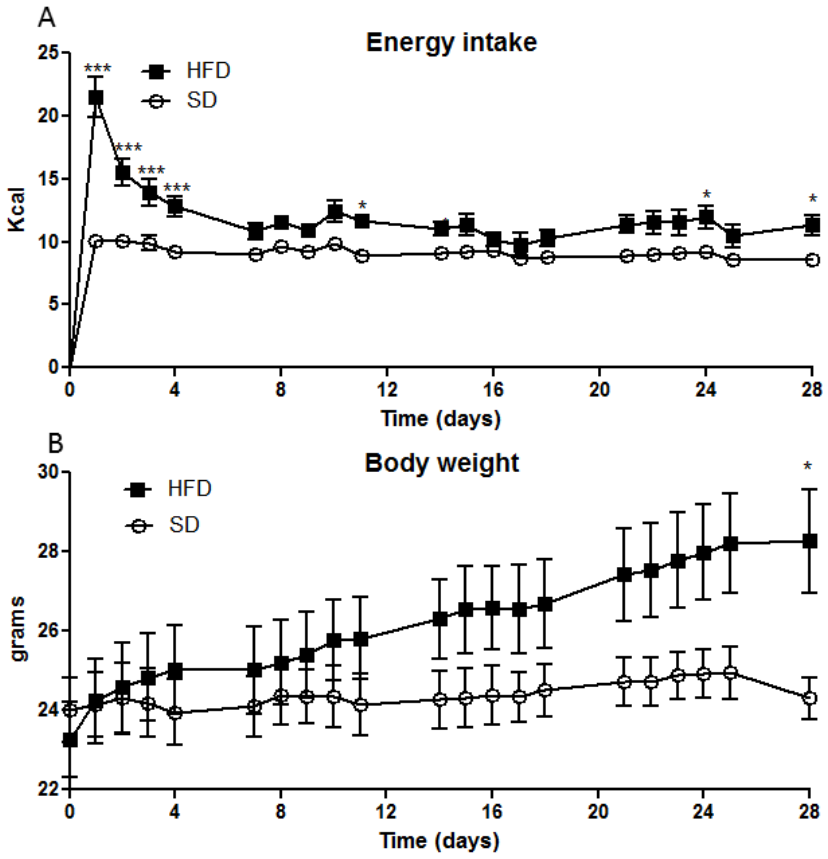

Fig. 1. (A) Energy intake and (B) body weight of mice fed standard diet (SD) or high fat diet (HFD). Results are expressed as mean ± SEM (n = 8/group). * $p < 0.05$, ** $p < 0.01$, *** $p < 0.001$; two-way ANOVA followed by Bonferroni post-hoc test.

4.3.2 Effects of HFD on hypothalamic sphingolipids.

Mice were fed a HFD *ad libitum* for 1, 3, 7, 14 or 28 days to investigate the effect of a short-term exposure to a fat-enriched diet (60% Kcal from fat). We used the LC-MS/MS based method previously developed by our lab (Basit, Piomelli et al. 2015) to characterize sphingolipid profile in tissue extracts from whole hypothalamus. As shown in Fig. 2A-C, when compared to mice fed a standard diet (SD), 1 day of exposure to HFD was sufficient to reduce levels of very long-chain ceramide (d18:1/24:0) and ceramide (d18:1/24:1), but failed to do so on the most abundant cerebral ceramide specie, (d18:1/18:0). Similar results were observed after 14 days of HFD (Fig. 2A-C). By contrast, no alterations were observed after 3, 7 or 28 days with any ceramide.

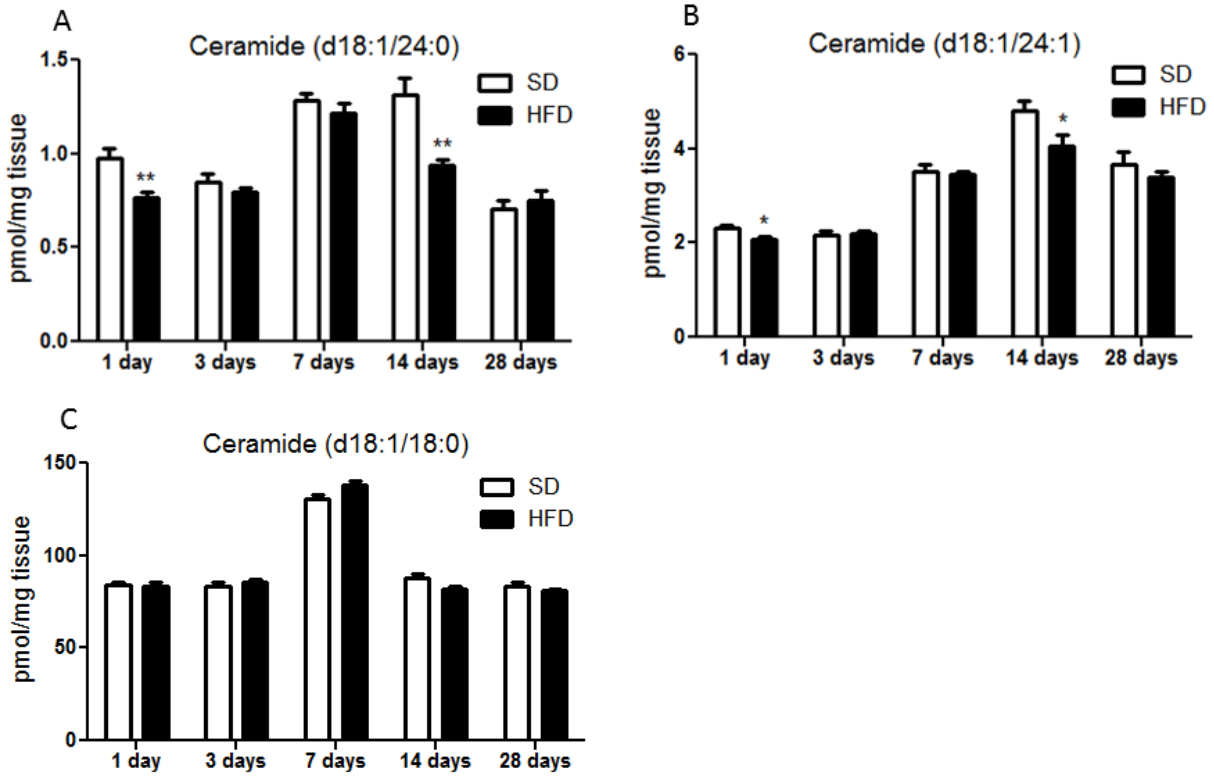

Fig. 2. Effects of standard diet (SD, white bars) and high fat diet (HFD, black bars) on (A) ceramide (d18:1/24:0), (B) ceramide (d18:1/24:1), (C) ceramide (d18:1/18:0) in hypothalamus after 1-3-7-14-28 days. Results are expressed as mean ± SEM (n = 8/group). * $p < 0.05$, ** $p < 0.01$, *** $p < 0.001$; Student's unpaired *t*-test.

To determine whether the low ceramide levels at day 1 and 14 were correlated with an impaired *de novo* biosynthesis, we quantified ceramide precursors: dihydroceramide (d18:0/24:0), dihydroceramide (d18:0/24:1) and dihydroceramide (d18:0/18:0). Dihydroceramide (d18:0/24:0) levels (Fig. 3A) decreased after 1 and 14 days of HFD exposure but, surprisingly, such changes were not detected with dihydroceramide (d18:0/24:1), which showed a slight increase at day 3 (Fig. 3B). Even though ceramide (d18:1/18:0) levels were not changed, we observed small but significant fluctuations in dihydroceramide (d18:0/18:0) after 14 and 28 days of exposure to a HFD (Fig. 3C).

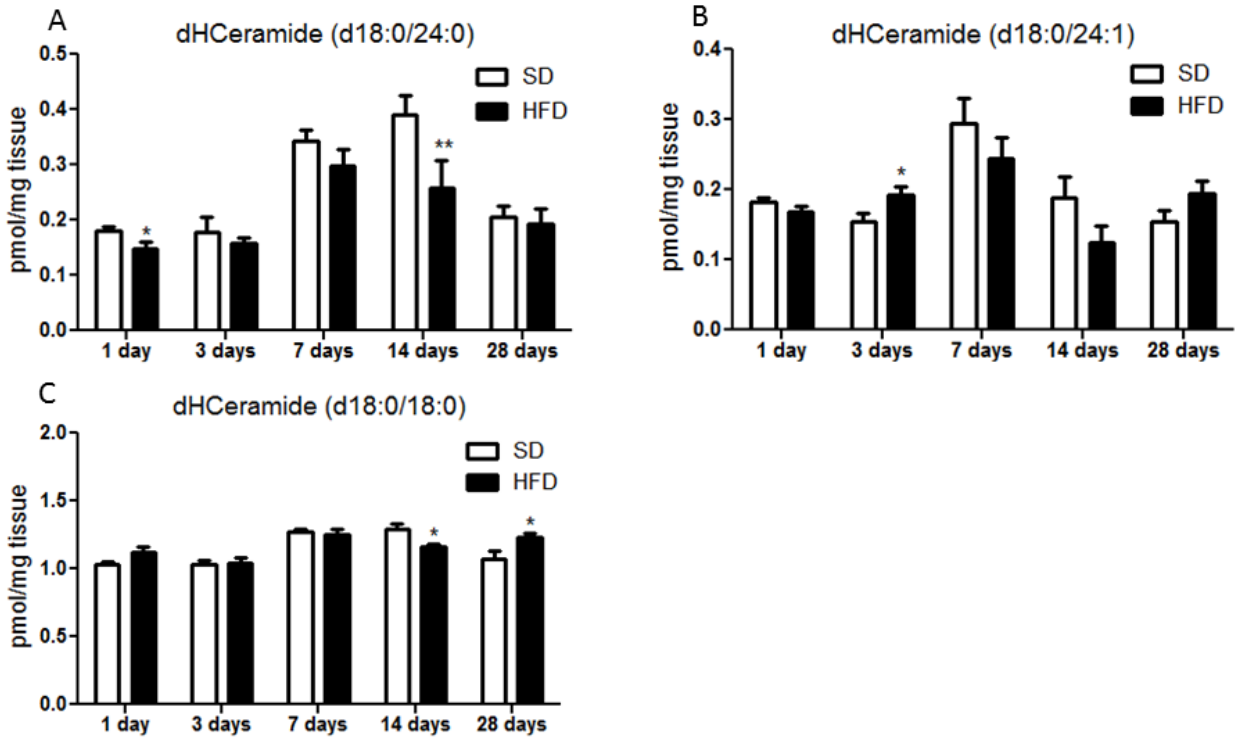

Fig. 3. Effects of standard diet (SD, white bars) and high fat diet (HFD, black bars) on dihydroceramides (dHCeramide) (A) dHCeramide (d18:0/24:0), (B) dHCeramide (d18:0/24:1) and (C) dHCeramide (d18:0/18:0) in hypothalamus after 1-3-7-14-28 days. Results are expressed as mean ± SEM (n = 8/group). * $p < 0.05$, ** $p < 0.01$, *** $p < 0.001$; Student's unpaired *t*-test.

As shown in Fig. 4A, no differences in the ceramide breakdown product SO were found in HFD-treated mice when compared to SD. By contrast, we observed a significant decrease of SO-1-P after 7 and 14 days of HFD and a similar trend, albeit not significant, after 1 and 3 days (Fig. 4B).

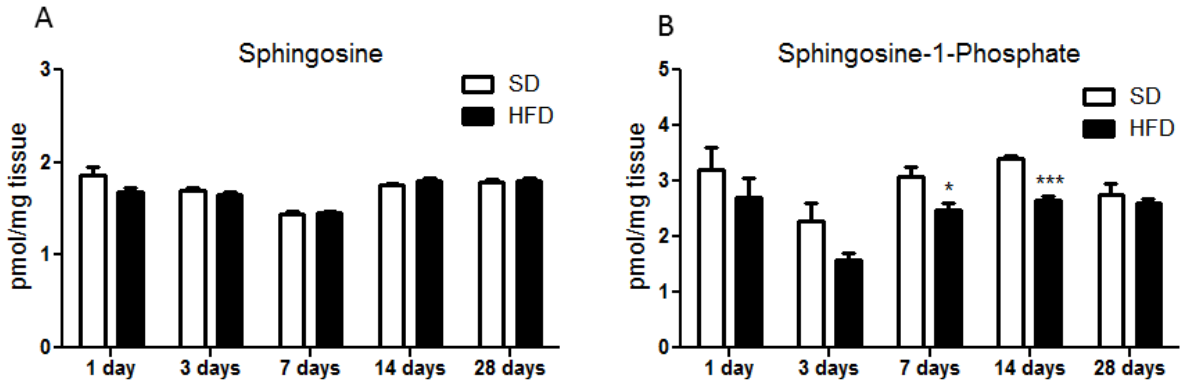

Fig. 4. Effects of standard diet (SD, white bars) and high fat diet (HFD, black bars) on (A) sphingosine and (B) sphingosine-1-phosphate in hypothalamus after 1-3-7-14-28 days. Results are expressed as mean ± SEM (n = 8/group). * $p < 0.05$, ** $p < 0.01$, *** $p < 0.001$; Student's unpaired *t*-test.

4.3.3 Effects of HFD on de novo synthesis gene expression.

*Sptlc*2 encodes the catalytic subunit 2 of serine palmitoyltransferase (SPT), which catalyzes the condensation of L-serine and palmitoyl-CoA. *Lass1* and *Lass2* encode respectively ceramide synthase 1 (CerS1) and ceramide synthase 2 (CerS2), which catalyze the N-acylation of dihydrosphingosine (sphinganine) to form dihydroceramide of different chain-lengths. As these enzymes play a key role in *de novo* sphingolipid biosynthesis, we examined their expression after 1 or 14 days of HFD, but we did not observe significant changes (Fig. 5).

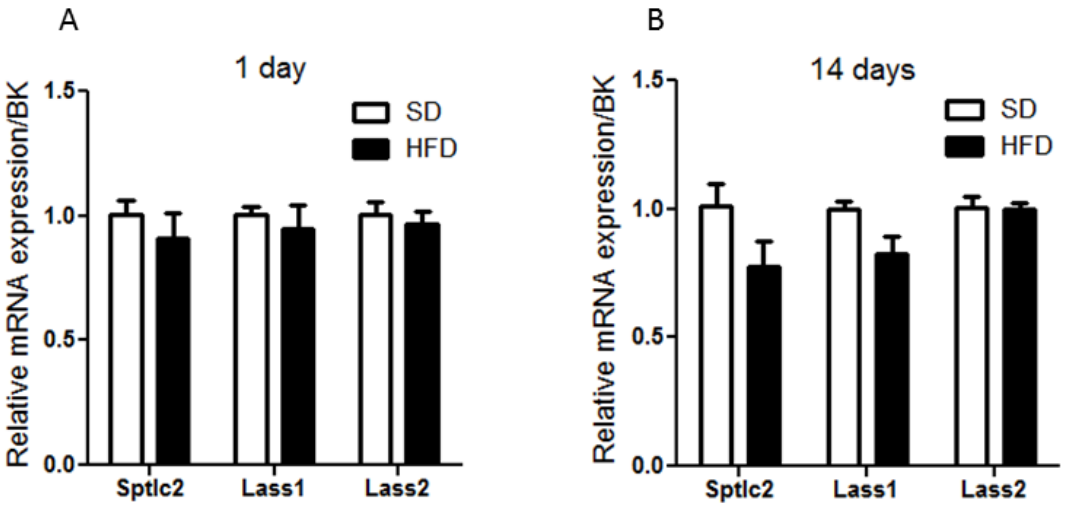

Fig. 5. Effects of standard diet (SD, white bars) and high fat diet (HFD, black bars) on *Sptlc2* (serine palmitoyltransferase), *Lass1* (ceramide synthase 1), *Lass2* (ceramide synthase 2) transcription in hypothalamus (A) after 1 day and (B) 14 days. Results are expressed as mean ± SEM (n = 5/group). * $p < 0.05$, ** $p < 0.01$, *** $p < 0.001$; Student's unpaired *t*-test .

4.3.4 Effects of 12h of food deprivation and refeeding on energy intake.

To assess the effect of an opposite feeding condition on hypothalamic sphingolipid metabolism, mice were food deprived for 12 hours and re-exposed to standard chow diet *ad libitum* for 1 hour or 6 hours. After 1 hour of refeeding, mice showed an intake of 2 ± 0.3 Kcal (Fig. 6), which is around 20% of their 24 h energy intake and is significantly higher, compared to free fed mice. After 4 h the energy intake was comparable with the control group and remained linear until 6 h.

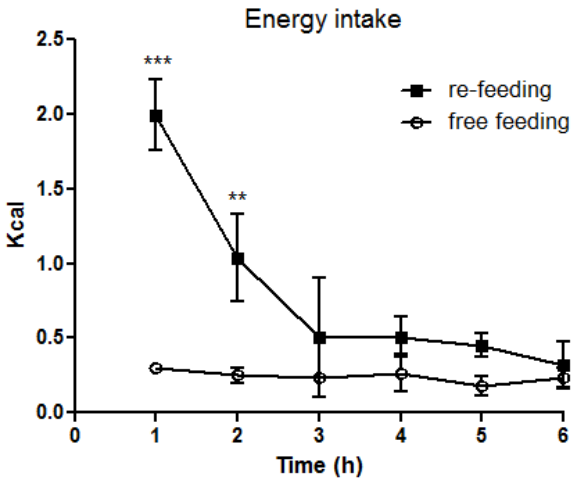

Fig. 6. Energy intake of free-fed mice and mice re-exposed to food. Results are expressed as mean ± SEM (n = 8/group). * $p < 0.05$, ** $p < 0.01$, *** $p < 0.001$; two-way ANOVA followed by Bonferroni post-hoc test.

4.3.5 Effects of food deprivation and refeeding on hypothalamic sphingolipids.

Food-deprived mice showed significant alterations of *de novo* ceramide biosynthesis. We found that sphinganine (Fig. 7A) and its metabolite sphinganine-1-phosphate (Fig. 7B) were reduced following 12 h food deprivation. Sphinganine levels remained low also during refeeding, while sphinganine-1-phosphate partially recovered after refeeding. Similarly, dihydroceramide (d18:0/18:0) showed decreasing levels after 12 h food deprivation and partial recovery after refeeding (Fig. 7C). By contrast, hypothalamic levels of ceramide (d18:1/18:0) were not altered either by fasting or refeeding (Fig. 7D). This result suggests that hypothalamic *de novo* biosynthesis of ceramides may be affected by the feeding status.

Since the balance between ceramide and SO-1-P is referred to as the “sphingolipid rheostat” (Newton, Lima et al. 2015), we next asked whether changes in ceramide precursors were accompanied by alterations in SO/SO-1-P levels. As shown in Fig. 7E, food deprivation (FD), a negative energy balance state, caused a significant accumulation of SO levels compared to free-fed mice. Such levels were re-established after 6 h refeeding (RF 6h). Concomitantly, fasting significantly decreased SO-1-P hypothalamic content (Fig. 7F), while RF 6h reinstated SO-1-P levels. These results suggest that 12 h food deprivation is sufficient to alter SO/SO-1-P balance (Fig. 7E-F).

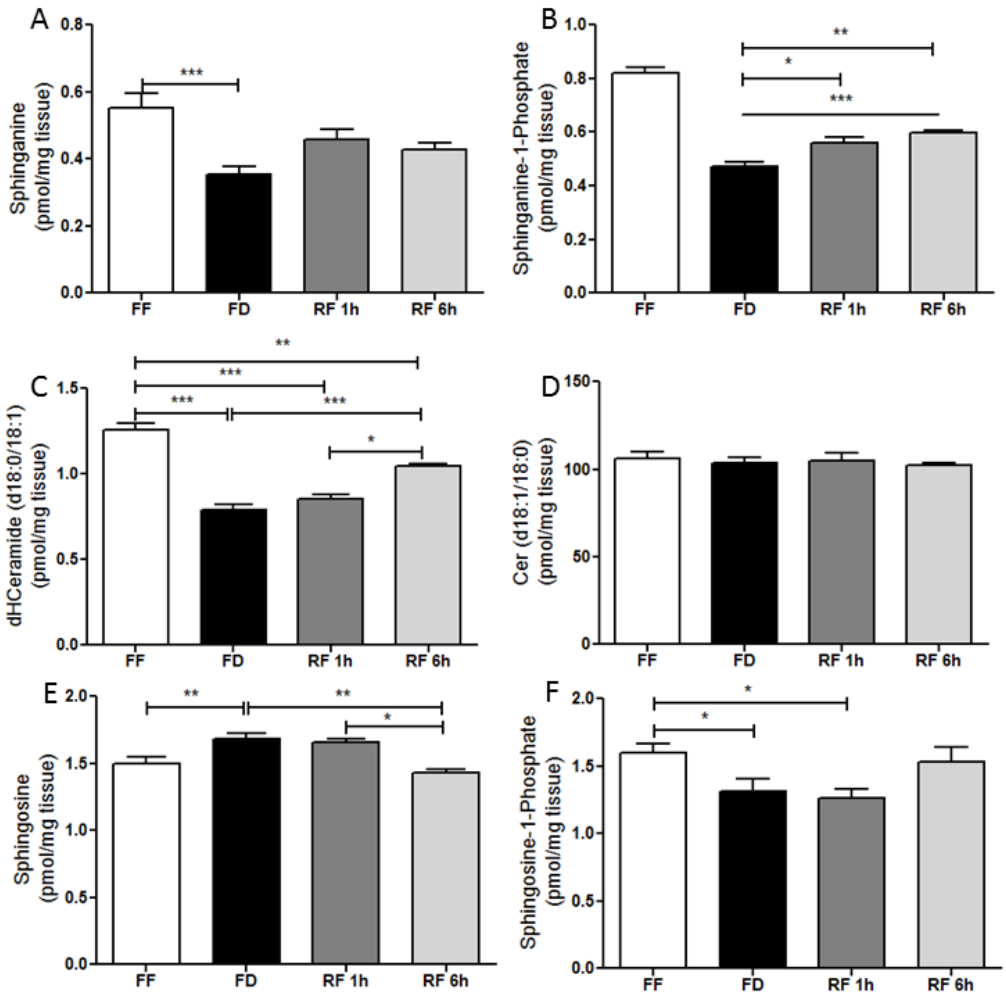

Fig. 7. Effects of free feeding (FF), 12 h food deprivation (FD), 1 h refeeding after food deprivation (RF 1h) and 6 h refeeding after food deprivation (RF 6h) on (A) sphinganine, (B) sphinganine-1-phosphate, (C) dHCeramide (d18:0/18:0), (D) ceramide (d18:1/18:0), (E) sphingosine, and (F) sphingosine-1-phosphate in hypothalamus. Results are expressed as mean ± SEM (n = 5-10/feeding condition). Independent experiments yielded similar results. *p < 0.05, **p < 0.01, ***p < 0.001; one-way ANOVA followed by Tukey's multiple comparison test.

4.3.6 Effects of food deprivation and refeeding on Sptlc2 and Lass1 gene expression.

Quantitative RT-PCR analysis showed that fasting significantly reduced *Sptlc2* and *Lass1* mRNA levels compared to free feeding control (Fig. 8A-B). *Sptlc2* gene transcription remained low through the whole refeeding interval (Fig. 8A), while *Lass1* gene expression was restored after 6 h refeeding (Fig. 8B). These results were consistent with the decreased levels of sphinganine and dihydroceramide during fasting.

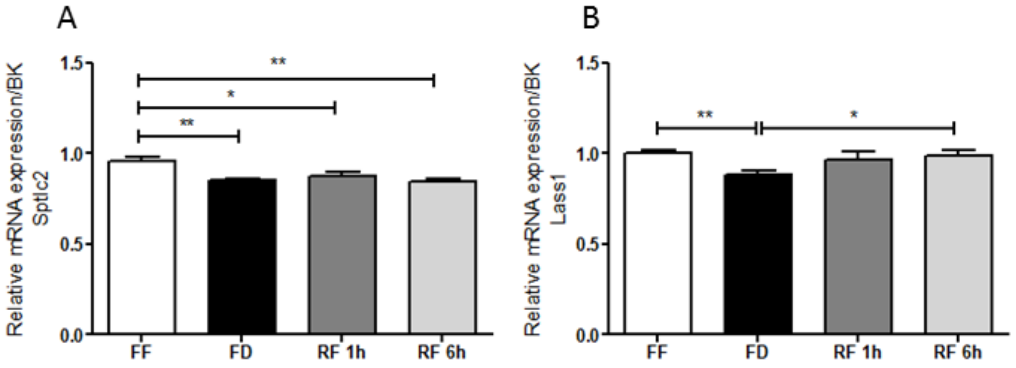

Fig. 8. Effects of free feeding (FF), 12 h food deprivation (FD), 1 h refeeding after food deprivation (RF 1h) and 6 h refeeding after food deprivation (RF 6h) on (A) *Sptlc2* (serine palmitoyltransferase), (B) *Lass1* (ceramide synthase 1). Results are expressed as mean ± SEM (n = 5-8/feeding condition). Two independent experiments yielded similar results. *p < 0.05, **p < 0.01, ***p < 0.001; one-way ANOVA followed by Tukey's multiple comparison test.

4.3.7 Effects of food deprivation and refeeding on SPT and CerS enzymatic activity.

To further investigate the involvement of *de novo* ceramide biosynthesis in this fasting model, serine palmitoyltransferase (SPT) and ceramide synthase 1 (CerS) enzymatic activity were assayed. As shown in Fig. 9 enzymatic activity was not affected by feeding status, even though we observed changes in mRNA expression of *Sptlc2* and *Lass1*.

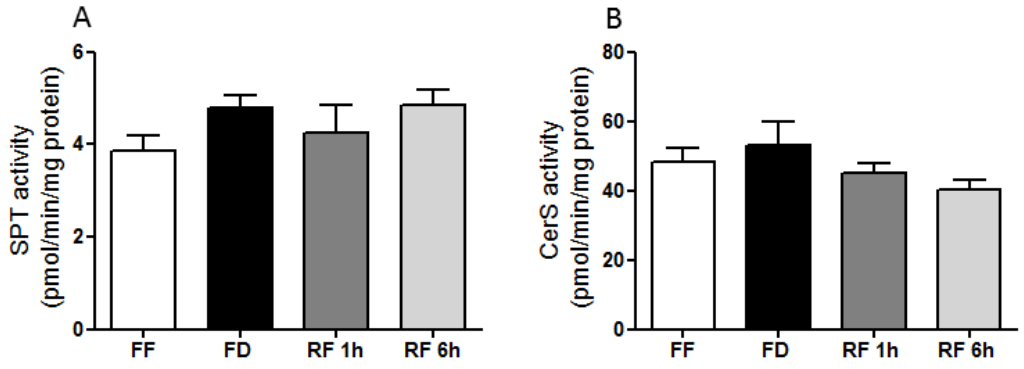

Fig. 9. Effects of free feeding (FF), 12 h food deprivation (FD), 1 h refeeding after food deprivation (RF 1h) and 6 h refeeding after food deprivation (RF 6h) on enzymatic activity of (A) SPT (serine palmitoyltransferase) and (B) CerS1 (ceramide synthase 1) in hypothalamus. Results are expressed as mean ± SEM (n = 5/feeding condition). *p < 0.05, **p < 0.01, ***p < 0.001; one-way ANOVA followed by Tukey's multiple comparison test.

4.3.8 Effects of food deprivation and refeeding on SphK1, SphK2 and S1PR1 gene expression.

Sphingosine kinase (SphK) catalyzes the synthesis of bioactive lipid SO-1-P, which in turn activates a family of five G-coupled receptors named sphingosine-1-phosphate receptor 1-5 (S1PR 1-5) (Maceyka, Sankala et al. 2005; Pyne, McNaughton et al. 2015). Two distinct isoforms of SphK are expressed in brain areas, SphK1 and SphK2 (Bryan, Kordula et al. 2008). As shown in Fig. 10A-B, 12 h fasting significantly decreased *SphK2* mRNA expression and slightly affected *SphK1*. After 6 h refeeding, *SphK2* was restored to baseline levels (Fig. 10B). SO-1-P/S1PR1 axis has an important role in the control of food consumption and energy homeostasis (Silva, Micheletti et al. 2014). We further confirmed this finding analyzing S1PR1 gene expression by qRT-PCR and we observed that 12 h food deprivation transcriptionally downregulates S1PR1 levels, an effect that is completely reversed by 6 h of refeeding (Fig. 10C).

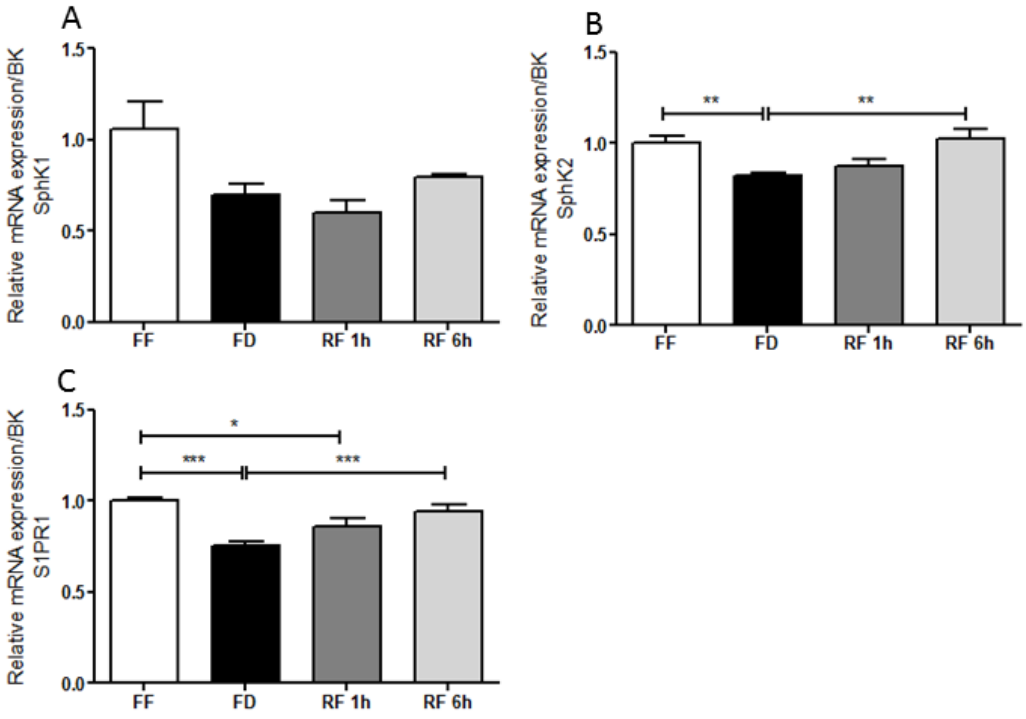

Fig. 10. Effects of free feeding (FF), 12 h food deprivation (FD), 1 h refeeding after food deprivation (RF 1h) and 6 h refeeding after food deprivation (RF 6h) on *SphK1* (Sphingosine kinase 1) (A), *SphK2* (Sphingosine kinase 2) (B), *S1PR1* (sphingosine-1-phosphate receptor 1) (C) transcription in hypothalamus. Results are expressed as mean ± SEM (n = 5-8/feeding condition). Two independent experiments yielded similar results. *p < 0.05, **p < 0.01, ***p < 0.001; one-way ANOVA followed by Tukey's multiple comparison test.

4.3.9 Effect of acid ceramidase inhibitor ARN14974 on feeding behavior.

Mice that received lateral ventricle injections of ARN14974 (50pmol/2µL, icv) did not show significant changes in the total amount of food intake or in cumulative food intake within the 24 hours of monitoring when compared to the vehicle group (Fig. 11).

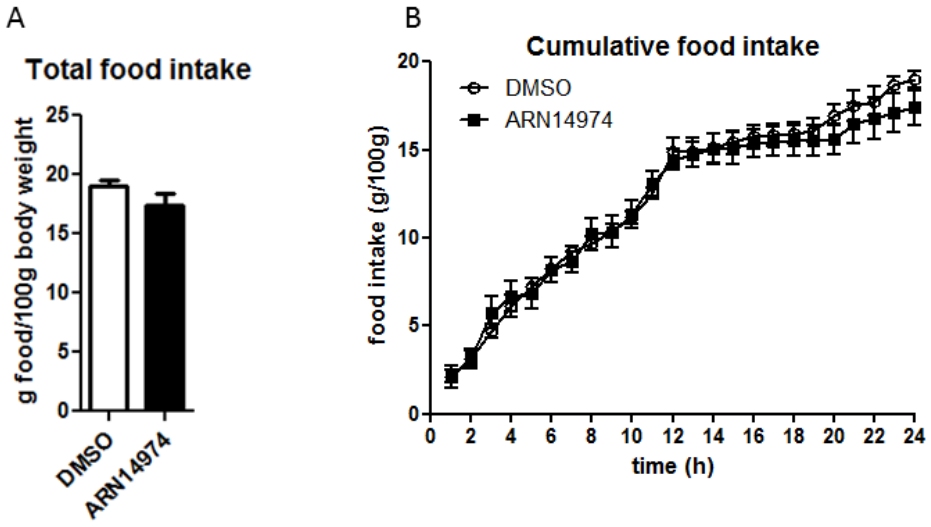

Fig. 11. Effects of ARN14974 (50 pmol, icv) on (A) total food intake and (B) cumulative food intake in free-fed mice after 24 h test period. Results are expressed as mean ± SEM (n = 8/group). * $p < 0.05$; Student's unpaired *t*-test was used for total food intake (A); two-way ANOVA followed by Bonferroni post-hoc test was used for cumulative food intake (B).

However, we explored the behavioral basis of ARN14974 action and we examined the effects of the acid ceramidase inhibitor on meal pattern during a 24 h period starting from the onset of dark phase. As shown in Fig. 12, ARN14974 altered various average-meal parameters. These included an increase of meal size (Fig. 12A) and post-meal interval (Fig. 12B), with a concomitant reduction of number of meals (Fig. 12C) and meal frequency (Fig. 12D). The parallel increase in post-meal interval and meal size caused the average satiety ratio to remain unchanged (Fig. 12E). Furthermore, there was no effect on meal duration (Fig. 12F) and average rate (Fig. 12G) at which mice consumed their meals.

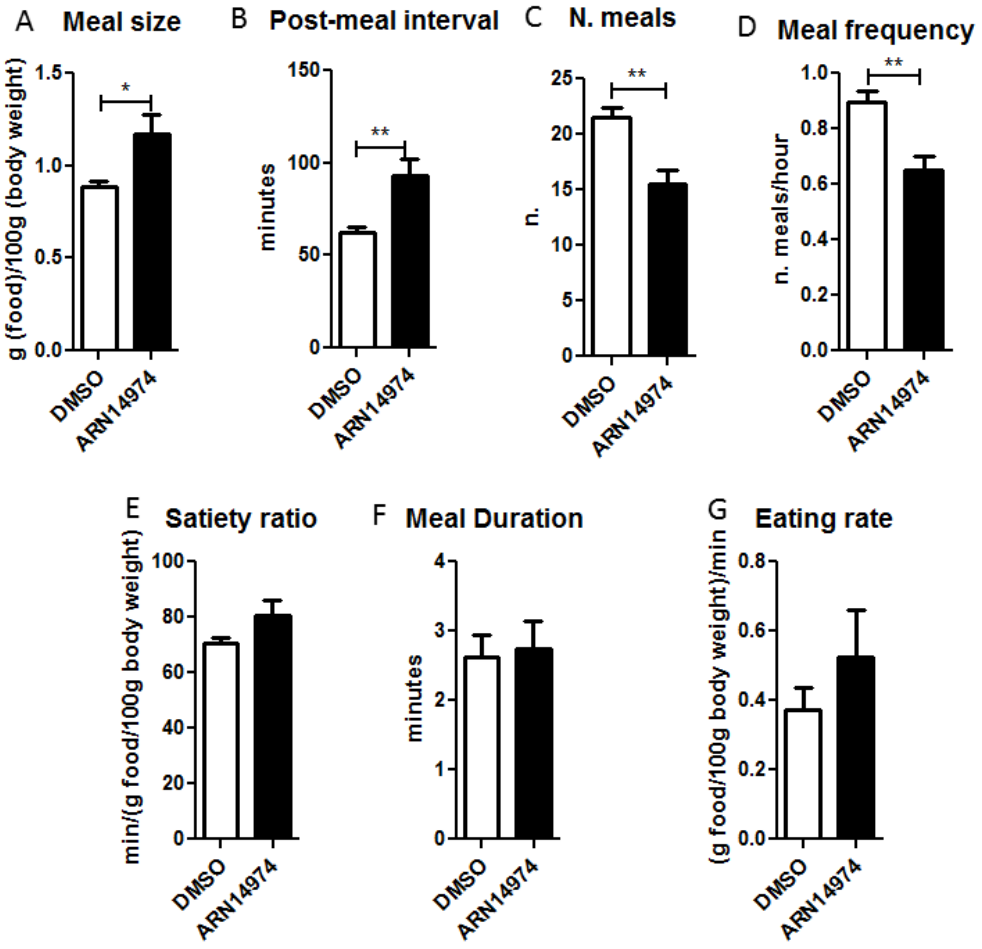

Fig. 12. Effects of ARN14974 (50 pmol, icv) on (A) meal size, (B) post-meal interval, (C) number of meals, (D) meal frequency, (E) satiety ratio, (F) meal duration, (G) eating rate in free-fed mice after 24 h test period. Results are expressed as mean ± SEM (n = 8/group). *p < 0.05, **p < 0.01, ***p < 0.001; Student's unpaired *t*-test.

4.4 Discussion

The roles of sphingolipids in obesity and co-morbidities such as diabetes (Summers 2006) and cardiovascular disease (Bismuth, Lin et al. 2008) have been widely investigated in recent years (Bikman and Summers 2011). Evidence suggests that ceramide is one of the most toxic lipids that can accumulate in obese rodent models and human patients and numerous studies indicate that ceramide and its metabolites have profound effects on cellular metabolism (Guenther and Edinger 2009). Previous works reported that hypothalamic ceramide levels are increased in mice after 12 weeks of HFD consumption (Borg, Omran et al. 2012), in streptozotocin-induced diabetic rats (Car, Zendzian-Piotrowska et al. 2012) and in obese Zucker rats (Contreras, Gonzalez-Garcia et al. 2014). However, despite these evidences, a systematic investigation of endogenous ceramide levels in hypothalamus after an acute and mid-term exposure to HFD has not been performed. In the present study, we described previously unreported alterations in hypothalamic sphingolipid metabolism in young mice exposed to a HDF for 1-3-7-14-28 days. Body weight and energy intake were monitored throughout the whole period of HFD exposure and compared to SD, in order to have readout of endogenous sphingolipid changes. Surprisingly, we found that young mice exposed to a fat-enriched diet for 24 h show a significantly high increase in energy intake paralleled by a reduction of the levels of ceramide (d18:1/24:0), its precursor dihydroceramide (d18:0/24:0), and ceramide (d18:1/24:1), whereas no changes were detected in ceramide (18:1/18:0). Changes in very long-chain ceramides are of particular interest since they have been involved also in aging and age-related disorders (Mielke, Haughey et al. 2010; Huang, Withers et al. 2014). Activation of astrocytes occurs as early as 1 day after HFD (Thaler, Yi et al. 2012; Buckman, Thompson et al. 2013) and this could initially function as a neuroprotective response and an attempt to maintain homeostasis. Similarly, a reduction in ceramide content may be considered as a defensive response to the high caloric load. However, the drawback of this defensive activation occurs when it is sustained over time, because inflammatory and neurotoxic factors can cause neuronal damage. We observed reduced levels of ceramide (d18:1/24:0), its precursor dihydroceramide (d18:0/24:0), ceramide (d18:1/24:1) and dihydroceramide (d18:0/18:0) up to day 14 of HFD exposure. After 14 days the energy intake of animals fed HFD was comparable to control animals, but a separation in body weight,

although still not significant, occurred. 14 days may be considered as the cut-off point between a putative protective role of ceramide and the induction of cerebral lipotoxicity. Molecular mechanisms underlying hypothalamic lipotoxicity may include inflammation, development of leptin and insulin resistance and ceramide overproduction. Contreras et al. suggested that ceramide-induced lipotoxicity was a key mechanism modulating energy balance (Contreras, Gonzalez-Garcia et al. 2014). Consistent with this hypothesis, we observed a significant increase of body weight in mice exposed to HFD for 28 days, that was accompanied by an increase in ceramide precursor dihydroceramide (d18:0/18:0) and increasing trend in dihydroceramide (d18:0/24:0), although no differences were detected in ceramides. *De novo* biosynthesis plays a key role in the pathogenesis of obesity and metabolic syndrome since it has been demonstrated that its inhibition in obese mice resulted in decreased body weight, without alterations in food intake (Yang, Badeanlou et al. 2009), indicating a shift in total energy balance toward enhanced metabolism and energy expenditure. By contrast, increased *de novo* synthesis of ceramides in hippocampus has been demonstrated to be responsible for decreased parasympathetic nervous activity and locomotor activity leading to increased body weight gain in rodents (Picard, Rouch et al. 2014). We then analyzed ceramide breakdown product SO-1-P, and we observed a significant decrease of this metabolite after 7 and 14 days of HFD exposure. SO-1-P has attracted great attention for his double pro-inflammatory or anti-inflammatory roles (Maceyka and Spiegel 2014). Circulating SO-1-P has been found to be elevated in obesity (Kowalski, Carey et al. 2013), and the work published by Silva et al. finally establishes the role of SO-1-P and SO-1-P/S1PR1 axis in the control of hypothalamic anorexigenic signals, food consumption and energy expenditure in hyperphagia and anorexia (Silva, Micheletti et al. 2014). These investigators found reduced S1PR1 protein and gene expression in hypothalamus of rats and mice fed HFD. They also observed a significant reduction of food intake when animals were treated by single injection of SO-1-P in the third ventricle.

Consumption of HFD and obesity development may have detrimental effects on hypothalamic control of energy balance. By contrast, it has been investigated and widely accepted that fasting, intermittent fasting (alternate day fasting or twice weekly fasting) or periodic fasting, may provide effective strategies to delay

aging and optimize health. Fasting for 24 hours twice weekly throughout adult life resulted in a significant increase in lifespan of black-hooded rats (Kendrick 1973). Furthermore, starvation may increase neuronal activity in brain regions involved in cognition, resulting in production of BDNF, enhanced synaptic plasticity and improved stress tolerance (Rothman, Griffioen et al. 2012). In the present study we used fasting and refeeding as a strong stimulus to stress the transition from a negative energy balance (12h food deprivation) to acute food intake (1h refeeding) and we examined sphingolipid metabolism activation in hypothalamus. We showed for the first time that food deprivation causes simultaneous acute changes of sphingolipid metabolites at different key points of sphingolipid metabolic pathway. *De novo* ceramide synthesis is affected by 12 h of food deprivation as we found a significant downregulation of sphinganine, its metabolite sphinganine-1-phosphate, and dihydroceramide (d18:0/18:0), but no differences were observed with ceramide (d18:0/18:0). These effects on ceramide biosynthesis could be accounted for by concomitant downregulation of *Sptlc2* and *Lass1* transcription but not SPT and CerS1 enzymatic activity. 6 h refeeding reinstated the energy intake to basal levels but was not sufficient to completely re-establish basal levels of lipids. The sphingolipid mediators sphingosine (SO) and SO-1-P were also quantified and found altered, with significant accumulation of SO and reduction of SO-1-P after 12 h of fasting. These results were supported by qRT-PCR experiments which showed downregulation of the sphingosine-metabolizing enzyme sphingosine kinase 2. The isoenzyme sphingosine kinase 1 displayed a similar decreasing trend, albeit not significant. Although highly similar in amino acid sequence, and although they use the same substrate and produce the same product, SphK1 and SphK2 have opposite roles with SphK1 enhancing proliferation and growth and the isoenzyme 2 enhancing apoptosis and suppressing growth (Maceyka, Sankala et al. 2005). It is possible that SO-1-P formed by SphK1 or SphK2 has distinct functions and responses to stimuli. SO-1-P/S1PR1 axis has been involved in the control of food consumption and energy expenditure also in food-deprived rodents. It has been shown that 12h fasting reduced S1PR1 protein level in hypothalamic neurons and 6 h refeeding was sufficient to reinstate it. We confirmed this observation analyzing the S1PR1 transcription in hypothalamus of 12 h food deprived mice and re-fed mice.

Acid ceramidase metabolizes ceramide into SO which is, in turn, phosphorylated to SO-1-P by SphK1 or SphK2. Ceramide breakdown into SO and SO-1-P has been termed “sphingolipid rheostat” as it involves enzymes which may be potential targets to tilt the balance between these bioactive molecules and determine cell fate. ARN14974 has been identified and characterized as a potent covalent acid ceramidase inhibitor (Pizzirani, Bach et al. 2015). When administered in standard chow free-fed mice by injection into the third ventricle, it promoted alterations in feeding behavior parameters. Even though the total food intake after 24 h of test was not affected in treated mice, the behavioral parameters changed. Of particular interest was the meal size, which was increased in ARN14974-treated mice compared to control. The acid ceramidase inhibitor causes an accumulation of ceramide and a reduction of SO and SO-1-P, which presumably results in increased meal size. Since also the post-meal interval was elevated, the satiety ratio, calculated by the ratio between those two parameters did not change. This means that treated animals eat bigger meals but they reach the same satiety as control group. The limit of this study is that only acute injections were performed but chronic treatments are required to better understand the role of long-term ceramide accumulation in free-fed mice. As previously mentioned, dysregulated ceramide metabolism may lead to lipotoxicity with consequences in energy intake regulation and the way animals approach to food.

4.5 Conclusions

In our study we quantified for the first time a broad panel of endogenous sphingolipids in hypothalamus, in distinct conditions of abnormal feeding such as consumption of a fat-enriched diet or fasting.

Our results revealed that *de novo* ceramide biosynthesis may have a critical role in hypothalamic regulation of feeding behavior and energy balance in response to drastic diet changes such as a high fat diet or food deprivation. Furthermore, we confirmed the importance of SO-1-P/SO1PR axis in the regulation of energy balance, showing that hypothalamic levels of SO-1-P, its precursor SO and enzymes involved in their conversion (sphingosine kinases) are influenced by feeding status. Since obesity and fasting may have respectively a detrimental or beneficial effect on aging, it will be important to establish the functional role of altered hypothalamic sphingolipid metabolism as it may represent a potential target for the treatment of altered feeding conditions.

References

(1996). "Research on the menopause in the 1990s. Report of a WHO Scientific Group." World Health Organ Tech Rep Ser **866**: 1-107.

Acaz-Fonseca, E., M. Avila-Rodriguez, et al. (2016). "Regulation of astroglia by gonadal steroid hormones under physiological and pathological conditions." Prog Neurobiol **144**: 5-26.

Alewijnse, A. E. and S. L. Peters (2008). "Sphingolipid signalling in the cardiovascular system: good, bad or both?" Eur J Pharmacol **585**(2-3): 292-302.

Almey, A., T. A. Milner, et al. (2015). "Estrogen receptors in the central nervous system and their implication for dopamine-dependent cognition in females." Horm Behav **74**: 125-138.

Astarita, G., A. Avanesian, et al. (2015). "Methamphetamine accelerates cellular senescence through stimulation of de novo ceramide biosynthesis." PLoS One **10**(2): e0116961.

Astarita, G., K. M. Jung, et al. (2011). "Elevated stearoyl-CoA desaturase in brains of patients with Alzheimer's disease." PLoS One **6**(10): e24777.

Babenko, N. A. and Y. A. Semenova (2010). "Effects of long-term fish oil-enriched diet on the sphingolipid metabolism in brain of old rats." Exp Gerontol **45**(5): 375-380.

Babenko, N. A. and E. G. Shakhova (2014). "Long-term food restriction prevents aging-associated sphingolipid turnover dysregulation in the brain." Arch Gerontol Geriatr **58**(3): 420-426.

Baker, L. D., S. Asthana, et al. (2012). "Cognitive response to estradiol in postmenopausal women is modified by high cortisol." Neurobiol Aging **33**(4): 829 e829-820.

Ball, M. J. (1977). "Neuronal loss, neurofibrillary tangles and granulovacuolar degeneration in the hippocampus with ageing and dementia. A quantitative study." Acta Neuropathol **37**(2): 111-118.

Bartke, N. and Y. A. Hannun (2009). "Bioactive sphingolipids: metabolism and function." J Lipid Res **50 Suppl**: S91-96.

Basit, A., D. Piomelli, et al. (2015). "Rapid evaluation of 25 key sphingolipids and phosphosphingolipids in human plasma by LC-MS/MS." Anal Bioanal Chem **407**(17): 5189-5198.

Bieberich, E. (2012). "Ceramide and sphingosine-1-phosphate signaling in embryonic stem cell differentiation." Methods Mol Biol **874**: 177-192.

Bikman, B. T. and S. A. Summers (2011). "Ceramides as modulators of cellular and whole-body metabolism." J Clin Invest **121**(11): 4222-4230.

Bismuth, J., P. Lin, et al. (2008). "Ceramide: a common pathway for atherosclerosis?" Atherosclerosis **196**(2): 497-504.

Borg, M. L., S. F. Omran, et al. (2012). "Consumption of a high-fat diet, but not regular endurance exercise training, regulates hypothalamic lipid accumulation in mice." J Physiol **590**(Pt 17): 4377-4389.

Brady, R. O., J. Kanfer, et al. (1965). "The Metabolism of Glucocerebrosides. I. Purification and Properties of a Glucocerebroside-Cleaving Enzyme from Spleen Tissue." J Biol Chem **240**: 39-43.

Brady, R. O., J. N. Kanfer, et al. (1966). "Demonstration of a deficiency of glucocerebroside-cleaving enzyme in Gaucher's disease." J Clin Invest **45**(7): 1112-1115.

Brady, R. O., J. N. Kanfer, et al. (1965). "Metabolism of Glucocerebrosides. II. Evidence of an Enzymatic Deficiency in Gaucher's Disease." Biochem Biophys Res Commun **18**: 221-225.

Brinton, R. D., S. Chen, et al. (2000). "The estrogen replacement therapy of the Women's Health Initiative promotes the cellular mechanisms of memory and neuronal survival in neurons vulnerable to Alzheimer's disease." Maturitas **34 Suppl 2**: S35-52.

Brooks, S. C., E. R. Locke, et al. (1973). "Estrogen receptor in a human cell line (MCF-7) from breast carcinoma." J Biol Chem **248**(17): 6251-6253.

Bryan, L., T. Kordula, et al. (2008). "Regulation and functions of sphingosine kinases in the brain." Biochim Biophys Acta **1781**(9): 459-466.

Buckman, L. B., M. M. Thompson, et al. (2013). "Regional astrogliosis in the mouse hypothalamus in response to obesity." J Comp Neurol **521**(6): 1322-1333.

Car, H., M. Zendzian-Piotrowska, et al. (2012). "Ceramide profiles in the brain of rats with diabetes induced by streptozotocin." FEBS J **279**(11): 1943-1952.

Carlesimo, G. A., C. Caltagirone, et al. (1996). "The Mental Deterioration Battery: normative data, diagnostic reliability and qualitative analyses of cognitive impairment. The Group for the Standardization of the Mental Deterioration Battery." Eur Neurol **36**(6): 378-384.

Castro, B. M., M. Prieto, et al. (2014). "Ceramide: a simple sphingolipid with unique biophysical properties." Prog Lipid Res **54**: 53-67.

Cerbai, F., D. Lana, et al. (2012). "The neuron-astrocyte-microglia triad in normal brain ageing and in a model of neuroinflammation in the rat hippocampus." PLoS One **7**(9): e45250.

Chaurasia, B. and S. A. Summers (2015). "Ceramides - Lipotoxic Inducers of Metabolic Disorders." Trends Endocrinol Metab **26**(10): 538-550.

Chavez, J. A. and S. A. Summers (2012). "A ceramide-centric view of insulin resistance." Cell Metab **15**(5): 585-594.

Choi, S. and A. J. Snider (2015). "Sphingolipids in High Fat Diet and Obesity-Related Diseases." Mediators Inflamm **2015**: 520618.

Cohen, P., J. M. Ntambi, et al. (2003). "Stearoyl-CoA desaturase-1 and the metabolic syndrome." Curr Drug Targets Immune Endocr Metabol Disord **3**(4): 271-280.

Collier, T. J., N. M. Kanaan, et al. (2011). "Ageing as a primary risk factor for Parkinson's disease: evidence from studies of non-human primates." Nat Rev Neurosci **12**(6): 359-366.

Contreras, C., I. Gonzalez-Garcia, et al. (2014). "Central ceramide-induced hypothalamic lipotoxicity and ER stress regulate energy balance." Cell Rep **9**(1): 366-377.

Corpeleijn, E., E. J. Feskens, et al. (2006). "Improvements in glucose tolerance and insulin sensitivity after lifestyle intervention are related to changes in serum fatty acid profile and desaturase activities: the SLIM study." Diabetologia **49**(10): 2392-2401.

Costantini, C., R. M. Kolasani, et al. (2005). "Ceramide and cholesterol: possible connections between normal aging of the brain and Alzheimer's disease. Just hypotheses or molecular pathways to be identified?" Alzheimers Dement **1**(1): 43-50.

Costantini, C., R. Weindruch, et al. (2005). "A TrkA-to-p75NTR molecular switch activates amyloid beta-peptide generation during aging." Biochem J **391**(Pt 1): 59-67.

Cutler, R. G., J. Kelly, et al. (2004). "Involvement of oxidative stress-induced abnormalities in ceramide and cholesterol metabolism in brain aging and Alzheimer's disease." Proc Natl Acad Sci U S A **101**(7): 2070-2075.

Cuvillier, O., G. Pirianov, et al. (1996). "Suppression of ceramide-mediated programmed cell death by sphingosine-1-phosphate." Nature **381**(6585): 800-803.

De Marinis, E., E. Acaz-Fonseca, et al. (2013). "17beta-Oestradiol anti-inflammatory effects in primary astrocytes require oestrogen receptor beta-mediated neuroglobin up-regulation." J Neuroendocrinol **25**(3): 260-270.

de Mello, V. D., M. Lankinen, et al. (2009). "Link between plasma ceramides, inflammation and insulin resistance: association with serum IL-6 concentration in patients with coronary heart disease." Diabetologia **52**(12): 2612-2615.

Deng, T. X., Z. X. Wang, et al. (2011). "[Alcohol-induced proliferation of neurons in mouse hippocampal dentate gyrus: a possible role of ceramide]." Sheng Li Xue Bao **63**(6): 479-490.

Di Stefano, G., T. Casoli, et al. (2001). "Distribution of map2 in hippocampus and cerebellum of young and old rats by quantitative immunohistochemistry." J Histochem Cytochem **49**(8): 1065-1066.

Dinoff, A., N. Herrmann, et al. (2017). "Ceramides and depression: A systematic review." J Affect Disord **213**: 35-43.

Dobrzyn, A. and J. M. Ntambi (2005). "Stearoyl-CoA desaturase as a new drug target for obesity treatment." Obes Rev **6**(2): 169-174.

Dobrzyn, P., H. Sampath, et al. (2008). "Loss of stearoyl-CoA desaturase 1 inhibits fatty acid oxidation and increases glucose utilization in the heart." Am J Physiol Endocrinol Metab **294**(2): E357-364.
Dominguez, L. J. and M. Barbagallo (2016). "The biology of the metabolic syndrome and aging." Curr Opin Clin Nutr Metab Care **19**(1): 5-11.
Edsfeldt, A., P. Duner, et al. (2016). "Sphingolipids Contribute to Human Atherosclerotic Plaque Inflammation." Arterioscler Thromb Vasc Biol **36**(6): 1132-1140.
Ellacott, K. L., G. J. Morton, et al. (2010). "Assessment of feeding behavior in laboratory mice." Cell Metab **12**(1): 10-17.
Ewers, M., M. M. Mielke, et al. (2010). "Blood-based biomarkers of microvascular pathology in Alzheimer's disease." Exp Gerontol **45**(1): 75-79.
Farfel-Becker, T., E. B. Vitner, et al. (2014). "Neuronal accumulation of glucosylceramide in a mouse model of neuronopathic Gaucher disease leads to neurodegeneration." Hum Mol Genet **23**(4): 843-854.
Farooqui, A. A., T. Farooqui, et al. (2012). "Metabolic syndrome as a risk factor for neurological disorders." Cell Mol Life Sci **69**(5): 741-762.
First, M. B. and H. A. Pincus (2002). "The DSM-IV Text Revision: rationale and potential impact on clinical practice." Psychiatr Serv **53**(3): 288-292.
Fjell, A. M., L. McEvoy, et al. (2014). "What is normal in normal aging? Effects of aging, amyloid and Alzheimer's disease on the cerebral cortex and the hippocampus." Prog Neurobiol **117**: 20-40.
Flood, D. G., S. J. Buell, et al. (1987). "Dendritic extent in human dentate gyrus granule cells in normal aging and senile dementia." Brain Res **402**(2): 205-216.
Flood, D. G., M. Guarnaccia, et al. (1987). "Dendritic extent in human CA2-3 hippocampal pyramidal neurons in normal aging and senile dementia." Brain Res **409**(1): 88-96.
Flowers, J. B., M. E. Rabaglia, et al. (2007). "Loss of stearoyl-CoA desaturase-1 improves insulin sensitivity in lean mice but worsens diabetes in leptin-deficient obese mice." Diabetes **56**(5): 1228-1239.
Folstein, M. F., S. E. Folstein, et al. (1975). ""Mini-mental state". A practical method for grading the cognitive state of patients for the clinician." J Psychiatr Res **12**(3): 189-198.
Fratiglioni, L., L. J. Launer, et al. (2000). "Incidence of dementia and major subtypes in Europe: A collaborative study of population-based cohorts. Neurologic Diseases in the Elderly Research Group." Neurology **54**(11 Suppl 5): S10-15.
Fu, J., S. Gaetani, et al. (2003). "Oleylethanolamide regulates feeding and body weight through activation of the nuclear receptor PPAR-alpha." Nature **425**(6953): 90-93.
Gaetani, S., F. Oveisi, et al. (2003). "Modulation of meal pattern in the rat by the anorexic lipid mediator oleoylethanolamide." Neuropsychopharmacology **28**(7): 1311-1316.
Galadari, S., A. Rahman, et al. (2013). "Role of ceramide in diabetes mellitus: evidence and mechanisms." Lipids Health Dis **12**: 98.
Gambacciani, M., M. Ciaponi, et al. (1997). "Body weight, body fat distribution, and hormonal replacement therapy in early postmenopausal women." J Clin Endocrinol Metab **82**(2): 414-417.
Garcia-Barros, M., N. Coant, et al. (2016). "Role of neutral ceramidase in colon cancer." FASEB J **30**(12): 4159-4171.
Gault, C. R., L. M. Obeid, et al. (2010). "An overview of sphingolipid metabolism: from synthesis to breakdown." Adv Exp Med Biol **688**: 1-23.
Geinisman, Y., W. Bondareff, et al. (1977). "Partial deafferentation of neurons in the dentate gyrus of the senescent rat." Brain Res **134**(3): 541-545.
Gerstner, B., M. Sifringer, et al. (2007). "Estradiol attenuates hyperoxia-induced cell death in the developing white matter." Ann Neurol **61**(6): 562-573.
Gonzalez, A., M. Valeiras, et al. (2014). "Lysosomal integral membrane protein-2: a new player in lysosome-related pathology." Mol Genet Metab **111**(2): 84-91.
Gracia-Garcia, P., V. Rao, et al. (2011). "Elevated plasma ceramides in depression." J Neuropsychiatry Clin Neurosci **23**(2): 215-218.

Grassme, H., J. Riethmuller, et al. (2007). "Biological aspects of ceramide-enriched membrane domains." Prog Lipid Res **46**(3-4): 161-170.
Grosch, S., S. Schiffmann, et al. (2012). "Chain length-specific properties of ceramides." Prog Lipid Res **51**(1): 50-62.
Guarner, V. and M. E. Rubio-Ruiz (2015). "Low-grade systemic inflammation connects aging, metabolic syndrome and cardiovascular disease." Interdiscip Top Gerontol **40**: 99-106.
Guenther, G. G. and A. L. Edinger (2009). "A new take on ceramide: starving cells by cutting off the nutrient supply." Cell Cycle **8**(8): 1122-1126.
Gutierrez-Juarez, R., A. Pocai, et al. (2006). "Critical role of stearoyl-CoA desaturase-1 (SCD1) in the onset of diet-induced hepatic insulin resistance." J Clin Invest **116**(6): 1686-1695.
Hamilton, D. J., L. J. Minze, et al. (2016). "Estrogen receptor alpha activation enhances mitochondrial function and systemic metabolism in high-fat-fed ovariectomized mice." Physiol Rep **4**(17).
Han, X., M. H. D, et al. (2002). "Substantial sulfatide deficiency and ceramide elevation in very early Alzheimer's disease: potential role in disease pathogenesis." J Neurochem **82**(4): 809-818.
Hanada, K., K. Kumagai, et al. (2003). "Molecular machinery for non-vesicular trafficking of ceramide." Nature **426**(6968): 803-809.
Hannun, Y. A. and L. M. Obeid (2008). "Principles of bioactive lipid signalling: lessons from sphingolipids." Nat Rev Mol Cell Biol **9**(2): 139-150.
Hattiangady, B. and A. K. Shetty (2008). "Aging does not alter the number or phenotype of putative stem/progenitor cells in the neurogenic region of the hippocampus." Neurobiol Aging **29**(1): 129-147.
Haus, J. M., S. R. Kashyap, et al. (2009). "Plasma ceramides are elevated in obese subjects with type 2 diabetes and correlate with the severity of insulin resistance." Diabetes **58**(2): 337-343.
Hawthorne, J. N. (1975). "A note on the life of J.L.W. Thudichum (1829-1901)." Biochem Soc Trans **3**(5): 591.
Hering, H., C. C. Lin, et al. (2003). "Lipid rafts in the maintenance of synapses, dendritic spines, and surface AMPA receptor stability." J Neurosci **23**(8): 3262-3271.
Hetz, C. A., M. Hunn, et al. (2002). "Caspase-dependent initiation of apoptosis and necrosis by the Fas receptor in lymphoid cells: onset of necrosis is associated with delayed ceramide increase." J Cell Sci **115**(Pt 23): 4671-4683.
Hof, P. R. and J. H. Morrison (2004). "The aging brain: morphomolecular senescence of cortical circuits." Trends Neurosci **27**(10): 607-613.
Hojjati, M. R., Z. Li, et al. (2005). "Effect of myriocin on plasma sphingolipid metabolism and atherosclerosis in apoE-deficient mice." J Biol Chem **280**(11): 10284-10289.
Hotamisligil, G. S. (2006). "Inflammation and metabolic disorders." Nature **444**(7121): 860-867.
Huang, X., B. R. Withers, et al. (2014). "Sphingolipids and lifespan regulation." Biochim Biophys Acta **1841**(5): 657-664.
Ichi, I., K. Nakahara, et al. (2006). "Association of ceramides in human plasma with risk factors of atherosclerosis." Lipids **41**(9): 859-863.
Iorio, M., G. Spalletta, et al. (2013). "White matter hyperintensities segmentation: a new semi-automated method." Front Aging Neurosci **5**: 76.
Ishikawa, M., Y. Tajima, et al. (2013). "Plasma and serum from nonfasting men and women differ in their lipidomic profiles." Biol Pharm Bull **36**(4): 682-685.
Jana, A., E. L. Hogan, et al. (2009). "Ceramide and neurodegeneration: susceptibility of neurons and oligodendrocytes to cell damage and death." J Neurol Sci **278**(1-2): 5-15.
Jazvinscak Jembrek, M., P. R. Hof, et al. (2015). "Ceramides in Alzheimer's Disease: Key Mediators of Neuronal Apoptosis Induced by Oxidative Stress and Abeta Accumulation." Oxid Med Cell Longev **2015**: 346783.
Jenkins, R. W., D. Canals, et al. (2010). "Regulated secretion of acid sphingomyelinase: implications for selectivity of ceramide formation." J Biol Chem **285**(46): 35706-35718.
Jequier, E. (1989). "Energy metabolism in human obesity." Soz Praventivmed **34**(2): 58-62.
Jiang, G., Z. Li, et al. (2005). "Prevention of obesity in mice by antisense oligonucleotide inhibitors of stearoyl-CoA desaturase-1." J Clin Invest **115**(4): 1030-1038.

Jiang, H., F. F. Hsu, et al. (2013). "Development and validation of LC-MS/MS method for determination of very long acyl chain (C22:0 and C24:0) ceramides in human plasma." Anal Bioanal Chem **405**(23): 7357-7365.
Kaestner, K. H., J. M. Ntambi, et al. (1989). "Differentiation-induced gene expression in 3T3-L1 preadipocytes. A second differentially expressed gene encoding stearoyl-CoA desaturase." J Biol Chem **264**(25): 14755-14761.
Karim, R., H. N. Hodis, et al. (2008). "Relationship between serum levels of sex hormones and progression of subclinical atherosclerosis in postmenopausal women." J Clin Endocrinol Metab **93**(1): 131-138.
Katsel, P., C. Li, et al. (2007). "Gene expression alterations in the sphingolipid metabolism pathways during progression of dementia and Alzheimer's disease: a shift toward ceramide accumulation at the earliest recognizable stages of Alzheimer's disease?" Neurochem Res **32**(4-5): 845-856.
Kendrick, D. C. (1973). "The effects of infantile stimulation and intermittent fasting and feeding on life span in the black-hooded rat." Dev Psychobiol **6**(3): 225-234.
Kishimoto, Y., M. Hiraiwa, et al. (1992). "Saposins: structure, function, distribution, and molecular genetics." J Lipid Res **33**(9): 1255-1267.
Kizhakkayil, J., F. Thayyullathil, et al. (2012). "Glutathione regulates caspase-dependent ceramide production and curcumin-induced apoptosis in human leukemic cells." Free Radic Biol Med **52**(9): 1854-1864.
Kowalski, G. M., A. L. Carey, et al. (2013). "Plasma sphingosine-1-phosphate is elevated in obesity." PLoS One **8**(9): e72449.
Landfield, P. W., L. D. Braun, et al. (1981). "Hippocampal aging in rats: a morphometric study of multiple variables in semithin sections." Neurobiol Aging **2**(4): 265-275.
Landfield, P. W., G. Rose, et al. (1977). "Patterns of astroglial hypertrophy and neuronal degeneration in the hippocampus of ages, memory-deficient rats." J Gerontol **32**(1): 3-12.
Lauterborn, J. C., L. C. Palmer, et al. (2016). "Chronic Ampakine Treatments Stimulate Dendritic Growth and Promote Learning in Middle-Aged Rats." J Neurosci **36**(5): 1636-1646.
Levy, M. and A. H. Futerman (2010). "Mammalian ceramide synthases." IUBMB Life **62**(5): 347-356.
Lightle, S. A., J. I. Oakley, et al. (2000). "Activation of sphingolipid turnover and chronic generation of ceramide and sphingosine in liver during aging." Mech Ageing Dev **120**(1-3): 111-125.
Livak, K. J. and T. D. Schmittgen (2001). "Analysis of relative gene expression data using real-time quantitative PCR and the 2(-Delta Delta C(T)) Method." Methods **25**(4): 402-408.
Lucki, N. C. and M. B. Sewer (2010). "The interplay between bioactive sphingolipids and steroid hormones." Steroids **75**(6): 390-399.
Maceyka, M., H. Sankala, et al. (2005). "SphK1 and SphK2, sphingosine kinase isoenzymes with opposing functions in sphingolipid metabolism." J Biol Chem **280**(44): 37118-37129.
Maceyka, M. and S. Spiegel (2014). "Sphingolipid metabolites in inflammatory disease." Nature **510**(7503): 58-67.
Maeng, H. J., J. H. Song, et al. (2017). "Celecoxib-mediated activation of endoplasmic reticulum stress induces de novo ceramide biosynthesis and apoptosis in hepatoma HepG2 cells mobilization." BMB Rep **50**(3): 144-149.
Majumdar, I. and L. D. Mastrandrea (2012). "Serum sphingolipids and inflammatory mediators in adolescents at risk for metabolic syndrome." Endocrine **41**(3): 442-449.
Mar-Heyming, R., M. Miyazaki, et al. (2008). "Association of stearoyl-CoA desaturase 1 activity with familial combined hyperlipidemia." Arterioscler Thromb Vasc Biol **28**(6): 1193-1199.
Mattson, M. P., W. Duan, et al. (2001). "Suppression of brain aging and neurodegenerative disorders by dietary restriction and environmental enrichment: molecular mechanisms." Mech Ageing Dev **122**(7): 757-778.
McKhann, G. M., D. S. Knopman, et al. (2011). "The diagnosis of dementia due to Alzheimer's disease: recommendations from the National Institute on Aging-Alzheimer's Association workgroups on diagnostic guidelines for Alzheimer's disease." Alzheimers Dement **7**(3): 263-269.
McNamara, R. K., Y. Liu, et al. (2008). "The aging human orbitofrontal cortex: decreasing polyunsaturated fatty acid composition and associated increases in lipogenic gene expression and stearoyl-CoA desaturase activity." Prostaglandins Leukot Essent Fatty Acids **78**(4-5): 293-304.

Melcangi, R. C., V. Magnaghi, et al. (2001). "Glial cells: a target for steroid hormones." Prog Brain Res **132**: 31-40.
Merrill, C. B., A. Basit, et al. (2017). "Patch clamp-assisted single neuron lipidomics." Sci Rep **7**(1): 5318.
Mielke, M. M., V. V. Bandaru, et al. (2015). "Demographic and clinical variables affecting mid- to late-life trajectories of plasma ceramide and dihydroceramide species." Aging Cell **14**(6): 1014-1023.
Mielke, M. M., V. V. Bandaru, et al. (2010). "Serum sphingomyelins and ceramides are early predictors of memory impairment." Neurobiol Aging **31**(1): 17-24.
Mielke, M. M., N. J. Haughey, et al. (2010). "Plasma ceramides are altered in mild cognitive impairment and predict cognitive decline and hippocampal volume loss." Alzheimers Dement **6**(5): 378-385.
Mielke, M. M., W. Maetzler, et al. (2013). "Plasma ceramide and glucosylceramide metabolism is altered in sporadic Parkinson's disease and associated with cognitive impairment: a pilot study." PLoS One **8**(9): e73094.
Mitsnefes, M., P. E. Scherer, et al. (2014). "Ceramides and cardiac function in children with chronic kidney disease." Pediatr Nephrol **29**(3): 415-422.
Miyazaki, M., M. J. Jacobson, et al. (2003). "Identification and characterization of murine SCD4, a novel heart-specific stearoyl-CoA desaturase isoform regulated by leptin and dietary factors." J Biol Chem **278**(36): 33904-33911.
Miyazaki, M., Y. C. Kim, et al. (2001). "A lipogenic diet in mice with a disruption of the stearoyl-CoA desaturase 1 gene reveals a stringent requirement of endogenous monounsaturated fatty acids for triglyceride synthesis." J Lipid Res **42**(7): 1018-1024.
Morrison, J. H. and P. R. Hof (1997). "Life and death of neurons in the aging brain." Science **278**(5337): 412-419.
Morselli, E., A. P. Frank, et al. (2016). "A sexually dimorphic hypothalamic response to chronic high-fat diet consumption." Int J Obes (Lond) **40**(2): 206-209.
Morselli, E., E. Fuente-Martin, et al. (2014). "Hypothalamic PGC-1alpha protects against high-fat diet exposure by regulating ERalpha." Cell Rep **9**(2): 633-645.
Moser, V. A. and C. J. Pike (2016). "Obesity and sex interact in the regulation of Alzheimer's disease." Neurosci Biobehav Rev **67**: 102-118.
Nagano, S., T. Yamada, et al. (1998). "Expression and processing of recombinant human galactosylceramidase." Clin Chim Acta **276**(1): 53-61.
Newton, J., S. Lima, et al. (2015). "Revisiting the sphingolipid rheostat: Evolving concepts in cancer therapy." Exp Cell Res **333**(2): 195-200.
Niccoli, T. and L. Partridge (2012). "Ageing as a risk factor for disease." Curr Biol **22**(17): R741-752.
Nichols, N. R., J. R. Day, et al. (1993). "GFAP mRNA increases with age in rat and human brain." Neurobiol Aging **14**(5): 421-429.
Ntambi, J. M., S. A. Buhrow, et al. (1988). "Differentiation-induced gene expression in 3T3-L1 preadipocytes. Characterization of a differentially expressed gene encoding stearoyl-CoA desaturase." J Biol Chem **263**(33): 17291-17300.
Ntambi, J. M., M. Miyazaki, et al. (2002). "Loss of stearoyl-CoA desaturase-1 function protects mice against adiposity." Proc Natl Acad Sci U S A **99**(17): 11482-11486.
Ogretmen, B. and Y. A. Hannun (2004). "Biologically active sphingolipids in cancer pathogenesis and treatment." Nat Rev Cancer **4**(8): 604-616.
Ogura, K., M. Ogawa, et al. (1994). "Effects of ageing on microglia in the normal rat brain: immunohistochemical observations." Neuroreport **5**(10): 1224-1226.
Paillard, F., D. Catheline, et al. (2008). "Plasma palmitoleic acid, a product of stearoyl-coA desaturase activity, is an independent marker of triglyceridemia and abdominal adiposity." Nutr Metab Cardiovasc Dis **18**(6): 436-440.
Pakkenberg, B., D. Pelvig, et al. (2003). "Aging and the human neocortex." Exp Gerontol **38**(1-2): 95-99.
Palmer, B. F. and D. J. Clegg (2015). "The sexual dimorphism of obesity." Mol Cell Endocrinol **402**: 113-119.
Patti, G. J., O. Yanes, et al. (2012). "Metabolomics implicates altered sphingolipids in chronic pain of neuropathic origin." Nat Chem Biol **8**(3): 232-234.

Perez, G. I., A. Jurisicova, et al. (2005). "A central role for ceramide in the age-related acceleration of apoptosis in the female germline." FASEB J **19**(7): 860-862.
Peters, A., J. H. Morrison, et al. (1998). "Feature article: are neurons lost from the primate cerebral cortex during normal aging?" Cereb Cortex **8**(4): 295-300.
Petersen, R. C. and J. C. Morris (2005). "Mild cognitive impairment as a clinical entity and treatment target." Arch Neurol **62**(7): 1160-1163; discussion 1167.
Pfaffl, M. W., A. Tichopad, et al. (2004). "Determination of stable housekeeping genes, differentially regulated target genes and sample integrity: BestKeeper--Excel-based tool using pair-wise correlations." Biotechnol Lett **26**(6): 509-515.
Picard, A., C. Rouch, et al. (2014). "Hippocampal lipoprotein lipase regulates energy balance in rodents." Mol Metab **3**(2): 167-176.
Pizzirani, D., A. Bach, et al. (2015). "Benzoxazolone carboxamides: potent and systemically active inhibitors of intracellular acid ceramidase." Angew Chem Int Ed Engl **54**(2): 485-489.
Pruett, S. T., A. Bushnev, et al. (2008). "Biodiversity of sphingoid bases ("sphingosines") and related amino alcohols." J Lipid Res **49**(8): 1621-1639.
Pyne, N. J., M. McNaughton, et al. (2015). "Role of sphingosine 1-phosphate receptors, sphingosine kinases and sphingosine in cancer and inflammation." Adv Biol Regul.
Rahman, S. M., A. Dobrzyn, et al. (2003). "Stearoyl-CoA desaturase 1 deficiency elevates insulin-signaling components and down-regulates protein-tyrosine phosphatase 1B in muscle." Proc Natl Acad Sci U S A **100**(19): 11110-11115.
Rahman, S. M., A. Dobrzyn, et al. (2005). "Stearoyl-CoA desaturase 1 deficiency increases insulin signaling and glycogen accumulation in brown adipose tissue." Am J Physiol Endocrinol Metab **288**(2): E381-387.
Ramirez, S., L. Martins, et al. (2013). "Hypothalamic ceramide levels regulated by CPT1C mediate the orexigenic effect of ghrelin." Diabetes **62**(7): 2329-2337.
Rothman, S. M., K. J. Griffioen, et al. (2012). "Brain-derived neurotrophic factor as a regulator of systemic and brain energy metabolism and cardiovascular health." Ann N Y Acad Sci **1264**: 49-63.
Sacket, S. J., H. Y. Chung, et al. (2009). "Increase in sphingolipid catabolic enzyme activity during aging." Acta Pharmacol Sin **30**(10): 1454-1461.
Saddoughi, S. A. and B. Ogretmen (2013). "Diverse functions of ceramide in cancer cell death and proliferation." Adv Cancer Res **117**: 37-58.
Salem, N., Jr., B. Litman, et al. (2001). "Mechanisms of action of docosahexaenoic acid in the nervous system." Lipids **36**(9): 945-959.
Samad, F., K. D. Hester, et al. (2006). "Altered adipose and plasma sphingolipid metabolism in obesity: a potential mechanism for cardiovascular and metabolic risk." Diabetes **55**(9): 2579-2587.
Saravia, F., J. Beauquis, et al. (2007). "Neuroprotective effects of estradiol in hippocampal neurons and glia of middle age mice." Psychoneuroendocrinology **32**(5): 480-492.
Satoi, H., H. Tomimoto, et al. (2005). "Astroglial expression of ceramide in Alzheimer's disease brains: a role during neuronal apoptosis." Neuroscience **130**(3): 657-666.
Savica, R., M. E. Murray, et al. (2016). "Plasma sphingolipid changes with autopsy-confirmed Lewy Body or Alzheimer's pathology." Alzheimers Dement (Amst) **3**: 43-50.
Schneider, M., B. Levant, et al. (2017). "Lipids in psychiatric disorders and preventive medicine." Neurosci Biobehav Rev **76**(Pt B): 336-362.
Schwartz, G. J., J. Fu, et al. (2008). "The lipid messenger OEA links dietary fat intake to satiety." Cell Metab **8**(4): 281-288.
Schwartz, M. W., S. C. Woods, et al. (2000). "Central nervous system control of food intake." Nature **404**(6778): 661-671.
Segovia, G., A. del Arco, et al. (2009). "Environmental enrichment, prefrontal cortex, stress, and aging of the brain." J Neural Transm (Vienna) **116**(8): 1007-1016.
Shaywitz, S. E., F. Naftolin, et al. (2003). "Better oral reading and short-term memory in midlife, postmenopausal women taking estrogen." Menopause **10**(5): 420-426.

Silva, V. R., T. O. Micheletti, et al. (2014). "Hypothalamic S1P/S1PR1 axis controls energy homeostasis." Nat Commun **5**: 4859.

Simstein, R., M. Burow, et al. (2003). "Apoptosis, chemoresistance, and breast cancer: insights from the MCF-7 cell model system." Exp Biol Med (Maywood) **228**(9): 995-1003.

Sugiura, Y., S. Shimma, et al. (2008). "Imaging mass spectrometry technology and application on ganglioside study; visualization of age-dependent accumulation of C20-ganglioside molecular species in the mouse hippocampus." PLoS One **3**(9): e3232.

Summers, S. A. (2006). "Ceramides in insulin resistance and lipotoxicity." Prog Lipid Res **45**(1): 42-72.

Tayebi, N., B. K. Stubblefield, et al. (2003). "Reciprocal and nonreciprocal recombination at the glucocerebrosidase gene region: implications for complexity in Gaucher disease." Am J Hum Genet **72**(3): 519-534.

Thaler, J. P., C. X. Yi, et al. (2012). "Obesity is associated with hypothalamic injury in rodents and humans." J Clin Invest **122**(1): 153-162.

van Blitterswijk, W. J., A. H. van der Luit, et al. (2003). "Ceramide: second messenger or modulator of membrane structure and dynamics?" Biochem J **369**(Pt 2): 199-211.

Velazquez-Zamora, D. A., D. Gonzalez-Tapia, et al. (2012). "Plastic changes in dendritic spines of hippocampal CA1 pyramidal neurons from ovariectomized rats after estradiol treatment." Brain Res **1470**: 1-10.

Venable, M. E., J. Y. Lee, et al. (1995). "Role of ceramide in cellular senescence." J Biol Chem **270**(51): 30701-30708.

Venable, M. E. and X. Yin (2009). "Ceramide induces endothelial cell senescence." Cell Biochem Funct **27**(8): 547-551.

Wang, C. Y. and J. K. Liao (2012). "A mouse model of diet-induced obesity and insulin resistance." Methods Mol Biol **821**: 421-433.

Weir, J. M., G. Wong, et al. (2013). "Plasma lipid profiling in a large population-based cohort." J Lipid Res **54**(10): 2898-2908.

West, M. J., P. D. Coleman, et al. (1994). "Differences in the pattern of hippocampal neuronal loss in normal ageing and Alzheimer's disease." Lancet **344**(8925): 769-772.

Wolf, O. T., B. M. Kudielka, et al. (1999). "Two weeks of transdermal estradiol treatment in postmenopausal elderly women and its effect on memory and mood: verbal memory changes are associated with the treatment induced estradiol levels." Psychoneuroendocrinology **24**(7): 727-741.

Yamada, J. and S. Jinno (2014). "Age-related differences in oligodendrogenesis across the dorsal-ventral axis of the mouse hippocampus." Hippocampus **24**(8): 1017-1029.

Yamazaki, Y., K. Kondo, et al. (2014). "Proportion of nervonic acid in serum lipids is associated with serum plasmalogen levels and metabolic syndrome." J Oleo Sci **63**(5): 527-537.

Yang, G., L. Badeanlou, et al. (2009). "Central role of ceramide biosynthesis in body weight regulation, energy metabolism, and the metabolic syndrome." Am J Physiol Endocrinol Metab **297**(1): E211-224.

Zhang, Q. G., R. Wang, et al. (2014). "Brain-derived estrogen exerts anti-inflammatory and neuroprotective actions in the rat hippocampus." Mol Cell Endocrinol **389**(1-2): 84-91.

Zheng, Y., S. M. Prouty, et al. (2001). "Scd3--a novel gene of the stearoyl-CoA desaturase family with restricted expression in skin." Genomics **71**(2): 182-191.

Acknowledgements

With great pleasure, I would like to express my deepest and most sincere gratitude to my supervisor Professor Daniele Piomelli for his countless support and mentorship and for training me as a young scientist since I joined his lab. His constructive suggestions, guidance and encouragement were the driving force behind the successful completion of my doctoral thesis. I wish to be as passionate, enthusiastic, and energetic as he is. I would also like to thank him for giving me the opportunity to spend one full year of my PhD program at the University of California Irvine.

My wholehearted thanks to my lab mate and friend Dr. Alessandra Misto for helping me in the lab, for daily support and also for sharing with me some frustrating moments.

I am very thankful to Dr. Andrea Armirotti, Dr. Natalia Realini and Dr. Silvia Pontis for their many insightful discussions and suggestions and for lending their valuable time to assist me in the development of this thesis. They all helped me a lot in moving my first steps as a researcher and they have been always available to answer my numerous questions, contributing to my professional growth.

I would like to thank Dr. Abdul Basit, whose availability and dedication allowed me to carry out the analytical parts of my projects and whose precious analytical competences helped me in technical issues.

I thank Dr. Francesca Palese for her helpful advices in molecular biology.

Special thanks to the D3 chemists, in particular my “bay mates”, for their friendship and for making my stay in the lab and in Genova wonderful and joyful.

I would also like to extend my thanks to the entire Drug Discovery and Development family, for the constant technical, administrative and informatics support.

I do wish to demonstrate my gratitude and appreciation to Dr. Kwang-Mook Jung and Dr. Faizy Ahmed for having been very welcoming since I have joined the lab of UCI and for their precious daily advices.

I would also like to thank my American lab mates Dr. Guillermo Moreno-Sanz, Dr. Karina Genaro, Yannick Fotio, Diane Lee and the undergrad students.

Finally, I thank my mother, my father, and my brother for their support and faith in me. No words can describe the immense love and motivation they provided me. Thank you for being with me in every situation.

If I am here today, it is mainly because of you.

Publications

1. **V. Vozella,** A. Basit, F. Piras, N. Realini, A. Armirotti, P. Bossù, F. Assogna, S. Sensi, G. Spalletta, D. Piomelli. "Elevated plasma ceramide levels in post-menopausal women" (manuscript under review, *Journal of Lipid Research-Patient oriented and epidemiological research*)

   Impact factor: 4.810

2. **V. Vozella,** A. Basit, A. Misto, D. Piomelli. "Age-dependent changes in nervonic acid-containing sphingolipids in mouse hippocampus", DOI: 10.1016/j.bbalip.2017.08.008. *Biochimica et Biophysica Acta (BBA) - Molecular and Cell Biology of Lipids*, **2017,** 1862, pp. 1502-1511.

   Impact factor: 5.557

3. A. Bach, D. Pizzirani, N. Realini, **V. Vozella**, D. Russo, I. Penna, L. Melzig, R. Scarpelli, D. Piomelli. "Benzoxazolone Carboxamides as Potent Acid Ceramidase Inhibitors: Synthesis and Structure-Activity Relationship (SAR) Studies", DOI: 10.1021/acs.jmedchem.5b01188. *J. Med. Chem.*, **2015**, *58*, pp 9258-9272.

   Impact factor: 6.259

4. A. Misto, A. Basit, G. Provensi, **V. Vozella**, M.B. Passani, D. Piomelli. "Mast cell-derived histamine controls liver ketogenesis via OEA signaling" (manuscript under review, *Cell Metabolism*)

   Impact factor: 17.303

Poster communications

1. **V. Vozella,** N. Realini, A. Misto, D. Piomelli. "Feeding regulates sphingolipid-mediated signaling in mouse hypothalamus".

   Poster presented at *Gordon Research Conference Lipids, molecular and cellular biology of* (Waterville Valley, New Hampshire, USA, July 30-August 4, **2017**)

2. **V. Vozella,** N. Realini, A. Misto, D. Piomelli. "Feeding regulates sphingolipid-mediated signaling in mouse hypothalamus".

   Poster presented at *Keystone Symposia on Molecular and Cell Biology, Lipidomics and Bioactive Lipids in Metabolism and Disease* (Tahoe City, California, USA, February 26-March 2, **2017**)

3. **V. Vozella,** N. Realini, A. Misto, D. Piomelli. "Feeding regulates sphingolipid-mediated signaling in mouse hypothalamus".

   Poster presented at *Society for Neuroscience (SfN)* (San Diego, California, USA, 12-16 November **2016**)

4. **V. Vozella,** N. Realini, A. Misto, D. Piomelli "Feeding status regulates ceramide signaling in mouse hypothalamus"

   Poster presented at *EMBO Workshop on Neural Control of Metabolism and Eating Behavior* (Cascais, Portugal, 5-7 May **2016**)